REPUBLIC OF TURKEY
AYDIN ADNAN MENDERES UNIVERSITY
GRADUATE SCHOOL OF NATURAL AND APPLIED SCIENCES
MECHANICAL ENGINEERING
2018-M.Sc.-026

THE INVESTIGATION OF CRACK INITIATION AND PROPAGATION IN COMPOSITE MATERIALS

Cihan ATİNTAŞ

Supervisor:

Assoc. Prof. Dr. Pınar DEMİRCİOĞLU

AYDIN

REPUBLIC OF TURKEY
AYDIN ADNAN MENDERES UNIVERSITY
GRADUATE SCHOOL OF NATURAL AND APPLIED SCIENCES
AYDIN

The thesis with the title of **"THE INVESTIGATION OF CRACK INITIATION AND PROPAGATION IN COMPOSITE MATERIALS"** prepared by Cihan ATİNTAŞ, Master Student at the Mechanical Engineering Program at the Department of Mechanical Engineering was accepted by the jury members whose names and titles presented below as a result of thesis defense on 12 July 2018.

	Title, Name Surname	Institution	Signature
President :	Assoc. Prof. Dr. Pınar DEMİRCİOĞLU	Aydın Adnan Menderes University	
Member :	Prof. Dr. İsmail BÖĞREKCİ	Aydın Adnan Menderes University	
Member :	Prof. Dr. Vural CEYHUN	Ege University	

This Master Thesis accepted by the jury members is endorsed by the decision of the Institute Board Members with ………… Serial Number and ………………… date.

Prof. Dr. Aydın ÜNAY
Institute Director

REPUBLIC OF TURKEY
AYDIN ADNAN MENDERES UNIVERSITY
GRADUATE SCHOOL OF NATURAL AND APPLIED SCIENCES
AYDIN

I hereby declare that all information and results reported in this thesis have been obtained by my part as a result of truthful experiments and observations carried out by the scientific methods, and that I referenced appropriately and completely all data, thought, result information which do not belong my part within this study by virtue of scientific ethical codes.

…./…./2018

Cihan ATİNTAŞ

ÖZET

KOMPOZİT MALZEMELERDE ÇATLAK BAŞLANGIÇ VE İLERLEMESİNİN ANALİZİ

Cihan ATİNTAŞ

Yüksek Lisans Tezi, Makine Mühendisliği Anabilim Dalı
Tez Danışmanı: Doç. Dr. Pınar DEMİRCİOĞLU
2018, 103 Sayfa

İyi tasarlanmış kompozit malzemelerin avantajı, genellikle bileşenlerinin en iyi özelliklerini sergilemeleri ve bazen ise bileşenlerinin bile sahip olmadığı bazı özelliklere sahip olmalarıdır.

Bu tezin ana amacı, zeytin pirinası partiküllü biyokompozit malzemedeki çatlak başlangıcını ve ilerlemesini sayısal olarak analiz etmek ve sonuçları analitik ve deneysel çözümlerle karşılaştırmaktır.

Çekme, bükülgenlik ve mikrosertlik testleri dahil olmak üzere farklı mekanik analiz teknikleri kullanılarak, zeytin pirinası partiküllerinin takviye malzemesi olarak kullanıldığı vinilester reçinedeki etkisi, ayrıntılı olarak araştırılmıştır. Darbe yüklemesine maruz kalan kompozit numunelerin çatlak başlangıcı ve ilerlemesi süreci Sonlu Elemanlar Yöntemi kullanılarak ANSYS'de incelenmiştir.

Sonuçlar, %5 (OP)p/VE numuneleri için malzeme mekanik özelliklerinden çekme mukavemetinde (%1,58) ve çekme modülünde (%0,49) iyileşme ve %10 ve %20 (OP)p/VE numuneleri için ise azalma göstermiştir. Bu sonuçlarla birlikte sonlu elemanlar analizi, %5 (OP)p/VE numuneleri için gerilme enerjisinde (%0,30) azalma, sırasıyla %10 ve %20 (OP)p/VE için (%5,44 ve %8,52) iyileşme olduğunu göstermiştir.

Anahtar Kelimeler: Biyokompozitler, kompozit malzemeler, çatlak başlangıcı ve ilerlemesi, hasar analizi, sonlu elemanlar yöntemi, doğal takviye malzemeleri, sayısal analiz, zeytin pirinası, atık yönetimi.

ABSTRACT

THE INVESTIGATION OF CRACK INITIATION AND PROPAGATION IN COMPOSITE MATERIALS

Cihan ATİNTAŞ

M. Sc. Thesis, Department of Mechanical Engineering
Supervisor: Assoc. Prof. Dr. Pınar DEMİRCİOĞLU
2018, 103 pages

The advantage of composite materials is that, if well designed, they usually show the best qualities of their constituents and often some qualities that neither constituent possesses.

The primary aim of this thesis is to analyze the crack initiation and propagation in olive pomace particulate biocomposite materials numerically and compare the results with the analytical and experimental solutions.

The influence of olive pomace particles as a reinforcing material for vinylester resin was investigated in detail using different mechanical analysis techniques, including tensile, flexural and microhardness tests. The process of the crack initiation and propagation of the composite materials, subjected to impact loading, was investigated using FEM with ANSYS.

The results indicated improvements in mechanical properties including tensile strength (%1,58) and tensile modulus (%0,49) for %5 (OP)p/VE specimens and declines for %10 and %20 (OP)p/VE specimens. However, the FEM analysis indicated declines in strain energy (% 0,30) for %5 (OP)p/VE specimens and improvements (%5,44 and %8,52) respectively for %10 and %20 (OP)p/VE specimens.

Key Words: Biocomposites, composite materials, crack initiation and propagation, failure analysis, finite element method, natural reinforcement materials, numerical analysis, olive pomace, waste management.

ACKNOWLEDGEMENTS

I wish to express my gratitude to my supervisor, Assoc. Prof. Dr. Pınar Demircioğlu who was offered invaluable support with her sincerity and belief in me. I am especially grateful to Prof. Dr. Ismail Böğrekci for his advices and comments. I would like to thank my valuable colleagues and superiors who supported and trusted me throughout my master study.

Also, I would like to thank my friend and mentor, Res. Asst. Saygın Sucuoğlu, who shares his knowledge and experiences with me during my thesis, for his invaluable efforts and help. I would like to acknowledge the efforts of both Oğulcan and Aslı for their help in the analysis process of my thesis work.

In addition, some of the experiments done for this study were carried out at the laboratories of Dokuz Eylül University, Department of Mechanical Engineering. I would also like to thank them for giving me the opportunity. I also thank Aydın Adnan Menderes University, Department of Food Engineering, for their help in the process of the preparation of the samples. I would also like to thank Mr. Hasan Filiz from Poliya Poliester San. ve Tic. Ltd. Sti., Mr. Mustafa Tuna from Dalan Yağ Endüstri A.Ş and Capt. Mesut Cin from Köşk, Aydın for their contributions.

I am always grateful to my mother for her prays and blessings.

Last but not least, I would like to give all my special thanks to my beloved wife Merve. Without her support I couldn’t been in this point both in academia and in my life. She is always with me when I felt hopeless and weak in solving problems.

I also want to express that this thesis is completed within the scope of the Department of Scientific Research Projects, Aydın Adnan Menderes University, with the same name and MF-17012 project number.

Cihan ATİNTAŞ

TABLE OF CONTENTS

LIST OF SUBSCRIPTS

c : composite

C : Critical value

f : flexural

I : Mode I

m : matrix

p : particle

LIST OF ABBREVIATIONS

APTES : 3-aminopropyltriethoxysilane

ASTM : American Society for Testing and Materials

DMA : Dynamic Mechanical Analysis

DSC : Differential Scanning Calorimetry

FEM : Finite Element Method

GFRP : Glass Fiber Reinforced Polymer

HDT : Heat Deflection Temperature

HR : Rockwell Hardness Number

ISO : International Organization for Standardization

LEFM : Linear Elastic Fracture Mechanics

MEKP : Methyl Ethyl Ketone Peroxide

MRPS : γ-mercaptopropyltrimethoxysilane

OP : Olive Pomace

PMC : Polymer Matrix Composite

ROM : Rule of Mixtures

SADT : Self-accelerating Decomposition Temperature

SIF : Stress Intensity Factor

STD : Standard Deviation

VE : Vinyl Ester / Vinylester

(OP)p/VE : Olive Pomace Particulate Vinylester

LIST OF FIGURES

LIST OF TABLES

LIST OF APPENDICES

1. INTRODUCTION

1.1. Background

Composite materials are of high interest at present due to their specific characteristics. Polymer matrix composite (PMC) is the most commonly used composite category, due to their lower density and cheapness as well higher specific modulus, higher specific strength and chemical inertness compared to aerospace aluminum and steel alloys. Natural fiber reinforced composites' importance has grown significantly, and they have become preferred materials in automotive, aerospace, marine, infrastructure, sporting goods, and defense industries (Thomas, 2013).

The industrial use of natural fibers serves as a source of income for farmers in developing economies. In addition, plant fibers are an alternative to the usage of wood materials, also reducing the exhaustion of forests.

Keeping with the effort to be environmentally friendly, experiments have been made by many researchers to use natural fiber reinforced composites instead of glass fiber composites in many applications. In fact, several automotive components which had been previously made with glass fiber composites are now being produced using environmentally friendly natural fiber composites (Vilaseca, et al., 2007).

Olive growing is among the most important sources of livelihood in the Turkish geographical regions of Marmara, Mediterranean and Aegean, which includes Aydin province. The solid waste produced in the production of olive oil is called "pomace" in Turkey. Due to the pieces of olive kernel in the content of this pomace, it has a cellulosic structure. For this reason, olive pomace can be used as reinforcements for biocomposites, which is made from renewable sources.

The primary aim of this thesis is to analyze the crack initiation and propagation in olive pomace particulate biocomposite materials numerically and compare the results with the analytical and experimental solutions. Particularly this thesis does

1. Predict the crack initiation in specifically produced composite material,
2. Find the mechanical properties of this material as a result of tensile, flexural and hardness tests,
3. Compare the numerical results with the previous studies and analytical solutions,
4. Investigate the crack propagation and failure in the material by using finite element methods.

In this study, a biocomposite of PMC class was produced by using olive pomace as reinforcing material and vinyl ester resin as matrix material. By adding 5%, 10% and 20% of pomace into the matrix, three specimens with different properties were formed. Thus, how the increase in the amount of pomace was reflected in the mechanical properties of the composite material were examined.

Because of studies on natural fiber reinforced composite materials or biocomposites in recent years, the effect of natural materials used as reinforcing materials on the mechanical properties of composite materials produced has been investigated.

Abessalam (Abessalam, 2011) dusted the cracked olive kernel in the range of 0.4-0.6 mm as reinforcing material in his research on damaging modes of natural fiber reinforced epoxy based composite materials. Some of the reinforcing material was used without chemical treatment and some of them were used by chemical treatment with '3-aminopropyltriethoxysilane' (APTES). Flexibility test, tensile test, microhardness test, impact test, dynamic mechanical analysis (DMA) of epoxy-based composite material and reinforcement material with reinforced material and untreated (10%, 20%, 30%, differential scanning calorimetry (DSC) test, and microscopic examination.

Gharbi et al. (Gharbi et al., 2014) used olive kernel dust in the weight range of 50-200 μm size (0% -60%) as reinforcing material in the study titled "silane" effect of olive kernel powder-reinforced unsaturated polyester based composite materials. In the produced samples, some of the reinforcing material was chemically treated with 'γ-mercaptopropyltrimethoxysilane' (MRPS). They have achieved the results they supported by DMA analysis by examining the flexural and impact strength of the composite specimens they prepared with the pressure molding method.

Erkliğ (Erkliğ, 2016) used two reinforcing materials at the same time in their work on the effect of olive pomace particles in the mechanical properties of glass fiber reinforced polymer (GFRP) composites. The method of hand laying with epoxy resin mixture containing 75 μm size of olive pomace reinforcing material in weight percentages (0.5%, 1%, 2%, 5%, 10%, and 15%) as synthetic fiber using eight layered glass fiber to produce composite specimens called hybrid composites. They investigated the tensile and elastic properties of the samples they produced with unreinforced epoxy and investigated the mechanical properties of GFRP type composite material by adding olive pomace particles.

This fundamental study will offer new information about olive pomace reinforced biocomposites by taking into consideration the crack initiation and propagation analyzed by finite element methods.

1.2. Literature Review

At the beginning, books, articles, journals, scientific standards, library and internet resources have been examined and reviewed. Previous studies including former researches on similar natural fiber reinforced composites as well as different testing standards of composites have been analyzed and considered. The performance of other natural fiber/filler composites, including the designs of reinforcement, the variations in the types of fiber's directions and textures has also been evaluated.

In the "Literature Review" chapter, it has been assessed the use of olive pomace with an environmentally friendly and 'green' look. In this second chapter also, the followings are presented:

1. Composite material generally and the at least three constituent phases,

2. The classification of composites regarding the environmentally friendly and natural way,

3. The fabrication and the applications of composites,

4. The characterizations of composites; tensile, flexural and microhardness tests,

5. The fracture mechanics of composites,

6. Finite Element Analysis, and lastly as mentioned above

7. The olive pomace as a reinforced material.

1.3. Material and Method

In the third chapter “Material and Method”;

1. The materials used are described thoroughly and the manufacturing process are presented,

2. The details of experiments and methods are presented and the preparation of olive pomace reinforced vinylester composites with different amount of content (0%, 5%, 10% and 20 %w/w) are described,

3. The finite element analysis are presented.

1.4. Results and Discussion

The results of the experimental investigations were analyzed and recorded before presenting the modes of crack initiation and propagation in the specimens. The following steps are in the “Results and Discussion” chapter as:

1. The physical and mechanical properties along with the finite element analysis are presented,

2. The test results of tensile, flexural, microhardness testing and Charpy analysis are presented,

3. The results of abovementioned are discussed.

1.5. Conclusions

In the last chapter “Conclusions”

1. The results of this investigation have been summarized and presented while the conclusion is studied.

2. Recommendations and suggestions for further works have been given and the benefits of this investigation are presented.

2. LITERATURE REVIEW

2.1. Composite Materials

A composite material is generally defined as the new constituted material which is a combination of two or more chemically insoluble and distinct materials at a macroscopic level, with a recognizable interphase between the phases (Kalpakjian et al., 2009; Miracle et al., 2001). Composite materials are generally divided into two classes by their origins: natural and synthetic (Other classifications were mentioned in Section 2.2. in detail). Natural composites are materials found in nature such as bone, teeth, wood, bamboo, and shell. Synthetic composites can be described as human production, and one of the oldest example is mudbrick used as building material of adobe houses in biblical times. The two constituent phases are clay and straw in that oldest application of composites (Beşergil, 2016; Kalpakjian et al., 2009).

The components forming composites are called phases. There are at least two bulk phases and an interphase in a composite material. The bulk phases are matrix and reinforcement phases. The interphase or interface, not a bulk phase in the true sense of the word, also may be called as a phase where matrix and reinforcement phases interact physically, chemically and mechanically with each other. Apart from interphase, matrix and reinforcement phases maintain their properties (Beşergil, 2016).

The advantage of a well-designed composite material is that it generally shows the best properties of its components and sometimes has certain properties that the components do not even possess (Jones, 1998). It is aimed to produce a material having superior properties than its components in an intended purpose.

When it comes to structural applications in mechanical engineering, the main reasons why composite materials are preferred to metals are as follows:

- Resistance to corrosion, chemicals and weather conditions,
- Providing a thermal, acoustical and electrical insulation,
- Having high strength-to-weight ratio,
- Mechanical and fatigue strength,
- Light weight and stiffness,

- Dimensional stability
- Design flexibility,
- Low costs and other desired qualities superior to metals (Beşergil, 2016; Jones, 1998; Kalpakjian et al., 2009; Kaw, 2006; Miracle et al., 2001).

In the production of composite materials, it is generally intended to develop one or more of the above features. It is possible to obtain the desired characteristics mentioned above when these following conditions met; pairing the suitable matrix and reinforcing material, a well production technique, optimization, strength properties of the components and consideration of other production factors.

2.1.1. Matrix Phase

The matrix material is the primary phase in a composite material. It has three principal functions:

- Holding the reinforcement materials, especially fibers together and transferring the load between them so that the fibers can carry most of the load,
- Protecting the reinforcement material against physical damage, mechanical abrasion, chemical reactions and the environment,
- Decreasing the propagation of cracks in the composite material by the higher ductility and toughness properties it has (Barbero, 1999; Beşergil, 2016; Kalpakjian et al., 2009).

The major matrix phases are metal, ceramic and organic. The term “organic-matrix” includes polymer and carbon matrixes (Miracle et al., 2001). Figure 2.1 shows the classification of matrix phases.

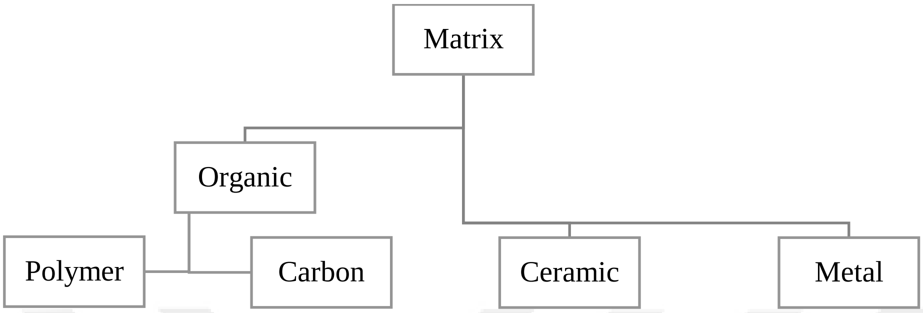

Figure 2.1. The classification of matrix phases

2.1.1.1. Polymer matrix composites

Polymer Matrix Composites (PMCs) are very popular in composites applications because they are cheaper and to apply fabrication methods to them is easy. Polymer alone as a structure material is limited by low mechanical properties, specifically strength, modulus and impact resistance. The main advantages of PMCs are, if reinforced with durable material networks:

- High specific strength and stiffness,
- High fracture resistance,
- Good abrasion, impact, corrosion, and fatigue resistances,
- Low cost.

Besides, the primary disadvantages of PMCs are low thermal resistance and high coefficient of thermal expansion (Jose et al., 2012).

The most important PMC - also a natural composite - is the wood, in which the matrix is lignin and the reinforcement is cellulose (Beşergil, 2016). The polymer matrix material, used in synthetic composites are categorized in three groups:

1) Thermosetting polymers,
2) Thermoplastic polymers,
3) Elastomers.

2.1.1.1.1. Thermosetting polymers

Thermosetting Polymers consist of molecules that have network or cross-linked structures with covalent bonds. They cannot be softened by the application of heat, and reshaped or reformed once solidified. On the other hand, they are durable and more resistant to heat, solvents and corrosion (Beşergil, 2016; Jose et al., 2012; Zweben, 2006). Most commercially produced PMC use a thermosetting matrix material called resin. Common examples are:

- Epoxy resins,
- Polyester resins,
- Vinylester resins,
- Phenolics,
- Ureas,
- Melamine,
- Silicone,
- Polyimides.

2.1.1.1.1.1. Vinylester resin

Vinylester resins have superior mechanical properties than polyester resins and lower cost than epoxy resins. They are widely used in commercial applications. They are remarkably resistant to solvents, acids, alkalis, peroxides and hypochlorites. They have greater corrosion resistance than polyester resins. They are preferred in highly moist environments (Barbero, 1999; Jose et al., 2012).

2.1.2. Reinforcement Phase

The reinforcement material is the secondary phase in a composite material. It is dispersed in the matrix and gives the desired properties to the composite material. Figure 2.2 shows the major types of reinforcement phases used in composite materials as follows:

- Continuous fiber laminated composites,
- Whisker (discontinuous or chopped) reinforcements,
- Particulate reinforcements,
- The various forms of fibrous architectures produced by textile technology, such as fabric and braid (Zweben, 2006).

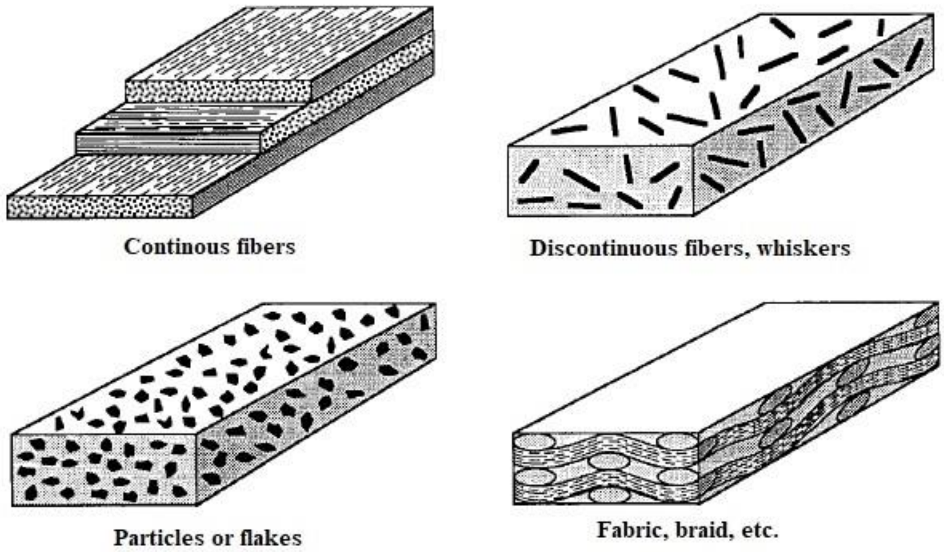

Figure 2.2. The forms of reinforcement phases (Zweben, 2006)

The principal function of the reinforcement phase is to provide strength and stiffness to the composite material. It may also provide electrical and thermal conductivity, wear resistance, and controlled thermal expansion (Miracle et al., 2001). Reinforcement materials are also divided into two classes by their origins: natural and synthetic (Beşergil, 2016; Thakur et al., 2014).

2.1.2.1. Particulate composites

Particulate composite materials are composed of particles or flakes of reinforcement material in a matrix material. One of the example of particulate composites is concrete, in which sand and gravel are reinforcement phase in the form of particles and the cement and water constitutes the matrix phase (Beşergil, 2016; Jones, 1998). It is possible to categorize particulate composites into two main categories as particle and flake reinforcements.

Particles may be of a wide variety, but their dimensions must be approximately the same in each direction. For effective strengthening, the particles must be very tiny and fully dispersed in the matrix, moreover the volume fractions of both phases are also influential. The elastic modulus of two-phased composites is related to the volume fractions of the phases and defined by two mathematic formulas. The first formula is called as rule of mixtures (ROM) and is applied to most of the calculations in composites, for example we can use ROM for determining the longitudinal modulus of fibrous composites. The elastic modulus of particle reinforced composites is determined between the Equations 2.1 and 2.2, as shown in Figure 2.3 (Beşergil, 2016).

Upper limit: (Eq.2.1)

$$E_c = V_m.E_m + V_p.E_p$$

Lower limit: (Eq.2.2)

$$\frac{1}{E_c} = \frac{V_m}{E_m} + \frac{V_p}{E_p}$$

E=Elastic Modulus, V=Volume fraction, and the subscripts are representing for composites (c), matrix (m), and particles (p) in Eq. 2.1-2 and Figure 2.3.

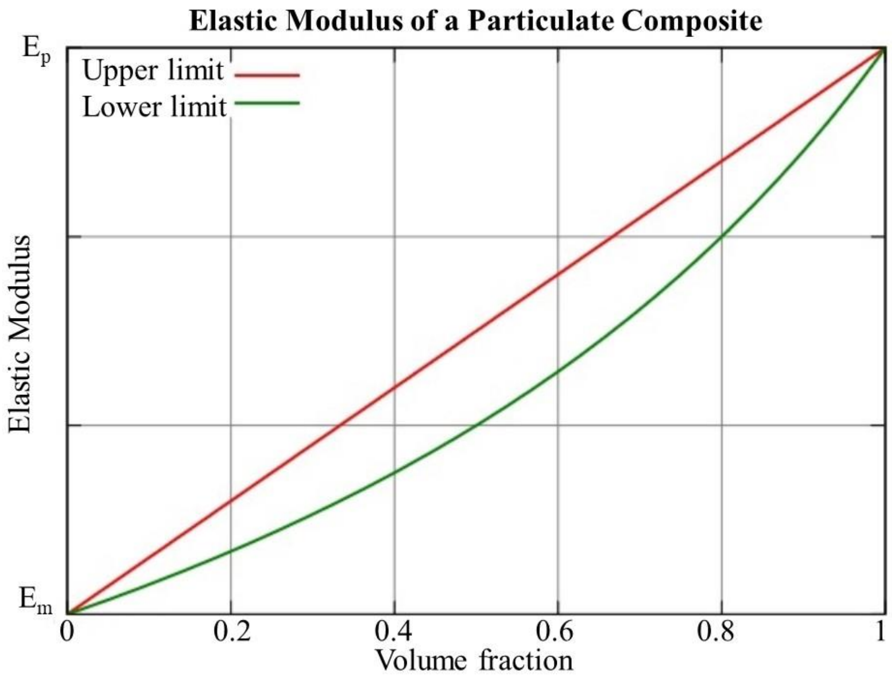

Figure 2.3. The elastic modulus of a particulate composites according to ROM

2.1.3. Interphase

The interphase or interface is the interaction region where the matrix and reinforcement phases are physically, chemically or mechanically joined in a composite material. Its principal function is to transfer the load from matrix phase to reinforcement phase. Although the interface is thought to be a two-dimensional region, researches has expanded this concept into that it exists in three dimensions (Drzal, 1985).

The interphase occurs from the point in the reinforcement phase where the local properties begin to transform from the properties of bulk reinforcement, through the actual interface, into the matrix phase where the local properties again match with the properties of bulk matrix. The complexity of the interphase can best be exemplified with the use of a schematic model, which allows the various distinct characteristics of this region and some of the factors that contribute to its formation to be listed, as shown in Fig. 2.4 (Drzal, 2001).

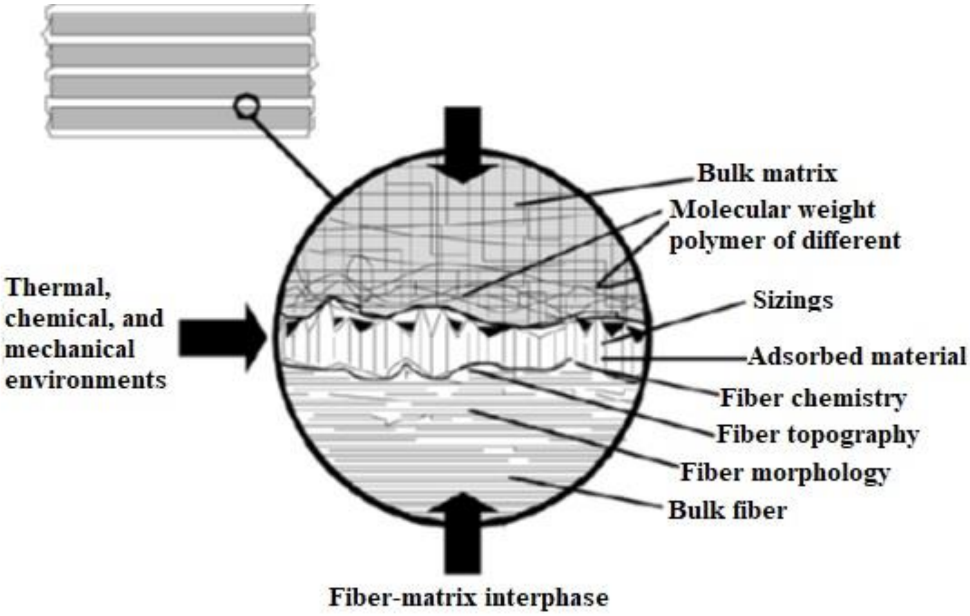

Figure 2.4. Schematic diagram of the fiber-matrix interphase (Drzal, 2001)

2.2. The Classification of Composites

Composites are generally classified at two separate levels apart from their origins. The first level of classification usually refers to the type of matrix and the second refers to the geometry of reinforcement (Miracle et al., 2001). Figure 2.5 shows all three levels of classifications basically. In addition to these general classification, it is possible to combine two or more of the geometries of reinforcement and also to create hybrid composites.

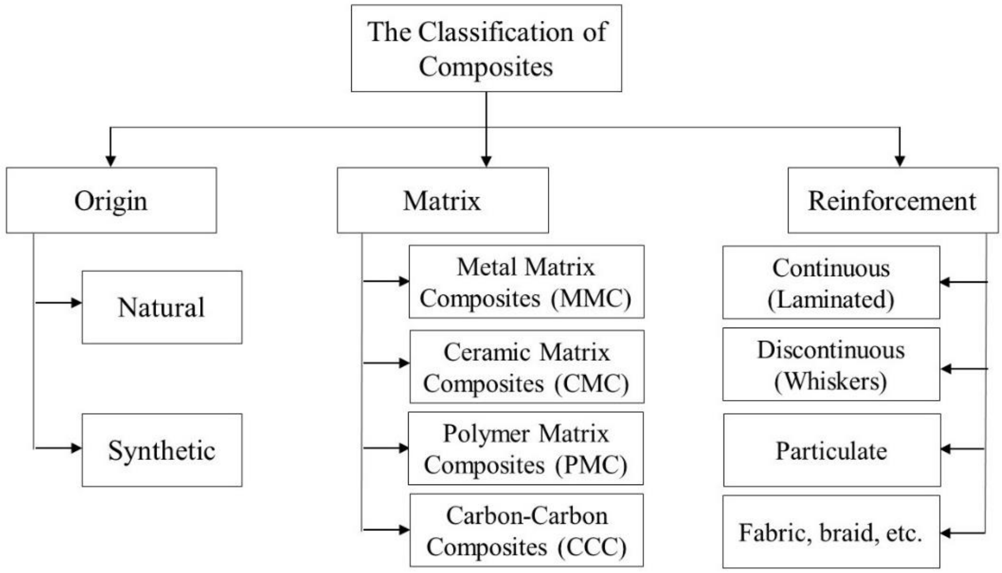

Figure 2.5. The general classification of composites

The most standard way to represent reinforced composites is to write the reinforcement and matrix separately with a slash. For example, carbon fiber-reinforced polyester is typically written as ‘‘carbon/polyester,’’ or, ‘‘C/PE.’’ Particle reinforcements are shown in parentheses followed by ‘‘p’’. For example, a cemented carbide, which has tungsten carbide particles as reinforcement and cobalt as matrix, appears to be written as ‘‘(WC)p/Co’’ (Beşergil, 2016; Zweben, 2006).

2.2.1. Biocomposites

Biocomposites are specific composites, in which at least one of its components is a biodegradable and renewable material derived from natural resources (Beşergil, 2016, Thakur et al., 2014). It is a specific classification that can also be subdivided into three main categories:

1) Totally biodegradable and renewable (*green*) composites, in which both the matrix and reinforcement are from natural resources.
2) Partly biodegradable and renewable (*ecofriendly*) composites, in which the matrix is obtained from natural resources and reinforced with a synthetic material.
3) Partly biodegradable and renewable (*ecofriendly*) composites, in which the reinforcement is obtained from natural resources and the matrix is a synthetic material (Mohanty et al., 2005; Thakur et al., 2014).

The terms biocomposites, green composites, and eco-composites or ecofriendly composites are all often used interchangeably. However, there are some examples of separate usages too (Beşergil, 2016; Goda et al., 2014; Mohanty et al., 2005; Thakur et al., 2014). Table 2.1 shows the features of the materials used in each phase of biocomposites.

Table 2.1. Phases of Biocomposites

	Biocomposites		
	Totally ecofriendly	Partly ecofriendly	
Matrix	Biopolymer	Biopolymer	Synthetic polymer
Reinforcement	Natural	Synthetic	Natural

2.2.1.1. Natural reinforcements

Over the last few years, many researchers have been involved in studying the using of natural reinforcements as load bearing materials in composites. The use of such materials in composites has increased because of their relative cheapness, strength per weight of material and ability to recycle. Natural reinforcements are subcategorized based on their origins as animal, mineral and plant reinforcements (Zavareze et al., 2012; John et al., 2012; Thakur et al., 2014).

Animal reinforcements, including silk and hair (or wool, feather, etc.), mainly consist of proteins.

Mineral reinforcements include asbestos which is the universal designation for a group of naturally occurring mineral silicate fibers.

Plant reinforcements, including cotton, flax, hemp, sisal, jute, kenaf, henequen, corn, coconut etc., mainly consist of cellulose, hemicellulose, lignin and pectin. They can be subcategorized into several classes as schematically shown in Figure 2.6 (John et al., 2012; Thakur et al., 2014).

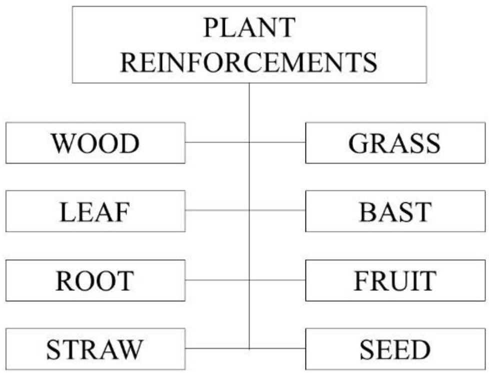

Figure 2.6. The classification of plant reinforcements

2.2.1.1.1. Olive seeds as a natural reinforcement

The olive seeds (olive pits or stones etc.) have been the subject of several investigations in composite applications and their physical, chemical, thermal properties, and mechanical behaviors have been investigated by many researchers (Abessalam 2011; Bledzki et al., 1996; Ayrılmış et al., 2010; Djidjelli et al., 2007; Erkliğ et. al., 2016; Ertürk, 2015; Kılıçaslan, 2016; Kılıçkan et al., 2008; Mousa et al., 2009; Naghmouchi et al., 2014; 2015; Papanicolaou et al., 2011; 2012). The findings of these investigations along with the history of olive and the usage of its seeds as a natural reinforcement were mentioned in detail, in section 2.7.

2.3. Fabrication and Application of Composites

When fabricating products and structures with traditional construction materials, manufacturing is generally a matter of machining, joining material or molding that once solidified and in such forms as block, rod or sheet. With composites, the circumstances are different in that both the component and material are manufactured simultaneously (Åström, 2001). Due to their low manufacturing costs, PMCs are the most common type of composites in a wide variety of applications.

2.3.1. Manufacturing of PMCs

The manufacturing and shaping of PMCs into final products often combines the formation of the materials (Jose et al., 2012). The common processing methods are as follows:

- Open molding process,
- Bag molding process,
- Pultrusion,
- Filament winding,
- Preformed molding compounds,
- Resin transfer molding,
- Injection molding,
- Reaction injection molding,
- Reinforced reaction injection molding and so on.

The open molding process - also known as wet lay-up process - which consists of hand lay-up and spray-up processes, is the oldest method used in PMC industry and still the selected manufacturing process for a wide range of products (Andressen, 2001). Advantages associated with the open molding process include:

- Simplicity,
- Design flexibility,
- Low costs of start-up, mold and tooling,
- Possibility of tailored properties, large-sized and high-strength large parts,

Disadvantages of the process include:

- Long cycle and long reworking times per molding,
- Labor intensive and operator-skill dependent,
- Sometimes only one surface has aesthetic appearance,
- Evaporation, exposure, and emission of volatile organic compounds,
- Sharp corners and limited edges.

2.3.2. Applications of PMCs

PMCs are extensively used for lightweight structures. It is possible to categorize the applications of PMCs into three main categories as engineering, structural and other miscellaneous applications.

2.3.2.1. Engineering applications

The use of PMCs has become increasingly appealing alternative to metals for many components of engineering applications mainly because of their increased strength, durability, resistance to fatigue and corrosion, and damage tolerance characteristics. PMCs also provide greater design flexibility because they can be tailored to meet the design requirements and they also offer significant lightweight advantages. The common engineering applications of PMCs are as follows:

- Aircraft industry; aerospace structures, air or space transports and general aviation applications,
- Automotive and rail industry; manufacturing of automobiles, road and rail transports and general automotive applications,
- Marine industry; naval engineering, maritime transports and general naval applications,
- General mechanical applications (Gay, 2014; Jose et al., 2012).

2.3.2.2. Structural applications

PMCs have been used in the construction industry for a long time. Applications range from non-structural claddings and gratings to full structural systems for industrial supports, long span roof structures, tanks, buildings, bridge components and complete bridge systems. Their benefits of resistance to corrosion and lightweight have proven attractive in many low stress applications. PMCs present immense opportunities to play developing role as an alternate material to take the place of steel, timber, aluminum and concrete in buildings. The common structural applications of PMCs are as follows:

- Construction industry; buildings and public works applications, profiles, panels and various covers (windows, domes etc.),
- Furniture industry; partitions, doors, bathrooms and portable toilets,
- Boards, laminates, pipes and so on (Gay, 2014).

2.3.2.3. Miscellaneous applications

The diversity of industrial products and the variety of consumer goods that incorporate PMCs, other than engineering and structural usage, includes numerous application areas of activity where PMCs have been introduced and are used in a significant way. These applications of PMCs are as follows:

- Electrical and electronics industry; panels, housing, insulators, switchgear, cables and connectors,
- Consumer and sports goods: golf and polo rods, skis, fishing rods, canoes and kayaks, tennis rackets, bicycles, archery equipment, protective sportswear and so on.
- Biomedical applications; medical implants, prosthetists or orthotists, orthopedic devices.
- And many more (Gay, 2014; Jose et al., 2012).

2.4. Characterizations of Composites

In terms of the direction where strain is induced in a specimen of PMCs, there are four specific modes of mechanical strength properties (Driscoll, 1998):

- Tensile,
- Compressive,
- Bending,
- Shear.

There are several types of testing methods applicable to help in characterizing these mechanical properties of PMCs. The testing techniques used in this study to characterize the properties of the (Olive Pomace)p/Vinylester composites include tensile, flexural and microhardness test methods.

2.4.1. Tensile Testing of PMCs

Tensile testing is one of the most commonly used characterization method for PMCs. The tensile test method resolves how the material responds to loads being applied in tension. It is possible to determine its strength and elongation at break by using this method. Tensile testing also produces a stress-strain diagram, that is used to determine mechanical properties like toughness, yield strength, ductility, tensile modulus and ultimate tensile strength.

There is one standard of American Society for Testing and Materials (ASTM D638 – 14) for testing unreinforced and reinforced plastics that is used internationally. Many nations individually, and the International Organization for Standardization (ISO), have a similar standard (Adams, 2006; Anonymous, 2014a).

2.4.1.1. Test specimen for tensile test

There are six types of test specimen by regards of the dimensions: Type I, II, III, IV, V and VI specimen. The Type I specimen is the preferred specimen in this study. It shall be used when the material has a thickness of 7 mm or less. It is also the recommended type for reinforced composites (Anonymous, 2014a; Beşergil, 2016).

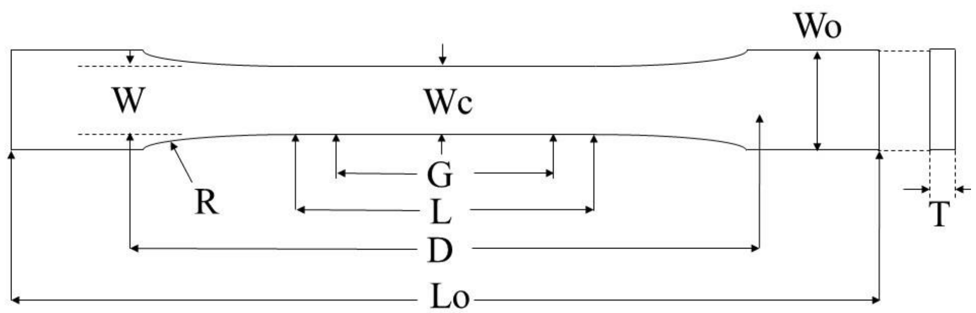

Figure 2.7. Type I specimen for tensile test

The dimensions for Type I specimen are illustrated in Figure 2.7 and the values are given in table 2.2.

Table 2.2. Dimensions of Type I specimen

Type I (see Fig.2.7)	W	L	Wo	Lo	G	D	R
Dimensions (mm)	13	57	19	165	50	115	76
Tolerances	± 0.5	± 0.5	+ 6.4	no max	± 0.25	± 5	± 1

W= Width of narrow section, L= Length of narrow section, Wo= Width overall, Lo= Length overall, G= Gage length, D= Distance between grips, R= Radius of fillet, Wc= Width at the center, T= Thickness and the T value is 7 mm or less for Type I specimens, but it shall be 3.2 ± 0.4 mm for all types of molded specimens and for other Type I specimens where possible.

2.4.2. Flexural Testing of PMCs

There are several methods for testing flexural properties of unreinforced and reinforced plastics and electrical insulating materials. Two main types of bending are cantilever and simple beam. The first method is the common cantilever beam test, ASTM D747 – 10. In it, the specimen is held in a fastener that rotates the specimen against a block (Figure 2.8.a). This method is rarely used and seldom discussed (Adams, D. F. 2006; Anonymous, 2017a).

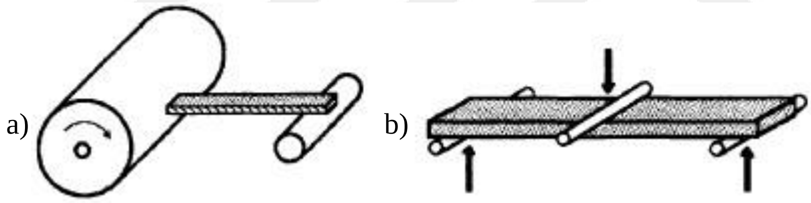

Figure 2.8. a) Cantilever beam bending b) 3-Point bending (Driscoll, 1998)

The second method is one of the most widely used of the mechanical property tests, as the specimen geometry and the hardware for supporting are both very simple. This method also was divided into two submethods:

- **3-point bending test** is ASTM D790 – 17, which consists of supporting the specimen at two points and loading it at the center with a single loading nose. The area of uniform stress is accumulated under the center loading point (Figure 2.8.b).
- **4-point bending test** is ASTM D6272 – 17, which consists of two loading noses. The area of uniform stress occurs between them.

ASTM D790 – 17 is the preferred flexural testing method in this study.

2.4.2.1. Test specimen for 3-Point bending test

The recommended specimen for molding thermosetting composite materials is 127 by 12.7 by 3.2 mm (length x width x depth) tested flatwise on a support span, resulting in a support span-to-depth ratio of 16 (tolerance ± 1). The loading nose and supports shall have cylindrical surfaces and the radii of them shall be 5.0 ± 0.1 mm (Beşergil, B. 2016; Anonymous, 2017a).

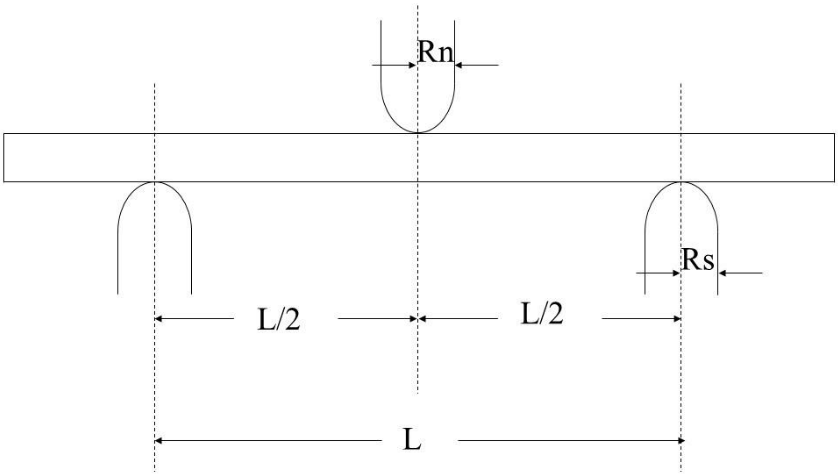

Figure 2.9. The dimensions of the specimen for 3-Point bending

Rn= Radius of the loading nose, Rs= Radius of the support, L= Distance between the supports, and D= depth of the specimen. The min Rn and Rs values are 3.2 mm and the max Rn= 4 x D and the max Rs= 16 x D.

2.4.3. Microhardness Testing of PMCs

Hardness is the most widely measured of the surface properties for PMCs. ASTM D785 – 08(2015) is a standard test method for Rockwell hardness of plastics and electrical insulating materials. It is done with a specialized instrument, which uses one of several possible steel ball or diamond shaped indenters. The indenter first is forced against the specimen for a short period of time under a minor load and then under a major load. A hardness reading is then taken from the appropriate scale, which are R, L, M, E and K scales (Adams, 2006; Anonymous, 2015a; Beşergil, 2016).

This method is divided into two submethods: Procedure A and B. Procedure B is used to characterize the surface microhardness of the specimens in this study. Furthermore, the R scale is the only scale approved for plastics testing by this procedure. Therefor the specimens were tested by using the R scale with a 12.7 mm (0.5 in.) indenter, 10-kg minor and 60-kg major loads (Anonymous, 2015a; Anonymous, 2018b).

The hardness determined by Procedure B shall be known as the alpha, α, Rockwell hardness number (HR) and it is derived from the following equation:

$$\alpha\ HR = 150 - e \qquad \text{(Eq. 2.3)}$$

where:

α HR = the Rockwell α hardness number, and

e = the depth of impression after removal of the major load, in units of 0.001 mm. This equation only holds for the R scale (Anonymous, 2015a; Anonymous, 2018b).

2.4.3.1. Test specimen for Rockwell hardness test

The test specimens shall be 25 by 25 mm-squares and have a thickness of 6 mm according to ASTM D785 – 08(2015). They shall have parallel flat surfaces so that there would not be deflections that might be caused by a poor contact with the anvil (Anonymous, 2015a).

2.5. Fracture Mechanics of Composites

Fracture is an unexpected failure of an intact body breaking into two or more pieces due to stress. The fracture mechanics deals with the behavior of cracks (Gross et al., 2011). Steps in fracture are as follows:

- Crack initiation,
- Crack propagation, and
- The fracture.

The cracks in composites always continue to grow until a residual strength has become so low that it subsequently leads to a fracture (Broek, 1982; Gross et al., 2011).

2.5.1. Linear Elastic Fracture Mechanics

The linear-elastic fracture mechanics (LEFM) was laid by Griffith (1921), who worked on glass for understanding the brittle fracture originating from a crack and later developed and modified by Irwin (1957a, 1957b), who worked on the crack-tip and its relationship with the approach of stress intensity factor (SIF) (Maiti, 2015; Perez, 2017).

The particulate composites are macroscopically homogeneous and often considered to be isotropic. Since PMCs exhibit nearly linear behavior almost to fracture, the LEFM is the theoretical basis used in this study. LEFM is applicable for many of the situations like brittle failures in PMCs or impact testing (Bert, 1989; Williams, 2001).

2.5.1.1. Modes of cracking

Considering the formation of a crack, there are three modes of crack opening which are illustrated in Figure 2.10 (Gross et al., 2011).

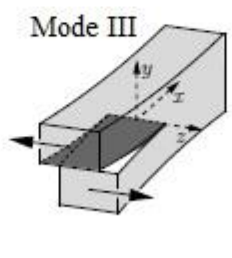

Figure 2.10. The three modes of cracking (Gross et al., 2011)

Mode I, which is denoted the **‘opening mode’**, is characterized by a symmetric crack opening, in which the displacements are in the direction perpendicular to the plane of the crack within y-direction.

Mode II, which is denoted the **'sliding mode'**, is described by an antisymmetric crack opening, in which the displacements are in the direction perpendicular to the leading edge of the crack and in the plane of the crack within x-direction.

Mode III, which is denoted the **'tearing mode'**, is defined as a crack opening, in which the displacements are parallel to the leading edge of the crack and in the plane of the crack within z-direction (Broek, 1982; Gross et al., 2011, Maiti, 2015).

Mode I occurs most often and is technically the most important type. The discussions in this study are limited to Mode I type of problems. K_I denotes SIF for Mode I. K_I is the most evaluated and studied experimentally for determining the critical stress intensity factor (K_{IC}) or usually called 'fracture toughness' of a composite material.

2.5.1.2. Fracture toughness

K_{IC} is a property which is a measure for the crack resistance of a material. When K_I reaches K_{IC}, the fracture must be expected to occur. PMCs with low K_{IC} values can tolerate only small cracks (Broek, 1982). The determination of K_{IC} of a PMC is generally performed in standardized tests, but in this study Finite Element Analysis is used instead.

2.6. Finite Element Method

The Finite Element Method (FEM) is a numerical tool for obtaining the closest solution for partial differential equations in engineering problems. FEM has been developed into a fundamental technology in modeling and simulation of engineering systems. One of the most important interests in solid mechanics problems is the simulation of damage and fracture phenomena. Engineering structures, which subjected to high loads, may result in stresses in the rigid body exceeding the strength of the material and thus, in dynamic failure. These material failures manifest themselves in various failure mechanisms such as the fracture or shear in ductile metals, or crack discontinuity in brittle materials (Khoei, 2014; Barbero, 2008; Liu et al., 2013).

Nowadays, many commercial programs exist with many finite element analysis capabilities for different disciplines of engineering systems. They help us to solve various problems from a simple linear static analysis to nonlinear transient analysis. A few of these, such as ANSYS^{TM} or ABAQUS™, have special capabilities to analyze composite materials. These programs accept user programmed formulations of element and constitutive custom equations (Khoei, 2014). The preferred program in this study is ANSYS^{TM}. The analysis for Charpy impact test has been simulated by using ANSYS^{TM} 17.2.

2.6.1. Test Specimen for Charpy Impact Analysis

The recommended test method is used to determine the resistance of plastics to breakage by flexural shock as indicated by the energy extracted from standardized pendulum type hammers, mounted in standardized machines, in breaking standard specimens with one pendulum swing, ASTM D6110-18 (Anonymous, 2018a). This test method requires specimens to be made with a milled notch (see Figure 2.11). The notch produces a stress concentration which promotes a brittle, rather than a ductile, fracture. The results of this test method are reported in terms of energy absorbed per unit of specimen width (see Table 2.3).

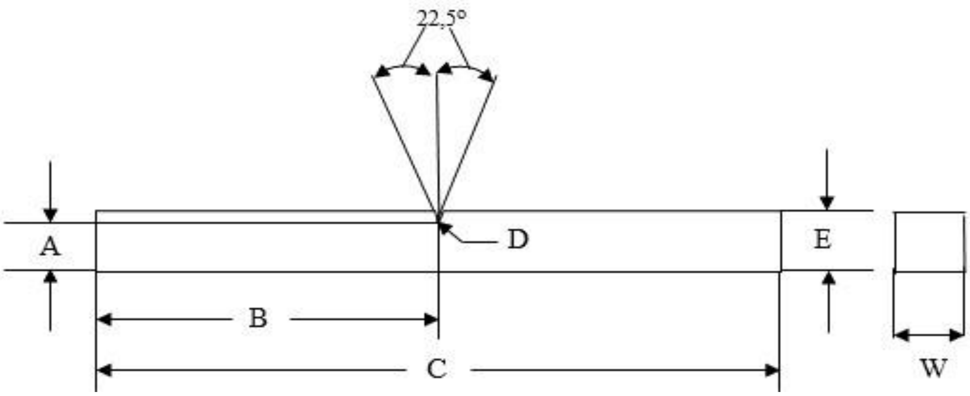

Figure 2.11. Simple Beam, Charpy Type, Impact Test Specimen

Table 2.3. Dimensions of Simple Beam, Charpy Type, Impact Test Specimen

see Fig.2.11	A	B	C	D	E	W
Dimensions (mm)	10.16	63.5	127	0.25 R	12.7	3.2
Tolerances	± 0.05	± 2.5	+ 5	± 0.05	± 0.15	± 0.2

2.7. Olive

Olives (Figure 2.12) are the most widely cultivated crops in the world. Olive cultivation is outspread throughout the Mediterranean region. It plays an important role in these rural economies and considers to be a local heritage. The largest producing countries are also in the Mediterranean and Middle East regions (Niaounakis et al., 2006).

Figure 2.12. Table olives (Anonymous, 2016a)

2.7.1. History of Olive

The olive tree (*Olea europaea L.*) is a member of the *Oleaceae* family, which includes approximately 30 species such as lilac, jasmine, privet and ash. The Asia Minor (Anatolia) is considered to be the birthplace of the wild olive tree (Anonymous, 2017b). It appears to have spread from Anatolia to entire Mediterranean Basin many millennia ago. Due to this region's characteristic soil and terrain, the Mediterranean is happened to be called as its native land. It has continued to spread outside the Mediterranean and at the present time is cultivated in places as far from its origins as China, Japan and Australia. Figure 2.13 shows the total production share of olives by region and Figure 2.14 shows the top production quantities of olives by country, respectively, between 2010 and 2014 (Anonymous, 2018e).

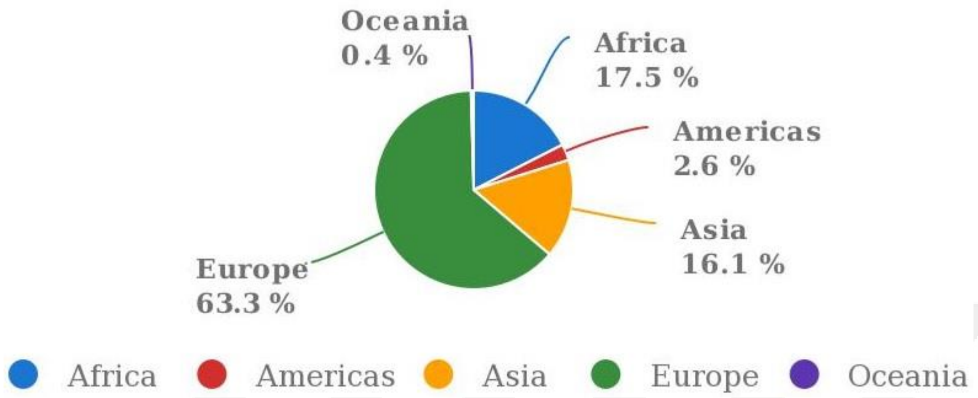

Figure 2.13. The production share of olives by region (Anonymous, 2018e)

Figure 2.14. The production quantities of olives by country (Anonymous, 2018e)

The olive tree is grown for its fruit, which is classed botanically as a drupe (Anonymous, 2017c). The olive fruit has a thin skin and flesh and a high oil content compared to other drupes. It is harvested mainly to produce olive oil because of this high content of oil (12-30% of fresh weight), which is depending on the variety and time of year (Anonymous, 2017b; Anonymous, 2017c).

The world harvested area of olive trees was reported as 10,272,547 hectares and the total world production of olives as 15,4 million tonnes, for the year of 2014. Figure 2.15 shows the top 10 producer countries, with Spain being first (4,56 tonnes), followed by Italy (1,96 tonnes), Greece (1,78 tonnes), and Turkey (1,77 tonnes) (Anonymous, 2018e).

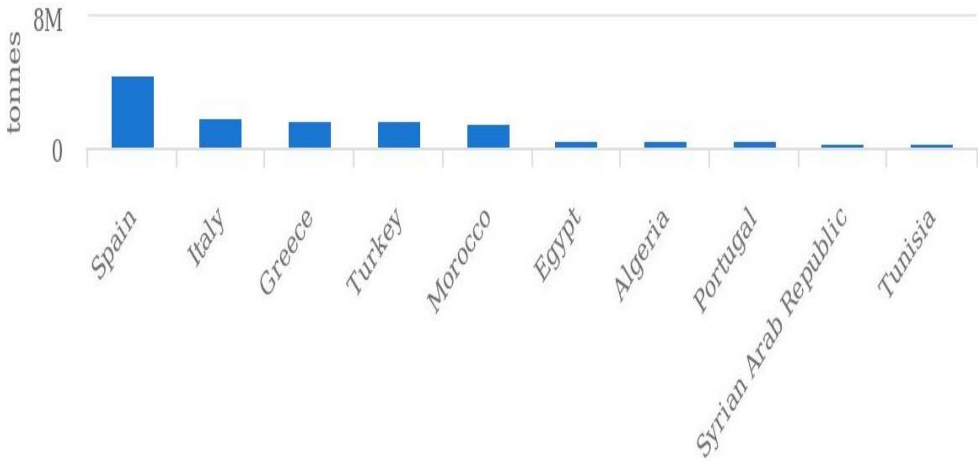

Figure 2.15. The production of olives: top 10 producer countries (Anonymous, 2018e)

2.7.2. Olive Oil Industry

The olive oil has been consumed for countless generations in the Mediterranean region. It is now extensively appreciated all around the world due to its nutritional properties with its wealth for health (Matos et. al, 2010). The way oil is extracted from olives is a tradition that has not changed in thousands of years. Nowadays extraction method is the same as some six thousand years ago. The olives are solely crushed into a smash where pressure is applied to extract the oil. The olive oil is then separated from the olive waste water. Technological developments saw the coming of hydraulic presses, which are used in today’s centrifugal systems (Anonymous, 2016a).

2.7.2.1. Olive waste

After the manufacturing process, beyond from the actual olive oil (20%), there outcomes a wet solid residue (30%) and olive waste water (50%) (Matos et. al, 2010). The solid olive residue is a composition of olive pulp and olive seeds. After being dried in rotary driers with the use of hot air (60 ◦C) and submitted to a hexane extraction to recover the seed oil, there leaves an olive pomace rich mass as a by-product (Niaounakis et al., 2006).

2.7.2.1.1. Olive pomace

The chemical composition of olive pomace produced by olive mills varies within large limits according to condition, type and origin of olives as well as to the extraction process of olive oil (Vlyssides A.G. et al., 1998). It can be seen in Table 2.4.

Table 2.4. Characteristics of olive pomace (Vlyssides A.G. et al., 1998)

Parameter	Pressure system	3-Phase system	2-Phase system
Moisture %	27.21 ± 1.048	50.23 ± 1.935	56.80 ± 2.188
Fats and oils %	8.72 ± 3.254	3.89 ± 1.449	4.65 ± 1.736
Proteins %	4.77 ± 0.024	3.43 ± 0.017	2.87 ± 0.014
Total sugars %	1.38 ± 0.016	0.99 ± 0.012	0.83 ± 0.010
Cellulose %	24.14 ± 0.283	17.37 ± 0.203	14.54 ± 0.170
Hemicellulose %	11.00 ± 0.608	7.92 ± 0.438	6.63 ± 0.366
Ash %	2.36 ± 0.145	1.70 ± 0.105	1.42 ± 0.088
Lignin %	14.18 ± 0.291	0.21 ± 0.209	8.54 ± 0.175
Kjeldahl Nitrogen %	0.71 ± 0.010	0.51 ± 0.007	0.43 ± 0.006
Phosphorous as P_2O_5 %	0.07 ± 0.005	0.05 ± 0.004	0.04 ± 0.003
Phenolic compounds %	1.146 ± 0.06	0.326 ± 0.035	2.43 ± 0.15
Potassium as K_2O %	0.54 ± 0.045	0.39 ± 0.033	0.32 ± 0.027
Calcium as CaO %	0.61 ± 0.059	0.44 ± 0.043	0.37 ± 0.036
Total Carbon %	42.90 ± 3.424	29.03 ± 2.317	25.37 ± 2.025
C/N ratio	60.79 ± 5.352	57.17 ± 5.033	59.68 ± 5.254

The olive pomace has a high lignin, cellulose, and hemicellulose content at all.

2.7.2.1.2. Lignin

Lignin is a component which is found in plants. Without lignin, the plants would not be able to reach great heights or the severity that is found in some crops like straw. The structure of lignin is amorphous, possesses a 3D polymer with high molecular weight. It is the sole one with the least closeness for water compared to the other three main compounds in fibers. It is thermoplastic, that means it starts to soften at around 90 °C temperatures and starts to flow at around 170 °C temperatures (Güner, 2007).

2.7.2.1.3. Cellulose

When the molecules of glucose attach end to end, a polymer form which known as cellulose, occurs. The chemical structure of cellulose form is an example of a polysaccharide. A molecule of cellulose may be from hundred to over ten thousand of glucose units long. The cellulose, that found in the pulp wood, has a chain with typical lengths between three hundred and seventeen hundred of units, at the same amount that found in cotton or other plant fibers ranges from eight hundred to ten thousand units (Klemm et al., 2005). It is crucial to consider the chemical shape of the 'cellobiose' molecule as it may indicate whether it may form a weak or strong bond with others such as polymer resin.

2.7.2.1.4. Hemicellulose

A hemicellulose is one of several heteropolymers (matrix polysaccharides), such as arabinoxylans, existing along with cellulose in the cell walls of almost all plants. While cellulose is crystalline, resistant and strong to hydrolysis, hemicellulose has an amorphous, random structure with little strength. It is simply hydrolyzed by dilute acid or base as well as myriad hemicellulose enzymes (Klemm et al., 2005).

3. MATERIAL AND METHOD

The materials used in experiments are described thoroughly and the manufacturing process of the samples are presented. The details of experiments and methods are presented and the preparation of olive pomace reinforced vinylester composites with different amount of content (0%, 5%, 10% and 20 %w/w) are described and finally the finite element analysis is presented.

3.1. Materials Used

3.1.1. Matrix Resin

The matrix resin used in this research was vinylester resin Polives 701, supplied by Poliya Composite Resins and Polymers Inc. Vinylester resin was selected as matrix material because its properties and bulk cost are intermediate between the polyester and epoxy resins. Vinylester resins have the best chemical resistance among the unsaturated resins. As polyester resins generally don’t resist much alkaline-based materials and oxidizing acids, Polives 701 can be used against these chemicals (Anonymous, 2004a).

Figure 3.1 shows the 1-liter container for the vinylester resin and Table 3.1 provides the physical and mechanical properties of the cured vinylester resin - Polives 701.

Table 3.1. Physical and mechanical properties for the cured vinylester resin - Polives 701 (Anonymous, 2004a)

Test	Value	Unit	Method
Water Absorption	0,15	%	ISO 62
Flexural Strength	160	MPa	ISO 178
Flexural Modulus	4360	MPa	ISO 178
Elongation at Break, flexural	6,9	%	ISO 178
Tensile Strength	80	MPa	ISO 527
Modulus of Elasticity in Tensile	3200	MPa	ISO 527
Elongation at Break, tensile	5-6	%	ISO 527
Izod Impact Strength	17	kJ/m²	ISO 180
Heat Deflection Temperature (HDT)	95 100	°C	ISO 75-A ISO 75-B
Barcol Hardness (Barcol 934-1)	35		ASTM D2583
Total Volume Shrinkage	7,7	%	ISO 2114

Figure 3.1. Vinylester resin Polives 701

3.1.2. Curing Additives

The vinylester resin was cured using additives: a catalyst and an accelerator both supplied by Poliya Composite Resins and Polymers Inc. The curing was carried out at room temperature.

3.1.2.1. Catalyst

The catalyst used in this research was Butanox M-60, a MEKP (Methyl ethyl ketone peroxide) hardener. The container is shown in Figure 3.2 and Table 3.2 provides the physical and chemical properties of Butanox M-60.

Table 3.2. Specifications and characteristic properties for Butanox M-60 (Anonymous, 2017d)

Specifications and Characteristics	**Parameters**
Appearance	Clear and colorless liquid
Active Oxygen Content	9,8 - 10,0 %
Density (relative)	1,17 g/cm^3 (at 20 °C)
Viscosity (dynamic)	25 mPa.s (at 20 °C)
Tensile Strength	ISO 527
Water solubility	Partly miscible (at 20 °C)
Self-accelerating decomposition temperature (SADT)	60 °C

Figure 3.2. Hardener Butanox M-60

3.1.2.2. Accelerator

The accelerator used in this research was Cobalt %6, a chemical accelerator. The container is shown in Figure 3.3 and Table 3.3 provides the Physical and chemical properties of Cobalt %6.

Table 3.3. Specifications and characteristic properties for Cobalt %6 (Anonymous, 2017e)

Specifications and Characteristics	Parameters
Appearance	Violet liquid
Odour	Faint
Density (relative)	0,963 g/cm^3 (at 20 °C)
Viscosity (dynamic)	16,5 mPa.s (at 20 °C)
pH	Neutral
Water solubility	Immiscible (at 20 °C)
Melting point	-10 °C

Figure 3.3. Accelerator Cobalt %6

3.1.3. Reinforcement

In this research olive pomace was used as a reinforcement material for vinylester resin. Olive pomace can be obtained from the waste by-product of the olive oil process.

In the production of olive oil, unwanted olive-mill wastewater and solid waste of olive pomace by-products are exposed together with olive oil. Olive pomace is sometimes used as animal feed in Turkey and mostly used as in pellet form for fuel (Figure 3.4). Studies on the use of the cellulose as a reinforcing material in polymer-based composites due to the richness of the cellulose, hemicellulose and lignin components in the content of the olive pomace are explained.

Figure 3.4. Olive pomace as pellets (Anonymous, 2018c)

The olive pomace used in this thesis study for the production of composite samples were supplied from a business establishment located in Köşk district of Aydın province. The olive pomace is from a variety of olive oil factories in Aydın, Manisa, İzmir, Muğla, Denizli and Antalya provinces. They are processed in this facility and subjected to a series of operations for seed oil extraction.

Then the wet olive pomace is subjected to a dehydration process. In large ovens, approximately 50% of the moisture content is evaporated. It is then subjected to an extraction process to separate seed oil in the pressurized tanks therein hexane gas. It contained with about 3% of seed oil for industrial usage.

Lastly, the residual olive pomace is washed and dried, leaving only a small amount of branch leaves, olive husks and seeds separated from the flesh, leaving only olive kernel pieces. In Figure 3.5, the production of olive pomace and the abovementioned process can be seen in a simple schema.

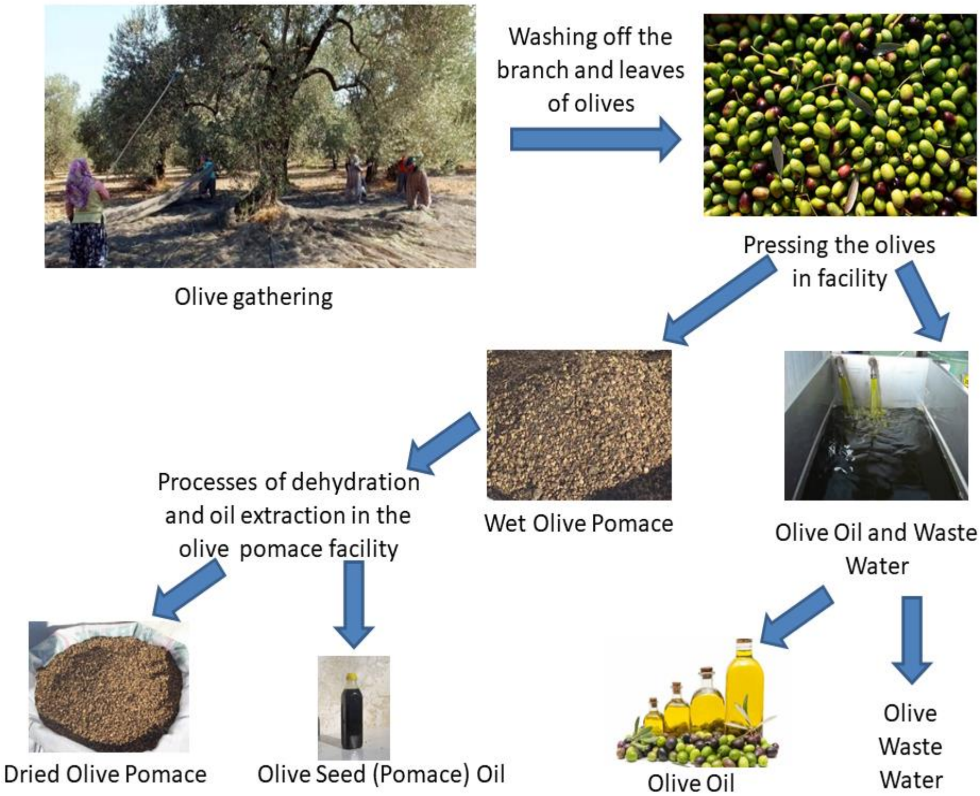

Figure 3.5. The production schema

The remaining dried olive pomace which contained the crushed olive seeds was then ground in a laboratory mill in Aydın Adnan Menderes University laboratories. Then finally the dried and grounded olive pomace sieved in a size range of 150 μm (by sieve analysis seen in Figure 3.6) using a sieve shaking machine of JEOTEST™.

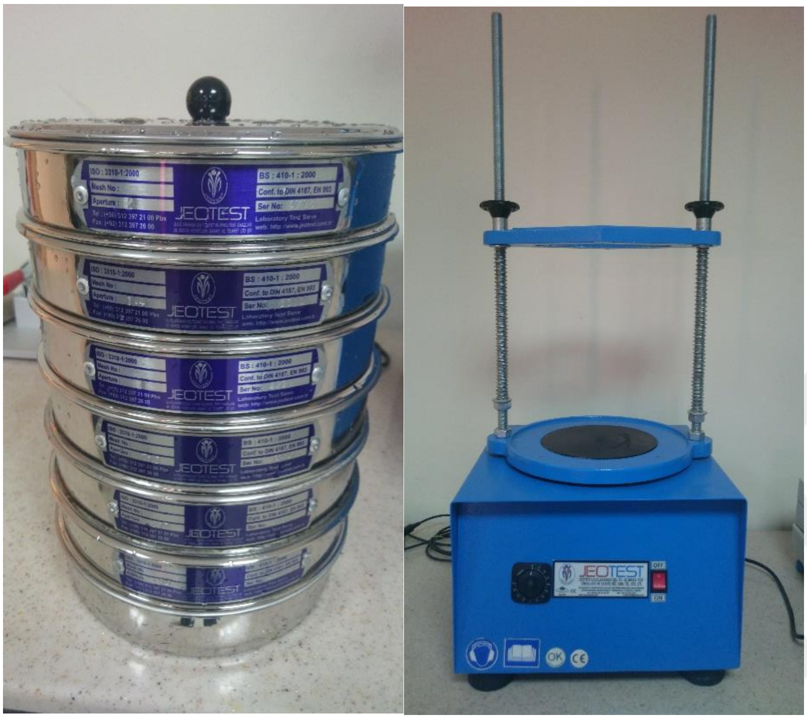

Figure 3.6. Sieve process and analysis

After the sieving process the grounded end sieved OP is ready for being a reinforcement filler for (OP)p/VE composites as seen in Figure 3.7.

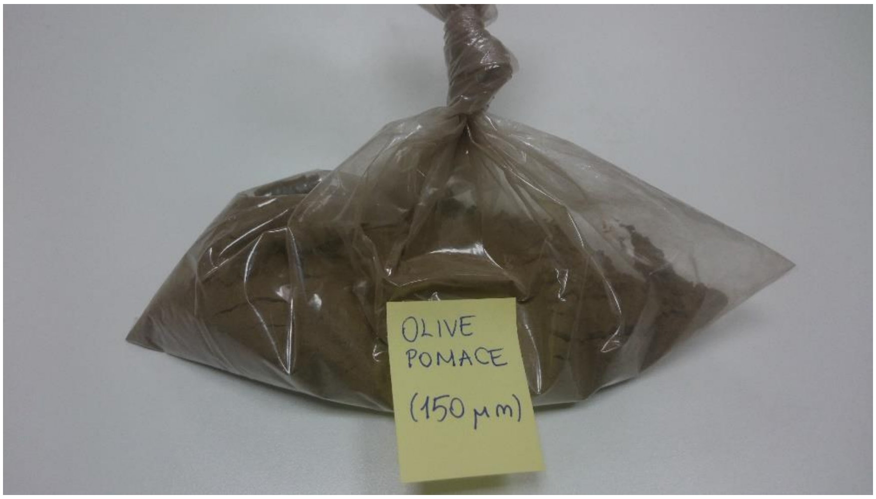

Figure 3.7. Olive Pomace - 150 μm

3.2. Methods

3.2.1. Preparation of Samples

The composite samples have different amount of olive pomace. The proportion of pomace used included, 0%, 5%, 10% and 20% (w/w). Figure 3.8 shows the process flow chart for the steps followed in preparation of the (OP)p/VE composites.

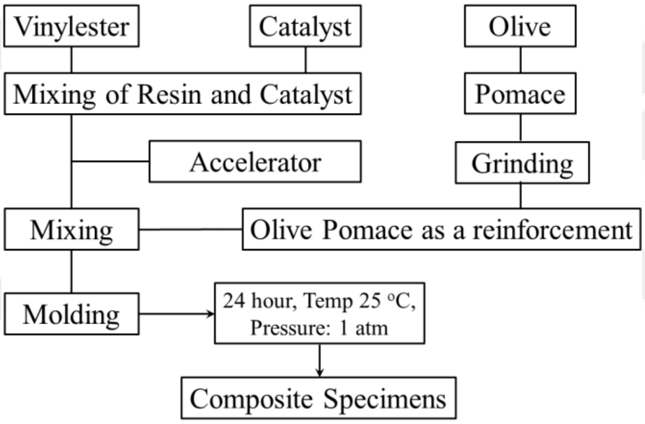

Figure 3.8. Steps for preparing the (OP)p/VE composites

For every specimen in this study, it has been prepared 125-gram mixtures, which can be seen in Figures 3.9 and 3.10, as weight to weight ratios are detailed below:

- VE(%0 OP w/w) = 125 gr Vinylester only,
- (OP)p/VE (%5 OP w/w) = 118,75 gr Vinylester and 6,25 gr Olive Pomace,
- (OP)p/VE (%10 OP w/w) = 112,5 gr Vinylester and 12,5 gr Olive Pomace,
- (OP)p/VE (%20 OP w/w) = 100 gr Vinylester and 25 gr Olive Pomace.

Figure 3.9. Olive Pomace as reinforcement

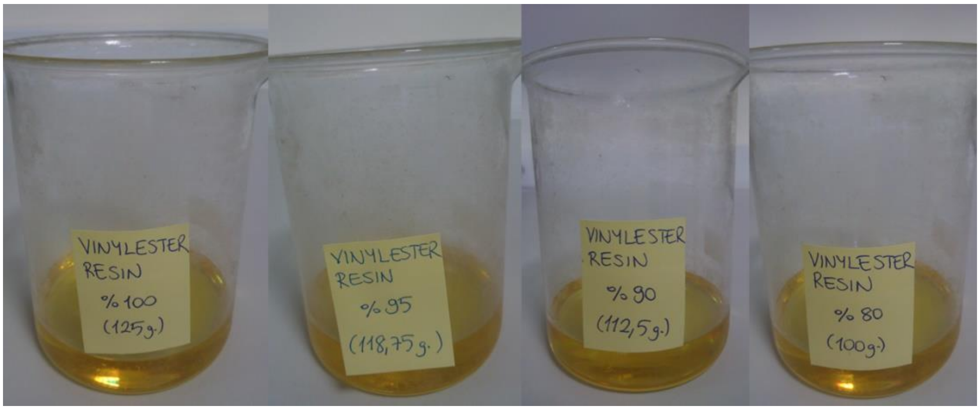

Figure 3.10. Vinylester resin as matrix

Open molding method was used to prepare the composite samples. This mold assembly consisted of two parts: mold base and mold top as shown in Figure 3.11. Mold drawings are made in Autodesk^{TM} Inventor.

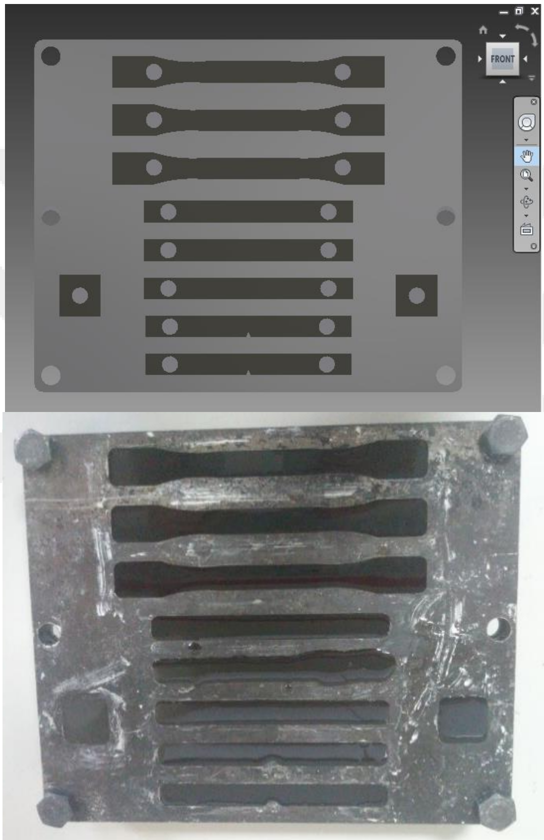

Figure 3.11. Mold (Drawing and base)

The mold was coated with a mold release wax, Polivaks SV-6 which can be seen in Figure 3.12.

Figure 3.12. Mold release agent

3.2.1.1. The test specimens

3.2.1.1.1. The specimens of tensile test

Three specimens were prepared from each mixture which consist of %0, %5, %10 and %20 OP w/w (Figure 3.13.a-d). According to the ASTM D638 – 14 which is explained in detail in section 2.4.1.1. The edges and harsh surfaces were polished with 1000 silicon carbide paper.

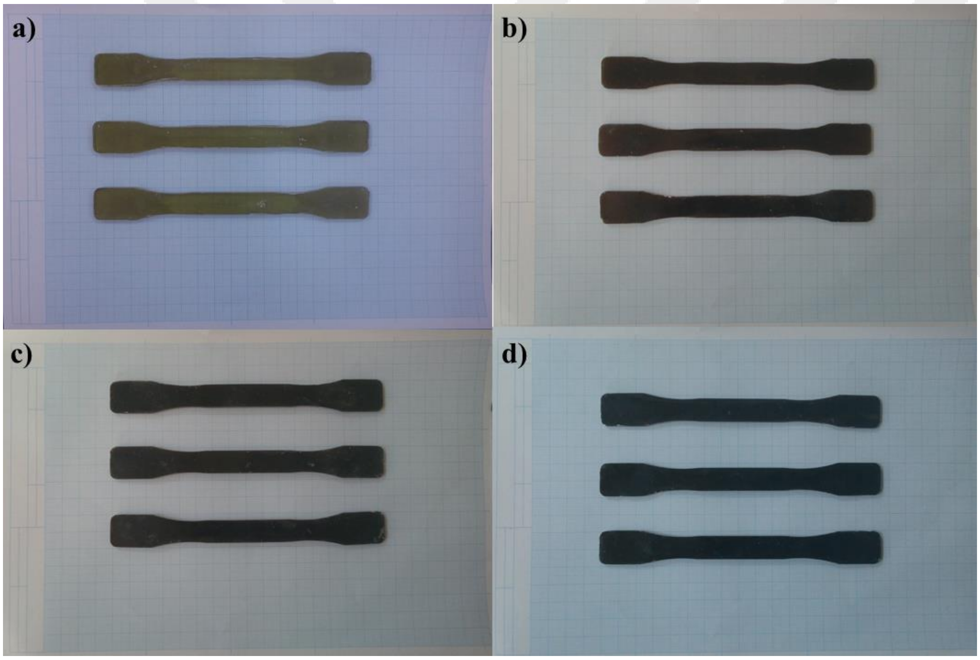

Figure 3.13. a) VE, %0 OP w/w b) (OP)p/VE, %5 OP w/w c) (OP)p/VE, %10 OP w/w d) (OP)p/VE, %20 OP w/w

3.2.1.1.2. The specimens of flexural test

Three specimens were prepared from each mixture which consist of %0, %5, %10 and %20 OP w/w (Figure 3.14.a-d). According to the ASTM D790 – 17 which is explained in detail in section 2.4.2.1. The edges and harsh surfaces were polished with 1000 silicon carbide paper.

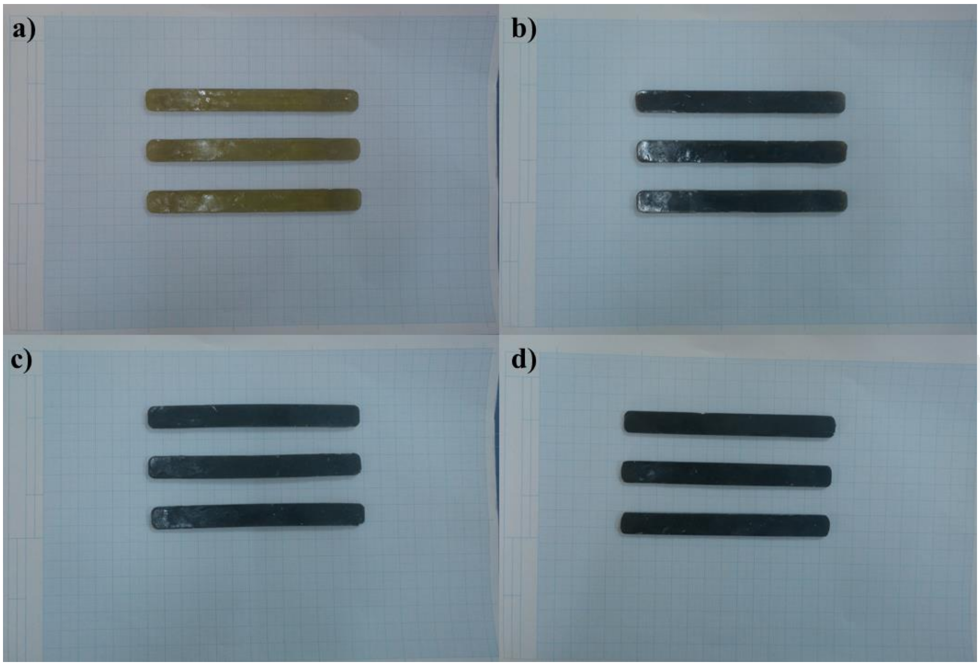

Figure 3.14. a) VE, %0 OP w/w b) (OP)p/VE, %5 OP w/w c) (OP)p/VE, %10 OP w/w d) (OP)p/VE, %20 OP w/w

3.2.1.1.3. The specimens of microhardness test

Three specimens were prepared from each mixture which consist of %0, %5, %10 and %20 OP w/w (Figure 3.15.a-d). According to the ASTM D785 – 08(2015) which is explained in detail in section 2.4.3.1. The edges and harsh surfaces were polished with 1000 silicon carbide paper.

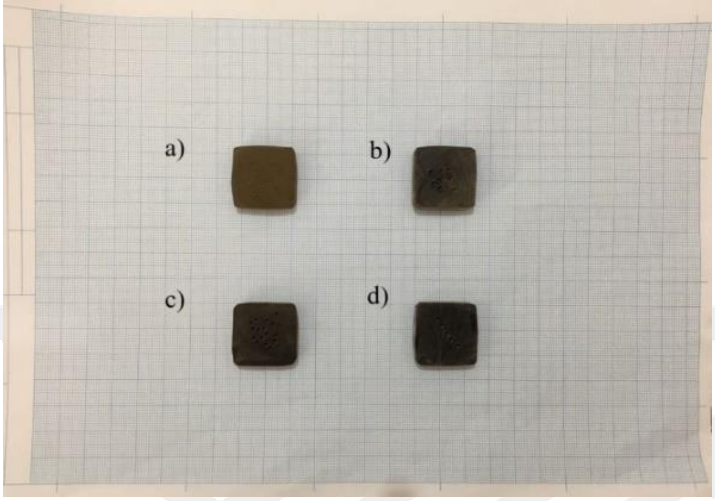

Figure 3.15. a) VE, %0 OP w/w b) (OP)p/VE, %5 OP w/w c) (OP)p/VE, %10 OP w/w d) (OP)p/VE, %20 OP w/w

3.3. Experimental Investigations

The experimental investigations are held in the laboratories of Aydın Adnan Menderes University in Aydın and Dokuz Eylül University in İzmir with the test machines in Figure 3.16.

Figure 3.16. The testing machines

3.3.1.Tensile Testing of (OP)p/VE

Tensile test measures the force required to break the specimen and the extent to which the specimen stretches or elongates at breaking point subjected to tension. Tensile tests produce force- displacement and stress-strain diagrams, which are used to determine tensile modulus. The data is generally used to characterize a material, to design a part to withstand applied force and as a quality control check of composite materials. Due to the physical properties of much of the composite materials (especially thermoplastics) can differ depending on ambient temperature.

Shimadzu AG-X series testing machine (Shimadzu Corporation, Kyoto, Japan) was used to carry out the tensile testing of (OP)p/VE composites (used in the Dokuz Eylül University’s laboratories with the permission of the Mechanical

Engineering Department, Dokuz Eylül University.) with a load cell of 100kN with a maximum speed of 2mm/min. The test was conducted in accordance with American standard methods, ASTM D638 – 14 (Anonymous, 2014a), for measurement of the for tensile properties of plastics. Figures 3.17 and 3.18 show the testing equipment and the tensile test claws (including the specimen after the tensile loading) respectively.

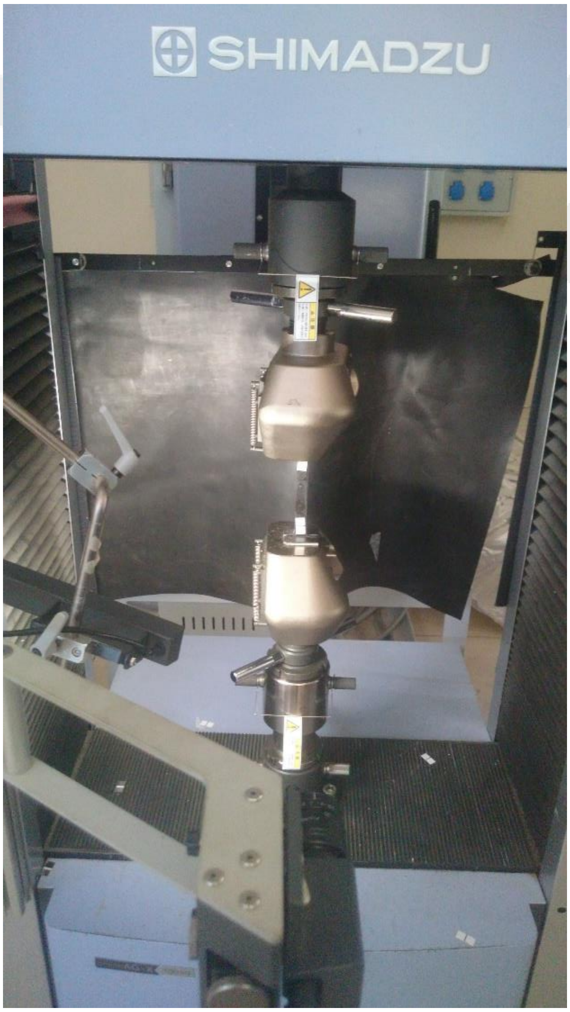

Figure 3.17. Tensile testing equipment

Figure 3.18. The specimen after the tensile loading

The force-displacement values were recorded during the test (Figure 3.19), then imported the data into an excel spreadsheet to calculate and acquire plots of tensile stress (σ) vs. strain (ε). The following equations (Equations 3.1 and 3.2) were used to calculate the tensile stress and tensile strain (Wambua, et al., 2003):

$$\sigma = \frac{F}{A}$$ (A = W x T in section 2.4.2.1) (Eq.3.1)

$$\varepsilon = \frac{\Delta L}{L}$$ (Eq.3.2)

Where;

σ = tensile stress (MPa).
ε = tensile strain (mm/mm)
F = load (N).
A = cross sectional area.
W = initial average width of the specimen (mm).
T = initial average thickness of the specimen (mm).
L = gauge length (mm).
ΔL = change in the length (mm).

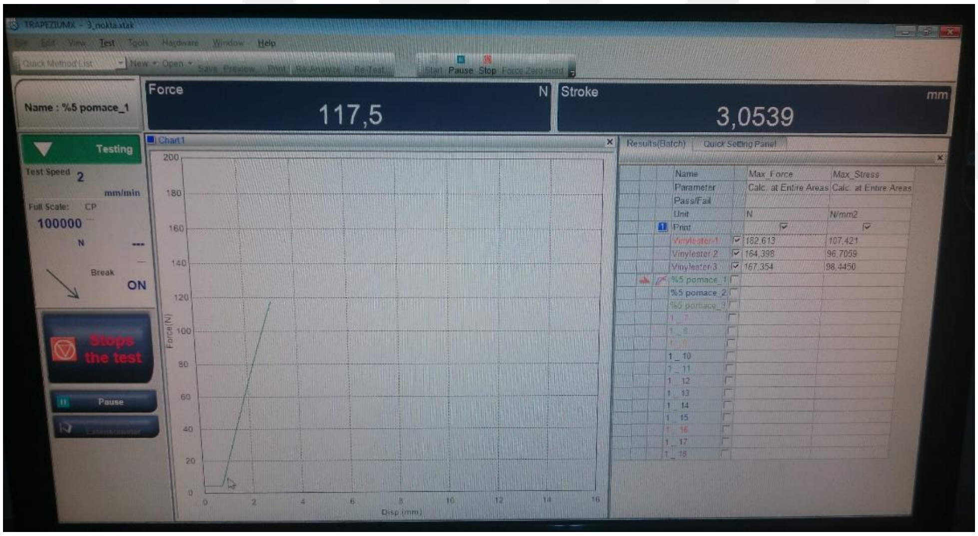

Figure 3.19. Test computer interface

3.3.2. Flexural Testing of (OP)p/VE

3-point bending test was carried out on (OP)p/VE composite specimens with different amount of OP w/w, according to testing standard ASTM D790 – 17 (Anonymous, 2017a). In this test, the specimen lies on a support span and the load is applied to the midpoint by the loading nose producing 3-point bending, at a specified rate of 2 mm/min. Each specimen was designed to have the specified dimensions, which described in section 2.4.2.1. Shimadzu AG-X series testing machine (Figure 3.20) was used to conduct flexural testing, with the permission of the Mechanical Engineering Department, Dokuz Eylül University.

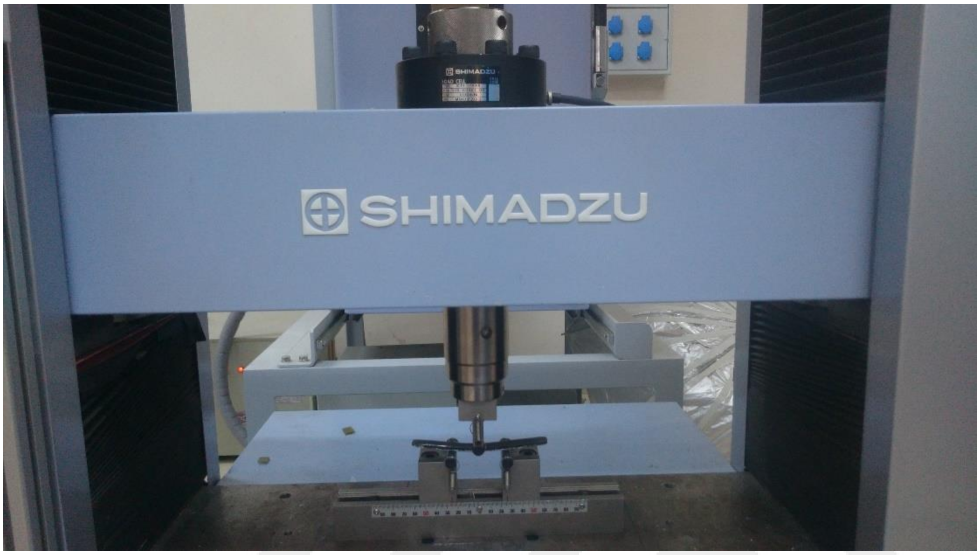

Figure 3.20. Flexural testing equipment

The machine was equipped with the flexural test apparatus after the tensile test. It was possible to adjust the span of the apparatus to provide for specimens of different thicknesses. Figures 3.20 and 3.21 show pictures of the equipment and the test apparatus (loading nose and supports) respectively.

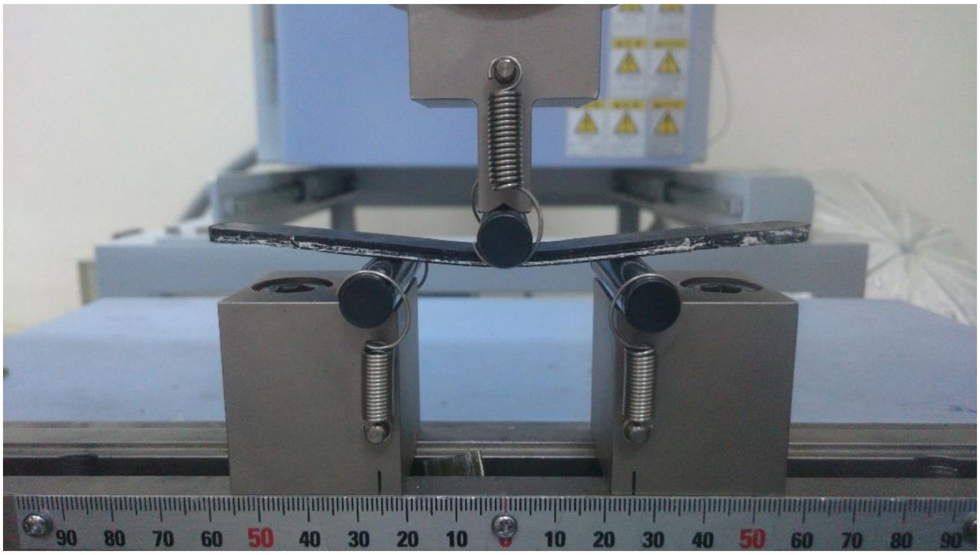

Figure 3.21. The specimen during the flexural loading

The load-deflection values were recorded during the 3-point bending test. It was then possible for the equipment software to provide plots of flexural stress (σ_f) vs. flexural strain (ε_f) as well as values for the flexural modulus (E_f). The software used the following equations (Equations 3.3, 3.4 and 3.5) to calculate the flexural stress, strain and modulus (Hastings et al., 2008):

$$\sigma_f = \frac{3FL}{2WD^2} \quad \text{(Eq.3.3)}$$

$$\varepsilon_f = -\frac{6dD}{L^2} \quad \text{(Eq.3.4)}$$

$$E_f = \frac{L^3 m}{4WD^3} \quad \text{(Eq.3.5)}$$

Where;

σ_f = flexural stress at center (MPa).
ε_f = flexural strain in the outer surface (mm/mm).
E_f = flexural Modulus of elasticity, (MPa).
F = load at a given point on the load deflection curve (N).
L = distance between the support spans (mm).
W = initial average width of the specimen (mm).
D= depth of the specimen
d = maximum deflection of the center of the beam, (mm).
m = gradient of the initial straight-line portion of the load deflection curve, (N/mm).

3.3.3. Microhardness Testing of (OP)p/VE

Hardness is the physical property of a material that helps to measure the resistance to grating. Microhardness testing was carried out using the Vickers Rockwell & Brinell Hardness Testing machine BMS 200-RB supplied by BMS Bulut Makina as shown in Figures 3.22 and 3.23 (used in the Aydın Adnan Menderes University laboratories).

The calculation and equations were mentioned in section 2.4.3. in details.

Figure 3.22. Hardness testing machine

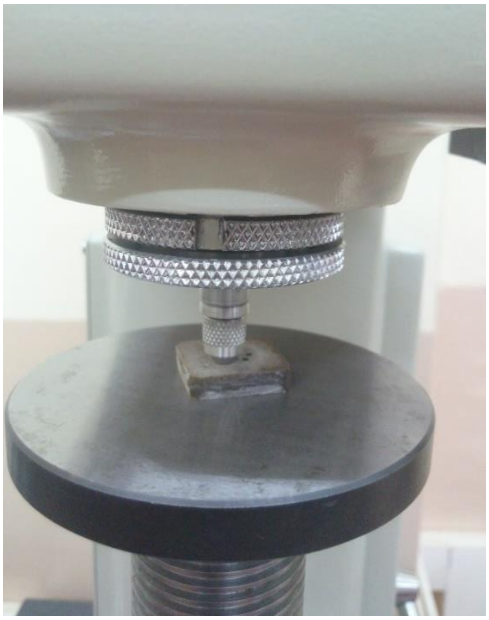

Figure 3.23. The specimen during the hardness test

3.3.4. Density Measurement

The density of the (OP)p/VE composites, for different weight fraction, has been determined using the experimental techniques, mentioned in Section 2.1.2.1. and the values have been compared with the theoretical Rule of Mixtures (ROM) equation (Eq.2.1). Table 3.4 presents the results of the density measurement for each weight fraction category of the composites. The density measurement was then calculated on four different specimens for each formulation.

Table 3.4. The results of the density measurement

Olive Pomace	Experimental densities	
w/w	Mean (g/cm^3)	STD
%0	4,40	0,078
%5	4,53	0,081
%10	4,60	0,082
%20	4,78	0,084

3.4. Finite Element Analysis of Charpy Impact Test

The analysis for Charpy impact test has been simulated by using ANSYS™ 17.2. Mechanical properties were used from the values driven from the experimental investigations in this study. Autodesk™ Inventor program was used to draw the test specimen, the anvils and the pendulum for the Charpy impact test according to ASTM D6110-18 (Anonymous, 2018a).

The initial condition which in transient structural analysis can be seen in Figure 3.24. and the crush moment within the standard earth gravity can be seen in Figure 3.25 respectively.

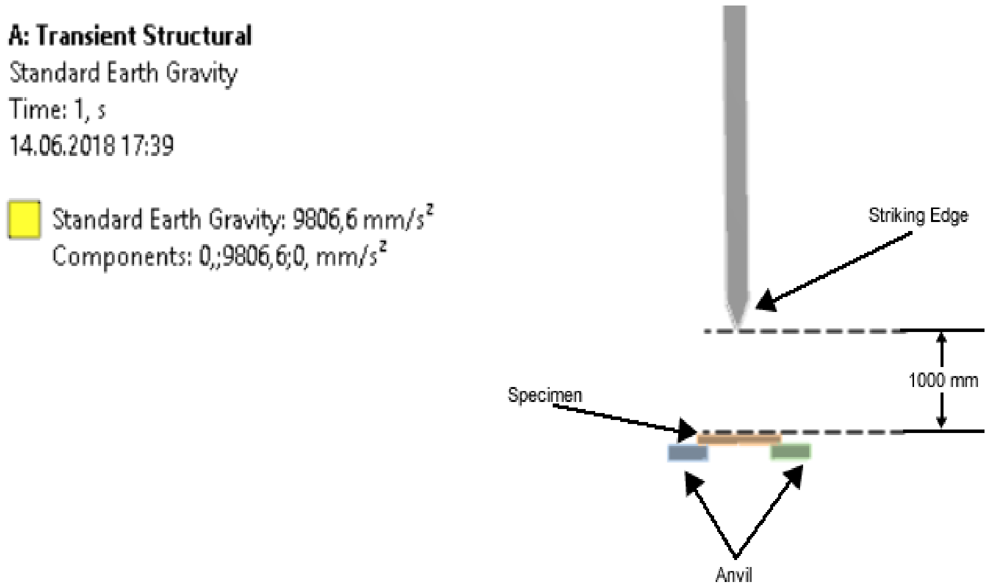

Figure 3.24. The initial condition of Charpy analysis

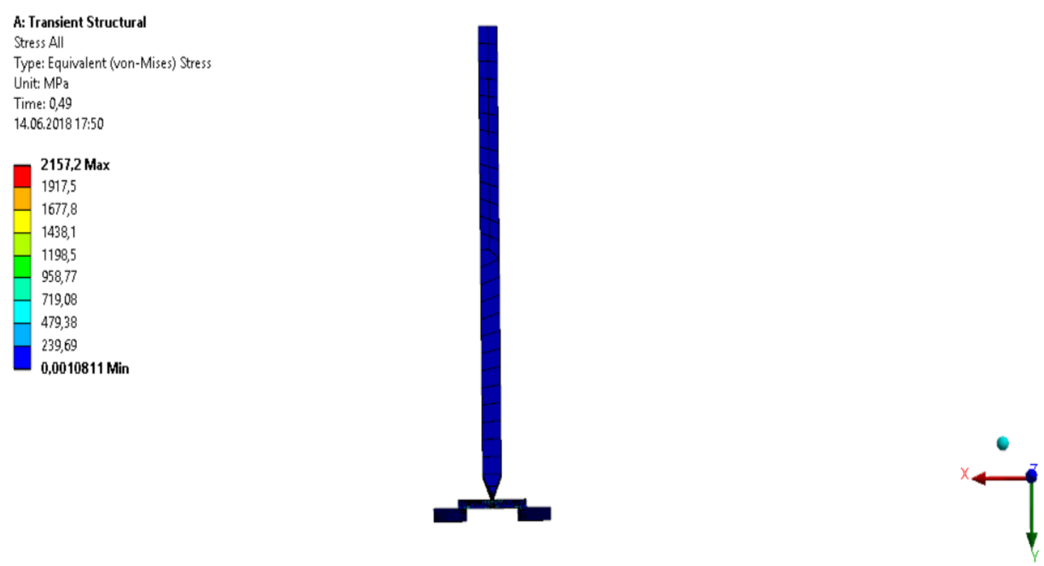

Figure 3.25. The impact moment

The simulation ran for the Charpy impact analysis in the transient structural of ANSYS. The strain values were recorded in the meshing parts of the specimens.

4.RESULTS AND DISCUSSION

In this chapter, it was presented and discussed the findings of the experiments and investigated the influence of OP on the crack initiation and propagation with the fracture mechanisms because of weak or strong fiber/matrix bond. It is considered the importance of the factors to get from the experimental findings and it also provides a link between the tests and the analysis.

4.1. Results

To achieve reliable results, it is very important to provide that the specimens produced have been prepared in accordance the relevant standards and methods under same conditions.

All specimens produced for the different tests have been precisely controlled for defects to make sure high-quality specimens have been produced. In this process various types of defects in the specimen preparation process have been found. These include defects like excessive localized voids, non-uniform thickness, surface defects, non-uniform distribution of olive pomace particles in the composites. High stages of such defects may significantly decrease the mechanical properties of the specimens.

Therefore, it was important to notice and eliminate the faulty specimens from the findings. However, not all preparation defects were noticed at the initial stage of this study and subsequently immature specimen failures were monitored.

4.1.1. Physical Properties of (OP)p/VE Samples

The structure of (OP)p/VE composites is quite complex. Olive pomace can be considered to have properties like wood, which consists of mostly cellulose, hemicellulose and lignin.

Cellulose is the dominant contributor to the harshness of the wood and is a linear polysaccharide polymer. Lignin fills the blanks between the cellulose and other compounds to give mechanical strength to wood and plays an important part in conducting water (Shiryaev et al., 2007). The physical appearances are described as follows:

- VE, %0 OP w/w is transparent, greenish yellow color and very smooth on the surface.
- (OP)p/VE, %5 OP w/w is semitransparent, greenish brown color and smooth on the surface
- (OP)p/VE, %10 OP w/w is not transparent, brownish khaki color and smooth on the surface.
- (OP)p/VE, %20 OP w/w is not transparent, dark brown color and a little rough on the surface.

4.1.2. Tensile Testing Results of (OP)p/VE Samples

The tensile stress - strain results for (OP)p/VE composites, including (OP) content are shown in Table 4.1. The mean and standard deviation values for the relevant tensile properties, including maximum force and ultimate (maximum) tensile stress (UTS) are presented.

Table 4.1. The results of tensile testing

Specimen	Max Force (Mean)	STD	Max Stress (Mean)	STD
Unit	(N)		(N/mm^2)	
VE - %0 OP	1309,613	35,70	35,470	7,89
(OP)p/VE - %5 OP	1330,350	51,69	31,258	1,21
(OP)p/VE - %10 OP	1000,018	74,22	23,497	1,74
(OP)p/VE - %20 OP	900,682	63,21	21,163	1,49

Relevant obtained stress – strain diagrams based on three specimens of each weight fractions of (OP)p/VE composites are summarized in between Figures 4.1 to 4.4. These diagrams were consolidated from the stress – strain diagrams of each individual specimen in Appendix A (Figures A.13 – 24)

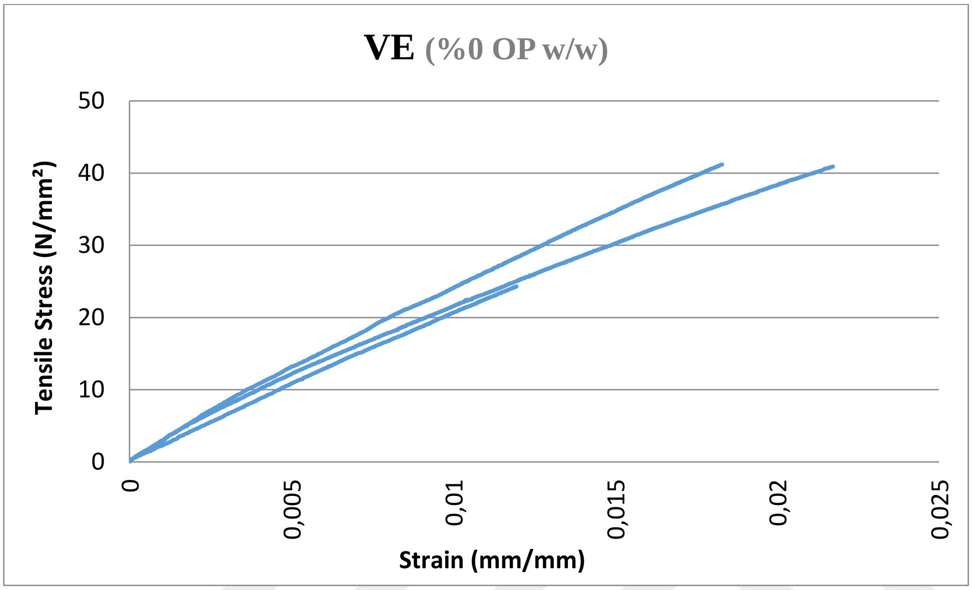

Figure 4.1. The tensile results of the specimens - VE (%0 OP w/w)

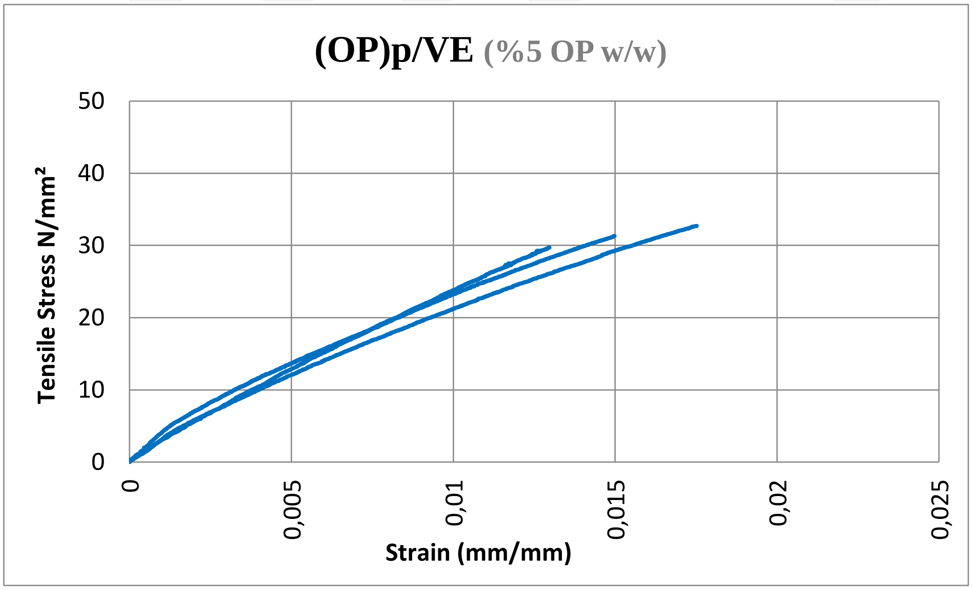

Figure 4.2. The tensile results of the specimens – (OP)p/VE (%5 OP w/w)

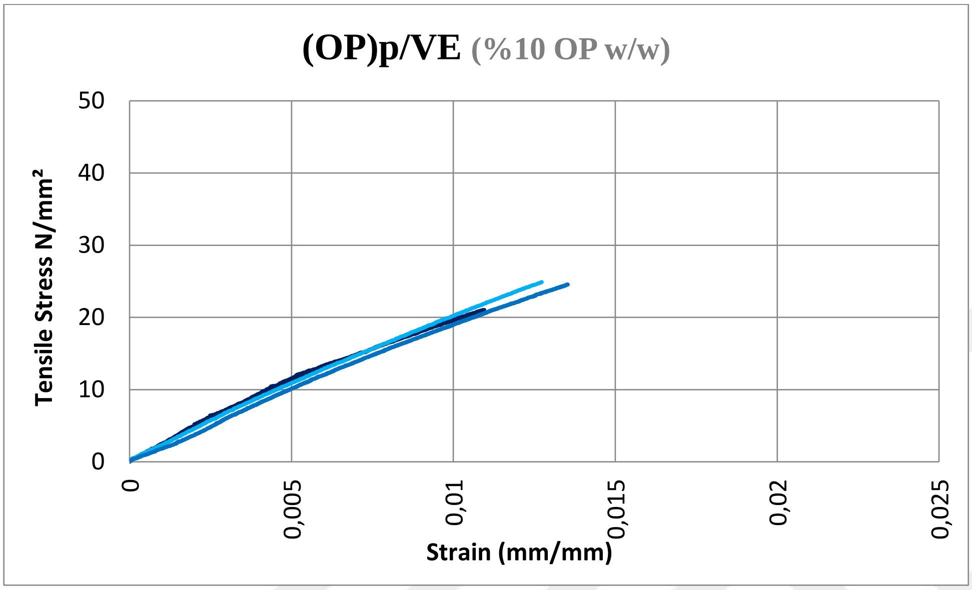

Figure 4.3. The tensile results of the specimens – (OP)p/VE (%10 OP w/w)

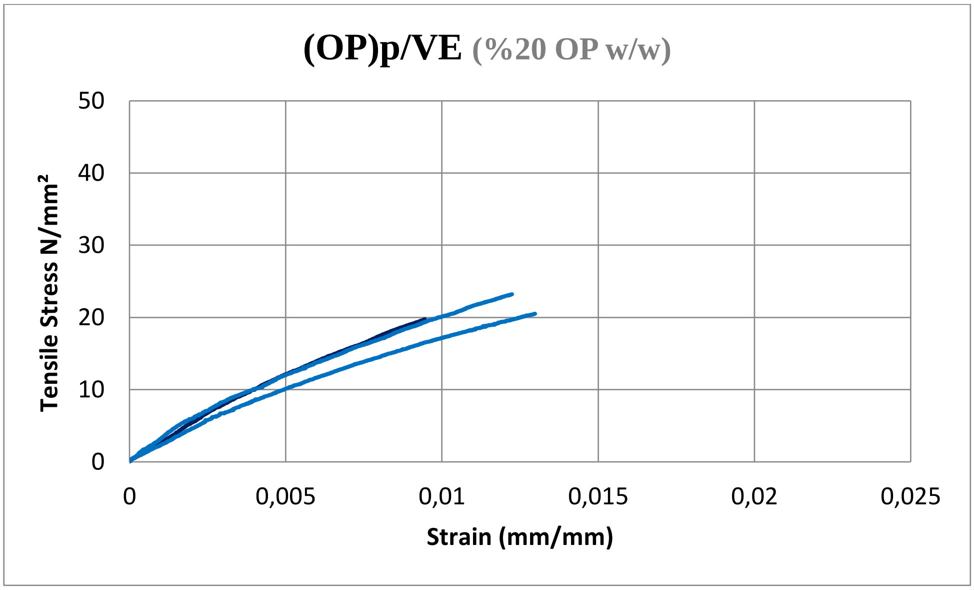

Figure 4.4. The tensile results of the specimens – (OP)p/VE (%20 OP w/w)

Table 4.2 shows the mean Elastic force values for each weight fractions of (OP)p/VE composites that are later used in the formulation in ANSYS.

Table 4.2. The values of Elastic force

Specimen	Elastic Modulus (Mean)	STD
Unit	(N/mm^2)	
VE - %0 OP	2748,650	63,85
(OP)p/VE - %5 OP	2762,333	51,24
(OP)p/VE - %10 OP	2524,150	34,87
(OP)p/VE - %20 OP	2406,317	73,83

The force – displacement diagrams of tensile tests can be seen in Appendix A (Figures A.1 -12)

4.1.3. Flexural Testing Results of (OP)p/VE Samples

The flexural stress - strain results for (OP)p/VE composites, including (OP) content are shown in between Figures 4.5 to 4.8. The mean and standard deviation values for the relevant flexural properties, including maximum force and maximum flexural stress are presented in Table 4.3.

Table 4.3. The mean and standard deviation values in flexural tests

Specimen	Max Force (Mean)	STD	Max Stress (Mean)	STD
Unit	(N)		(N/mm^2)	
VE - %0 OP	171,455	7,98	100,857	4,70
(OP)p/VE - %5 OP	146,442	6,85	86,144	4,03
(OP)p/VE - %10 OP	93,052	2,61	54,737	1,54
(OP)p/VE - %20 OP	82,699	8,57	48,648	5,04

Relevant obtained stress -strain diagrams based on three specimens of each weight fractions of (OP)p/VE composites are summarized in between Figures 4.5 to 4.8. These diagrams were consolidated from the stress – strain diagrams of each individual specimen in Appendix B (Figure B.13 – 24)

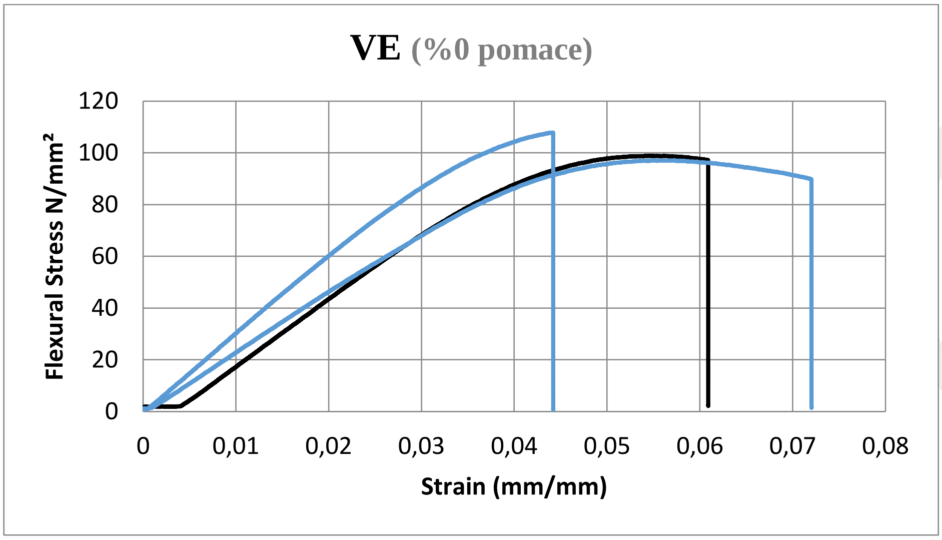

Figure 4.5. The flexural results of the specimens - VE (%0 OP w/w)

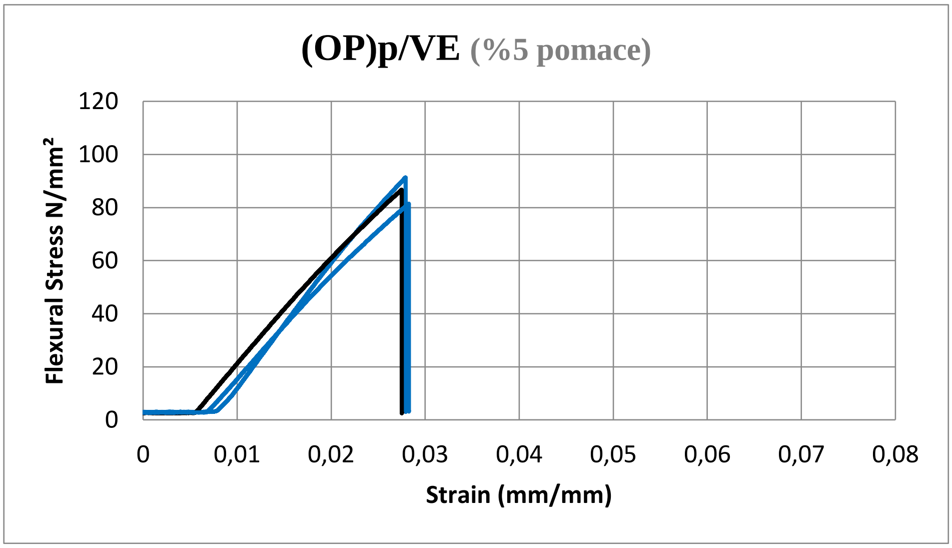

Figure 4.6. The flexural results of the specimens – (OP)p/VE (%5 OP w/w)

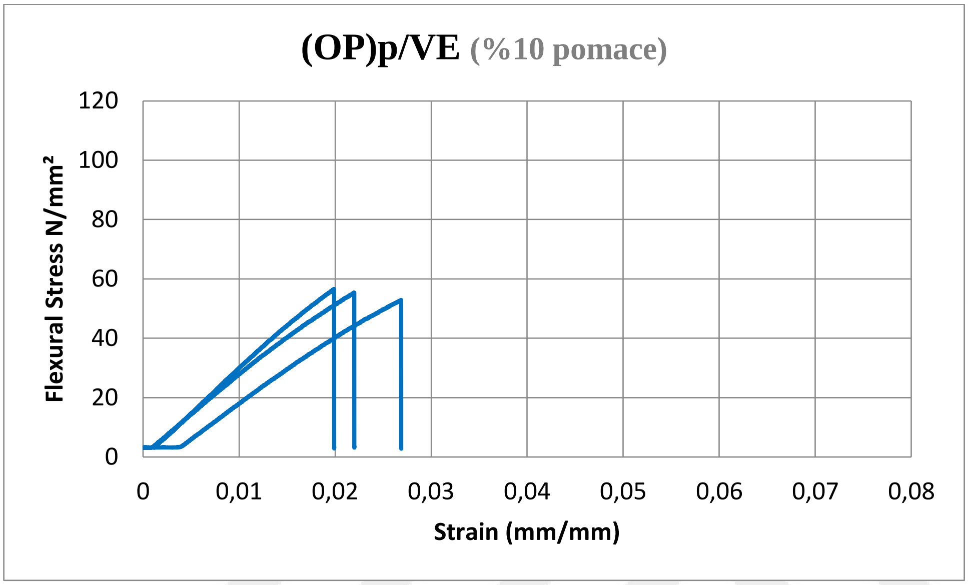

Figure 4.7. The flexural results of the specimens – (OP)p/VE (%10 OP w/w)

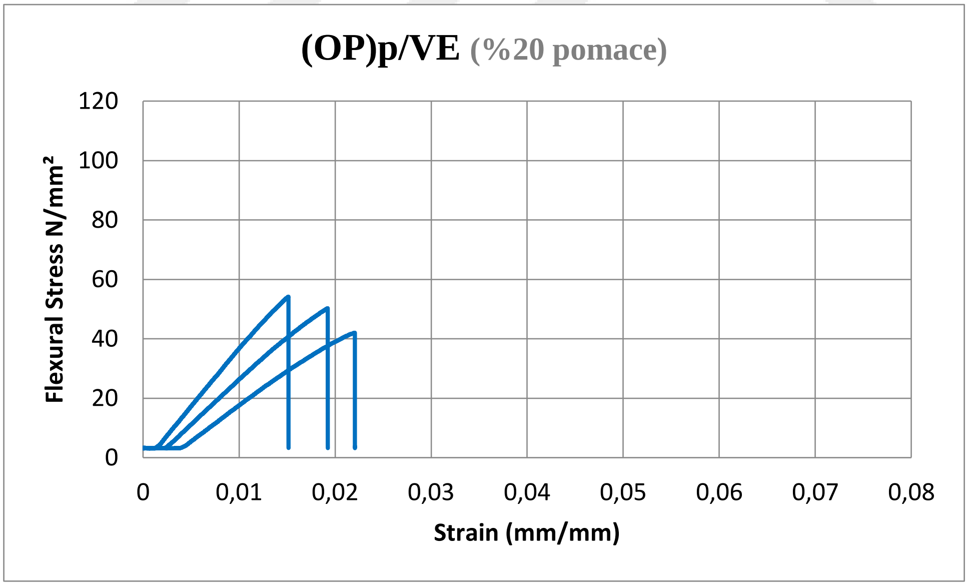

Figure 4.8. The flexural results of the specimens – (OP)p/VE (%20 OP w/w)

The force – displacement diagrams of flexural tests can be seen in Appendix B (Figures B.1 – 12).

4.1.4. Microhardness Testing Results of (OP)p/VE Samples

In this study, the R scale of Rockwell hardness test (HRR) was used to measure the microhardness valued of the (OP)p/VE composite specimens. The mean and standard deviation values of the microhardness test results for the composite specimens with different weight fractions of OP are presented in Table 4.4.

Table 4.4. The values of hardness test for the specimens

	VE %0 OP w/w	(OP)p/VE %5 OP w/w	(OP)p/VE %10 OP w/w	(OP)p/VE %20 OP w/w
e	22,4	31,6	36,6	41,2
e	25,0	34,8	39,1	38,4
e	23,0	37,5	32,3	41,4
e	22,9	34,0	34,6	44,1
e	26,0	35,0	36,2	47,3
e	28,0	35,2	37,5	41,6
e	27,4	32,0	34,0	42,0
e	26,0	35,4	35,4	44,8
e	24,0	38,0	36,5	43,7
e	25,0	34,1	39,0	39,6

After calculating with the Eq.2.3, it is observed that when olive pomace particles are used in vinylester, the hardness decreases by approximately %7,3, %8,9 and %13,94 for %5, %10 and %20 w/w (OP)p/VE composites respectively (Table 4.5). The lower the number means the softer the specimens are.

Table 4.5. The Rockwell hardness values

Specimen	α HR (Mean)	STD
VE - %0 OP	125,03	1,91
(OP)p/VE - %5 OP	115,24	2,04
(OP)p/VE - %10 OP	113,88	2,14
(OP)p/VE - %20 OP	107,59	2,61

This test does not serve well as a predicter such as strength or resistance to scratches, abrasion or wear and should not be used alone for product design specifications. It is used to measure the hardness of (OP)p/VE composites resistance to penetration.

4.2. Charpy Test Analysis

As described in Section 3.4. The analysis for Charpy impact test has been simulated by using ANSYS^{TM} 17.2. The data for the specimens were derived from experimental results. Like in Figure 4.10, all data related to specimens in the Table 4.6 were formulated in the transient structural analysis of (OP)p/VE composites' Charpy tests.

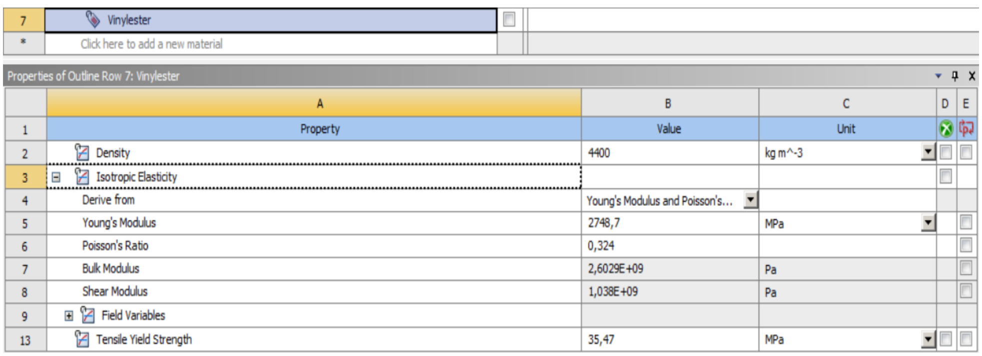

Figure 4.9. The computer interface of ANSY for the properties

Table 4.6. The experimental properties of the specimens

Name	Young's Modulus	Tensile Yield Stress	Density
Unit	(N/mm^2)	(N/mm^2)	(kg/m^3)
VE - %0 OP	2748,650	35,470	4400
(OP)p/VE - %5 OP	2762,333	31,258	4533
(OP)p/VE - %10 OP	2524,150	23,497	4600
(OP)p/VE - %20 OP	2406,317	21,163	4778

In structural materials the strain energy is as the energy which is stored within a material when work has been done on the material. The strain energy stored in a material upon deformation is calculated below for a number of different geometries and loading conditions as Equation 4.1 (Kelly, 2013). These expressions for stored energy then were used for the function relates the energy stored in an elastic material, and thus the stress–strain relationship.

$$U = \frac{1}{2}V\sigma\varepsilon = \frac{1}{2}VE\varepsilon^2 = \frac{1}{2}VE\sigma^2 \qquad \text{(Eq.4.1)}$$

Where;

σ = stress (MPa).
ε = strain (mm/mm).
V= Volume (m^3)
E = Young's Modulus (MPa).
U = Strain Energy (Joule or Nm or Pam^3).

The Ansys results, which can be seen in Figures 4.11 to 4.14, show that the Strain Energy and the experimental results are match up with each other.

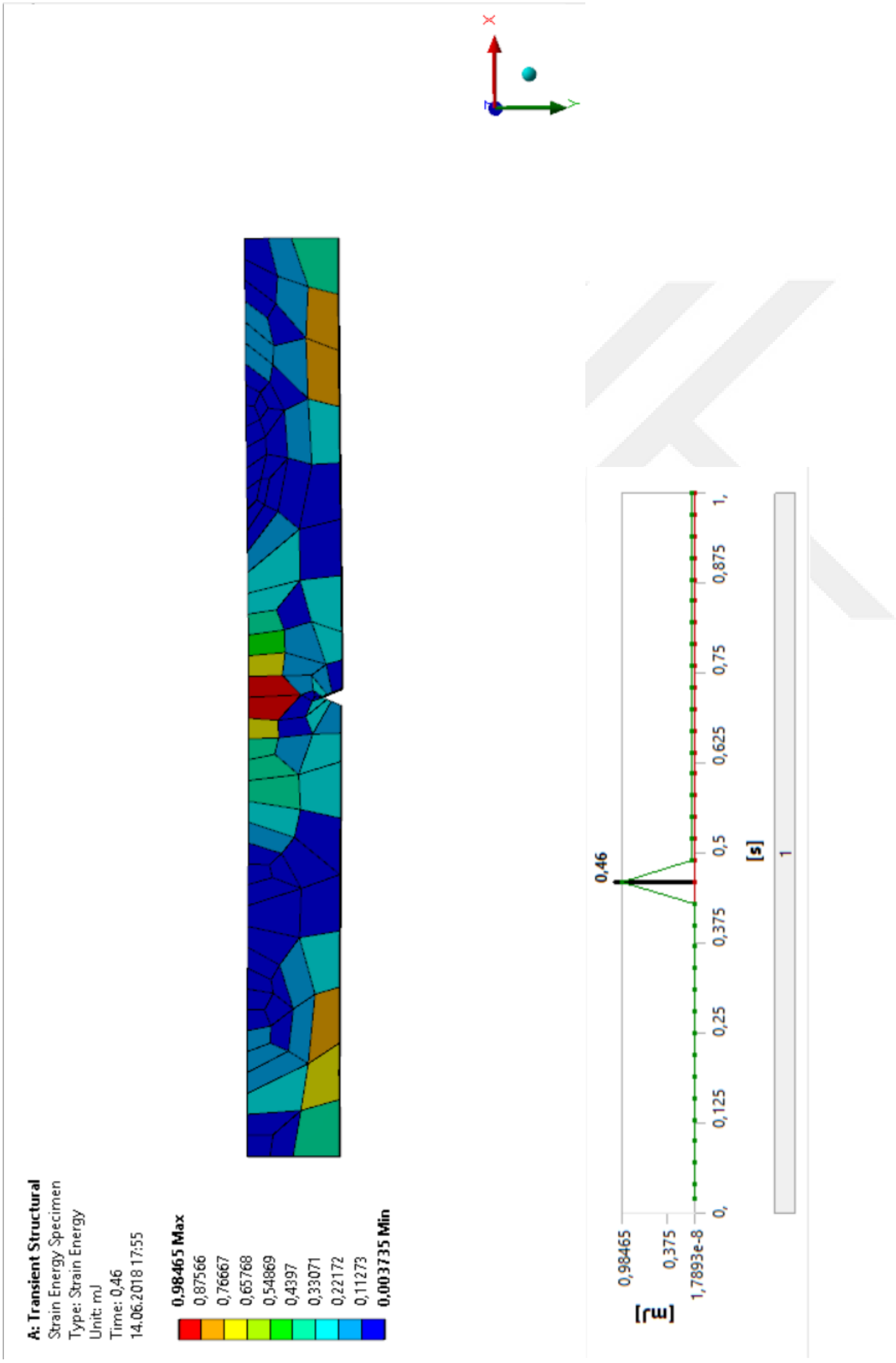

Figure 4.10. Charpy analysis of VE (%0 OP w/w)

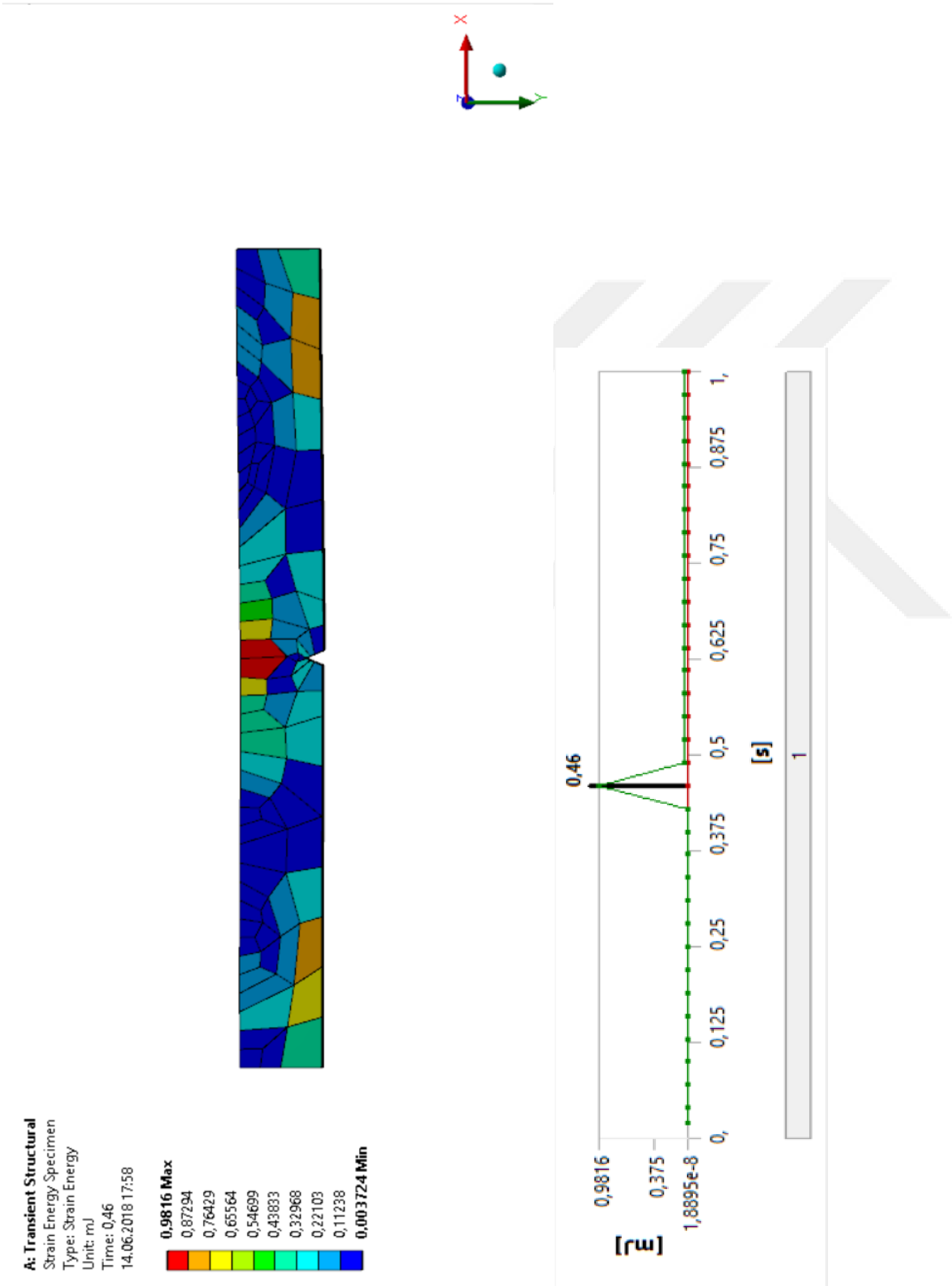

Figure 4.11. Charpy analysis of (OP)p/VE (%5 OP w/w)

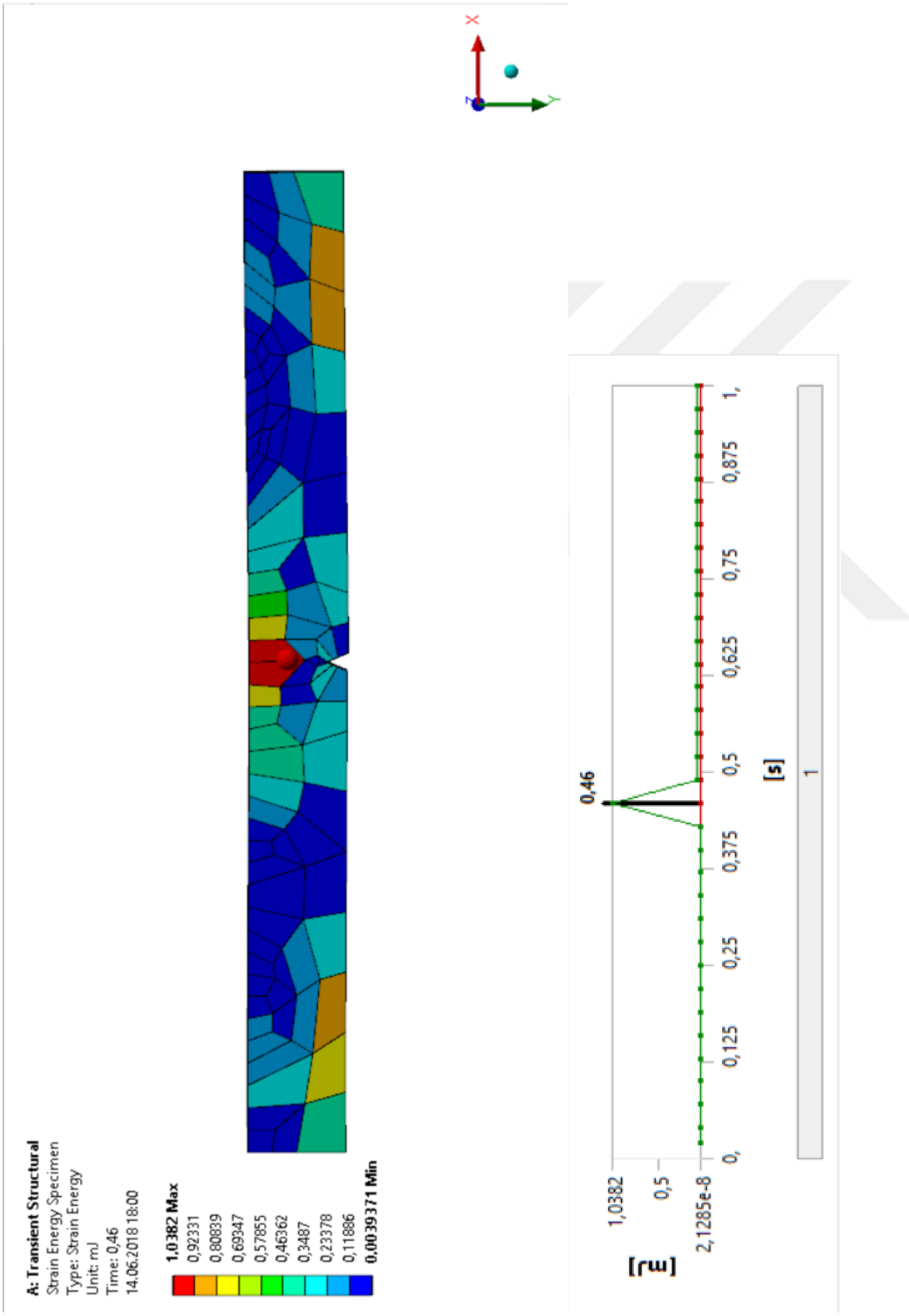

Figure 4.12. Charpy analysis of (OP)p/VE (%10 OP w/w)

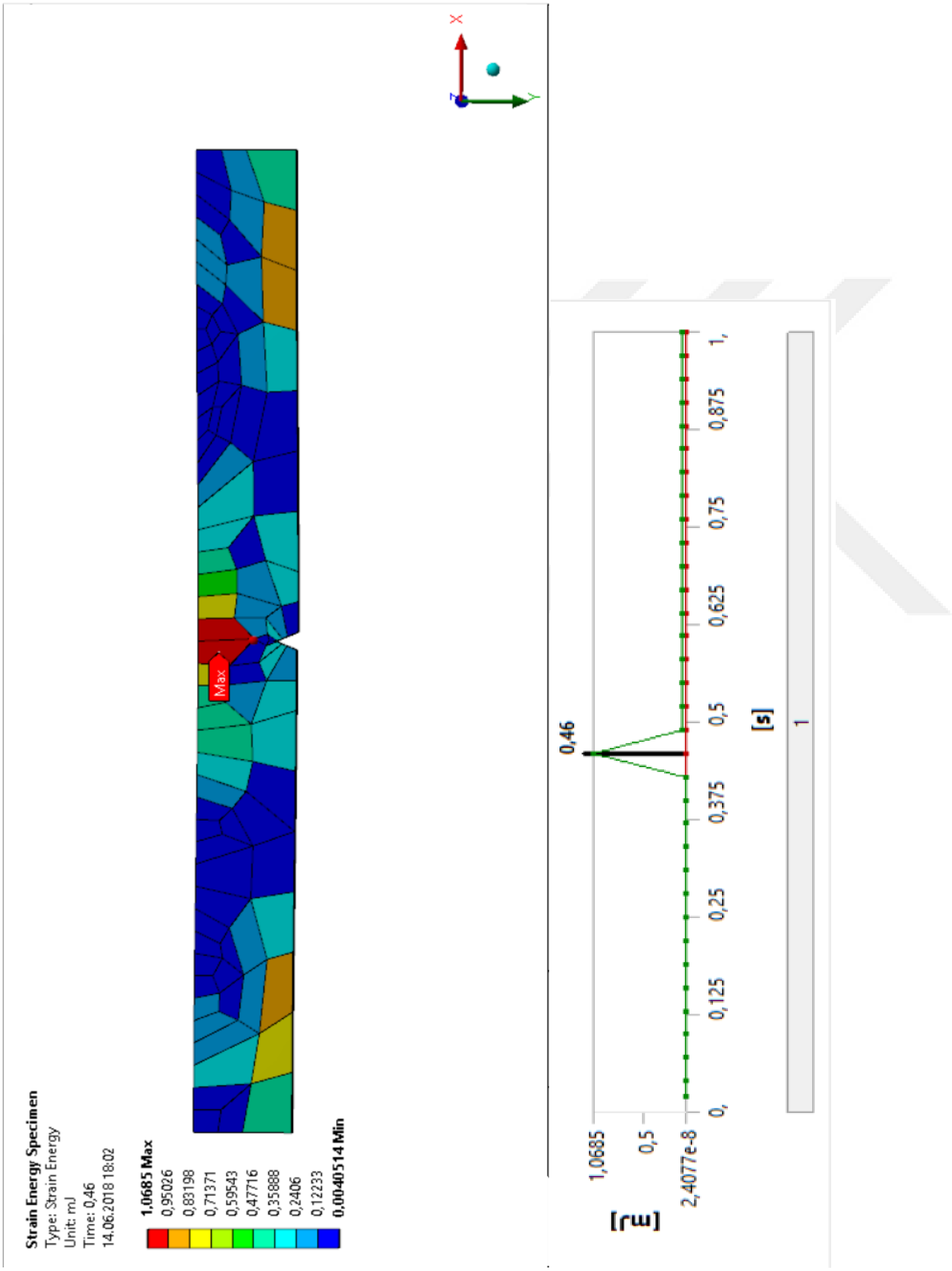

Figure 4.13. Charpy analysis of (OP)p/VE (%20 OP w/w)

After analyzing with ANSYS, it is observed that when olive pomace particles are used in vinylester, the strain energy increases by approximately %5,44 and %8,52 for %10 and %20 w/w (OP)p/VE composites respectively and on the contrary it decreases by slightly %0,30 for %5 (OP)p/VE (Table 4.7).

Table 4.7. ANSYS values of Maximum strain energy

Specimen	Maximum Strain Energy (mJ)
VE - %0 OP	0,9846
(OP)p/VE - %5 OP	0,9816
(OP)p/VE - %10 OP	1,0382
(OP)p/VE - %20 OP	1,0685

5. CONCLUSIONS

5.1. Conclusions

The influence of olive pomace particles as a reinforcing material for vinylester resin has been investigated in detail using different mechanical analysis techniques, including tensile, flexural and microhardness tests. The process of the crack initiation and propagation of the composite materials, subjected to impact loading, which has been investigated using FEM with ANSYS.

The differences in the results have been related to the amount of OP in the (OP)p/VE composites include, %0, %5, %10 and %20.

The following conclusions are based on the findings of this study which summarizes the damage and failure in the composites:

- The average density of the (OP)p/VE composite specimens have been measured. The experimental density values for the specimens have been found to be increasing with the increase of reinforcement (by approximately %2,95, %4,54 and %8,41 for 5%, 10% and 20% w/w than %0 (OP)p/VE respectively). The improvement in the density is due to the adding of olive pomace particles.
- Tensile test results indicate improvement in tensile strength and tensile modulus values only for %5 (OP)p/VE specimen according to VE (%0 OP w/w), with %1,58 improvement in tensile strength and %0,49 improvement in tensile modulus respectively. However, the results indicate declines in tensile strength and tensile modulus values for %10 and %20 (OP)p/VE specimens, with %23,64 and %31,22 decline in tensile strength and %8,16 and %12,45 decline in tensile modulus respectively according to VE (%0 OP w/w). Only improvement (%0,49) in tensile modulus was achieved when %5 OP w/w particles was used, this is due to better particle/matrix interaction which leads to a stronger chemical interphase between matrix and the cellulose surface of the olive pomace. However, by increasing the OP to %10 and %20 w/w the tensile strength decreases by approximately %27. The reason for this may be due to the immense number of particles.

- Flexural test carried out on all the specimens show significant declines in the results when the vinylester resin is reinforced with olive pomace particles, with %14,58, %45,72 and %51,76 decline in flexural strength and stress for %5, %10 and %20 respectively according to VE %0 OP w/w. This is due to having higher percentage of olive pomace particles, higher void content and lower interfacial bonding.
- Microhardness test results show that the addition of olive pomace particles to the vinylester resin decreases the hardness of the vinylester resin by %7,83, %8,91 and %13,94 for %5, %10 and %20 respectively according to VE %0 OP w/w. This decrease in the hardness is due to declined stiffness on the surface of the specimens.
- ANSYS simulations results indicate improvements in the Charpy test for %10 and %20 (OP)p/VE specimens, with approximately %5,44 and %8,52 improvement in strain energy respectively according to VE (%0 OP w/w). However, the results indicate decline in tensile the Charpy test for %5 (OP)p/VE specimens with slightly % 0,30 decline in strain energy according to VE (%0 OP w/w).

5.2. Recommendations for Future Work

This study has provided fundamental data on the behavior of olive pomace particulate reinforced vinylester composites in fracture. It should be emphasized that the work that has been conducted is not exhaustive and a lot more information needs to be obtained on the behavior of plant based natural fiber composites under fracture loading. The trend towards adoption practices with low impact to the environment will in the future require more information on the performance of ‘ecofriendly’ products.

This study also has highlighted the significant changes – improvements and declines - in mechanical properties such as tensile and flexural strength, impact resistance and microhardness, when olive pomace particles is used as fillers to reinforce vinylester resin. The scope of this area should be investigated deeply and an extension of the quantitative approach on evaluation of the crack initiation to include a factor dependent on the bond strength. However further work is proposed to investigate, in more details, the interfacial effects of (OP)p/VE composites.

- It is recommended that more fracture tests be conducted that include other commercially useful natural fibers such as cotton, flax, hemp, sisal, jute, kenaf, henequen, corn, coconut, pineapple etc., to provide an extensive database of fracture data for natural fiber composites.
- The results presented in this study need to be translated into applications by combining (OP)p/VE composites into products currently in use. A study of the behavior of such products under fracture loading will give us useful information on the suitability of natural fibers as reinforcement material for polymeric matrices in applications.
- The current use of natural fibers in automobile interior parts is a very good example of how natural fiber composites can be utilized in current products. The mechanical properties of cellulosic or lignocellulosic fiber composites will lead to more natural fiber composite parts being specified in automobiles.
- It has been shown that the different amount of OP particles has resulted in different damage and fracture mechanisms of the specimens under tensile, flexural and impact loadings. It is therefore a reasonable proposition to investigate, more in detail, the different failure events occurring in the composites during the loading processes. It is therefore recommended to operate different tools to help in elaborating the damage process concerning ultrasonic scan and acoustic emission analysis. These techniques can possibly identify the initiation of crack within the specimen resulting crack propagation. For that reason, further work is required to analyze the different failure mechanisms with these operating in these materials.

REFERENCES

Abessalam, Q. 2011. Investigation into the modes of damage and failure in natural fibre reinforced epoxy composite materials. University of East London, Doctoral dissertation, London, UK.

Adams, D. F. 2006. Test Methods for Mechanical Properties In: Test Methods, Nondestructive Evaluation, and Smart Materials, Volume 5 of Comprehensive Composite Material. (Carlsson, L. et. al. Eds.), pp. 13-27, London, UK.

Andressen, F.R. 2001. Open Molding: Hand Lay-Up and Spray-Up In: A. S. M. Handbook Volume 21: Composites (Miracle, D. B., Donaldson, S. L. Eds), ASM International, pp. 450-451, Ohio.

Anonymous. 2004a. Polives™ 701, Product Technical Bulletin, doc.cod UTB Polipvesver 2004, www.poliya.com.tr, Last accessed in July 2018.

Anonymous. 2014a. ASTM D638-14, Standard Test Method for Tensile Properties of Plastics, ASTM International, West Conshohocken, PA, 2014, https://www.astm.org/Standards/D638.htm, Last accessed in July 2018.

Anonymous. 2015a. ASTM D785-08(2015), Standard Test Method for Rockwell Hardness of Plastics and Electrical Insulating Materials, ASTM International, West Conshohocken, PA, 2015, https://www.astm.org/Standards/D785.htm, Last accessed in July 2018.

Anonymous. 2016a. Olivae No: 123 English Ed. November 2016, **Official Journal of The International Olive Council**, pp. 8, Madrid, Spain.

Anonymous. 2017a. ASTM D790-17, Standard Test Methods for Flexural Properties of Unreinforced and Reinforced Plastics and Electrical Insulating Materials, ASTM International, West Conshohocken, PA, 2017, https://www.astm.org/Standards/D790.htm, Last accessed in July 2018.

Anonymous. 2017b. International Olive Council. (2017). The olive tree. http://www.internationaloliveoil.org/estaticos/view/76-the-olive-tree, Last accessed in July 2018.

Anonymous. 2017c. Encyclopædia Britannica (2017). Olive plant. http://www.britannica.com/plant/olive-plant, Last accessed in July 2018.

Anonymous. 2017d. Butanox® M-60, Product Data Sheet, AkzoNobel, TS 65429.09/July 2017, www.akzonobel.com/, Last accessed in July 2018.

Anonymous. 2017e. Cobalt %6, Accelerator NL-51P, Saftey Data Sheet, AkzoNobel, Version 1. Revision Date 28.04.2015. Print Date 05.10.2017, www.akzonobel.com/, Last accessed in July 2018.

Anonymous. 2018a. ASTM D6110-18, Standard Test Method for Determining the Charpy Impact Resistance of Notched Specimens of Plastics, ASTM International, West Conshohocken, PA, 2018, www.astm.org/Standards/D6110, Last accessed in July 2018.

Anonymous. 2018b. BMS 200-RB (Rockwell&Brinell Sertlik Ölçme Cihazı), Operation Manual. Rev:00. http://www.bulutmak.com/uploads/2/0/0/3/20037867/bms_200-rb_kullanma_kilavuzu.pdf, Last accessed in July 2018.

Anonymous. 2018c. https://zeytinhakkindahersey.tr.gg/P%26%23304%3BR%26%23304%3BNA.htm, Last accessed in July 2018.

Anonymous. 2018d. https://www.poliya.com/en/stand-alone-mold-release-waxes, Last accessed in July 2018.

Anonymous. 2018e. Food and Agriculture Organization of the United Nations. 2018. Visualize data. http://www.fao.org/faostat/en/#data/QC/visualize, Last accessed in July 2018.

Åström, B. T. 2001. Introduction to Manufacturing of Polymer-Matrix Composites In: A. S. M. Handbook Volume 21: Composites (Miracle, D. B., Donaldson, S. L.), ASM International, pp. 421, Ohio.

Ayrılmış, N., Büyüksarı, U. 2010. Utilization of olive mill sludge in manufacture of lignocellulosic/polypropylene composite. **Journal of Materials Science**, 45(5): 1336-1342.

Barbero, E. J. 2008. Finite element analysis of composite materials. CRC press, pp. 46, Boca Raton, FL.

Barbero, E. J. 1999. Introduction to Composite Materials Design. Taylor & Francis, pp. 25-30, New York.

Bert, C. W. 1989. Section II A: Anisotropic-Material Behavior In: Manual on Experimental Methods for Mechanical Testing of Composites. (Pendleton, R., Tuttle, M. Eds.). Society for Experimental Mechanics Inc., pp. 5, Bethel, Connecticut.

Beşergil, B. 2016. Kompozitler Temel İlkeler Test Metotları. Gazi Kitabevi, pp. 37,38,51,114,459,493,518, Ankara.

Bledzki, A. K., Reihmane, S., Gassan, J. 1996. Properties and modification methods for vegetable fibers for natural fiber composites. **Journal of Applied Polymer Science**, 59(8): 1329-1336.

Broek, D. 1982. Elementary engineering fracture mechanics. Martinus Nijhoff Publishers, pp. 6-9,12-13, The Hague, The Netherlands.

Djidjelli, H., Benachour, D., Boukerrou, A., Zefouni, O., Martinez-Véga, J., Farenc, J., Kaci, M. 2007. Thermal, dielectric and mechanical study of poly (vinyl chloride)/olive pomace composites. **Express Polymer Letters**, 1: 846-852.

Driscoll, S. B. 1998. The Basics of testing plastics: mechanical properties, flame exposure, and general guidelines. ASTM, pp. 20-22, West Conshohocken, PA.

Drzal, L. T. 2001. Interfaces and Interphases. In: A. S. M. Handbook Volume 21: Composites (Miracle, D. B., Donaldson, S. L. Eds.), ASM International, pp. 169, Ohio.

Drzal, L.T. 1985. The Interphase in Epoxy Composites. In: Advances in Polymer Science II, Vol 75 (Dusek, K. Ed.), Springer-Verlag, pp. 3, Berlin.

Erkliğ, A., Shihan, A., Alsaadi, M. 2016. Effect of Olive Pomace on the Mechanical Property of glass fiber reinforced epoxy composites. **International Conference on Advanced Technology & Sciences (ICAT'16)**, (September 01-03, 2016). 1159-1162, Konya.

Ertürk, D. 2015. Synthesis of Pomace Composite Resin. Istanbul Technical University. PhD Thesis (unpublished), Istanbul.

Gay, D. 2014. Composite Materials: Design and Applications. CRC Press, pp. 7-9, Boca Raton, FL.

Gharbi, A., Hassen, R. B., Boufi, S. 2014. Composite Materials from Unsaturated Polyester Resin and Olive Nuts Residue: The Effect of Silane Treatment. **Industrial Crops and Products**, 62: 491-498.

Goda, K., Sreekala, M. S., Malhotra, S. K., Joseph, K., Thomas, S. 2014. Advances in Polymer Composites: Biocomposites – State of the Art, New Challenges, and Opportunities. In: Polymer Composites, Volume 3: Biocomposites, (Thomas, S., Joseph, K., Malhotra, S. K., Goda, K., Sreekala, M. S., Eds.), Wiley-VCH, pp.5-8, Weinheim, Germany.

Griffith, A.A. 1921. VI. The Phenomena of Rupture and Flow in Solids. **Philosophical Transactions of the Royal Society of London**, Series A 221: 163-69.

Gross, D., Seelig, T. 2011. Fracture mechanics: With an introduction to micromechanics (Second edition). Springer Science & Business Media, pp. 1,63, Heidelberg, Germany.

Guner, M. 2007. Pneumatic conveying characteristics of some agricultural seeds. **Journal of Food Engineering**, 80(3): 904-913.

Hastings, G. W., Williams, D. F., Biological Engineering Society. 2008. Chapter 4 Mechanical Properties of Biomaterials. Biomaterials - The intersection of Biology and Material Science. Pearson Prentice Hall Bioengineering, pp. 152, New Jersey.

Irwin, G.R. 1957a. Analysis of Stresses and Strains Near the End of a Crack Traversing a Plate. **Journal of Applied Mechanics**, Transactions of ASME 24: 361-64.

Irwin, G.R. 1957b. Relation of stresses near a crack to the crack extension force. Proceedings of **Ninth International Congress of Applied Mechanics**, Brussels.

John, M. J., Thomas, S. 2012. Natural Polymers: An Overview In: Natural Polymers, Volume 1: Composites. (Maya John, J., Thomas S. Eds.), The Royal Society of Chemistry Publishing, pp. 4-6, Cambridge, UK.

Jones, R. M. 1998. Mechanics of Composite Materials (2nd ed.). Taylor & Francis, pp. 2, Philadelphia.

Jose, J. P., Malhotra, S. K., Thomas, S., Joseph, K., Goda, K., Sreekala, M. S. 2012. Advances in Polymer Composites: Macro and Microcomposites – State of the Art, New Challenges, and Opportunities. In: Polymer Composites, Volume 1: Macro and Microcomposites, (Thomas, S., Joseph, K., Malhotra, S. K., Goda, K., Sreekala, M. S., Eds.), Wiley-VCH, pp.4-11, Weinheim, Germany.

Kalpakjian, S., Schmid, S. R. 2009. Manufacturing Engineering and Technology (Sixth Edition in SI Units). Pearson - Prentice Hall, pp. 216-222, New York.

Kaw, A. K. 2006. Mechanics of Composite Materials (2nd ed.). CRC Press, pp. 8-12, Boca Raton, FL.

Kelly, P. 2013. Solid mechanics lecture notes. Reological Models. http://www3.esc.auckland.ac.nz/people/staff/pkel015/SolidMechanicsBooks/Part_I/BookSM_Part_I/07_Viscoelasticity/PDF/Viscoelasticity_03_Rheological.pdf, Last accessed in July 2018.

Khoei, A. R. 2014. Extended finite element method: theory and applications. John Wiley & Sons. pp. 1, West Sussex, UK.

Kılıçaslan, C. 2016. Zeytin Pirinası/Polyester Kompozitin Basma Yükü Altındaki Mekanik Özelliklerinin Belirlenmesi. **Engineer & the Machinery Magazine**, 57(676).

Kılıçkan, A., Güner, M. 2008. Physical properties and mechanical behavior of olive fruits (Olea europaea L.) under compression loading. **Journal of Food Engineering**, 87(2): 222-228.

Klemm, K., Eguíluz, V. M., Toral, R., San Miguel, M. 2005. Globalization, polarization and cultural drift. **Journal of Economic Dynamics and Control**, 29(1-2): 321-334.

Liu, G. R., Quek, S. S. 2013. The finite element method: a practical course. Butterworth-Heinemann, pp. 18, Waltham, MA.

Maiti, S. K. 2015. Fracture Mechanics. Cambridge University Press, pp. 6-13, Delhi, India.

Matos, M., Barreiro, M. F., Gandini, A. 2010. Olive stone as a renewable source of biopolyols. **Industrial Crops and Products**, 32(1): 7-12.

Miracle, D. B., Donaldson, S. L. 2001. Introduction to Composites. In: A. S. M. Handbook Volume 21: Composites (Miracle, D. B., Donaldson, S. L. Eds.), ASM International, pp. 1, Ohio.

Mohanty, A. K., Misra, M., Drzal, L. T., Selke, S. E., Harte, B. R., Hinrichsen, G. 2005. Natural Fibers, Biopolymers, and Biocomposites: An Introduction. In: Natural Fibers, Biopolymers, and Biocomposites, Mohanty, A. K., Misra, M., Drzal, L. T. (Eds.), CRC Press, pp. 4-5, Boca Raton, FL.

Mousa, A., Heinrich, G., Gohs, U., Hässler, R., Wagenknecht, U. 2009. Application of renewable agro-waste-based olive pomace on the mechanical and thermal performance of toughened PVC. **Polymer-Plastics Technology and Engineering**, 48(10): 1030-1040.

Naghmouchi, I., Mutjé, P., Boufi, S.2014. Polyvinyl chloride composites filled with olive stone flour: mechanical, thermal, and water absorption properties. **Journal of Applied Polymer Science**, 131(22).

Naghmouchi, I., Mutjé, P., Boufi, S. 2015. Olive stones flour as reinforcement in polypropylene composites: A step forward in the valorization of the solid waste from the olive oil industry. **Industrial Crops and Products**, 72: 183-191.

Niaounakis, M., Halvadakis, C.P., 2006. Olive Processing Waste Management: Literature Review and Patent Survey. Elsevier, pp. 1-126, Amsterdam.

Papanicolaou, G. C., Xepapadaki, A. G., Angelakopoulos, G. C., Zabaniotou, A., Ioannidou, O. 2011. Use of solid residue from olive kernel pyrolysis for polymer matrix composite manufacturing: Physical and mechanical characterization. **Journal of Applied Polymer Science**, 119(4): 2167-2173.

Papanicolaou, G. C., Koutsomitopoulou, A. F., Sfakianakis, A. 2012. Effect of thermal fatigue on the mechanical properties of epoxy matrix composites reinforced with olive pits powder. **Journal of Applied Polymer Science**, 124(1): 67-76.

Perez, N. 2017. Fracture Mechanics. Springer International Publishing, pp. 62, Switzerland.

Shiryaev, A.A., Frost, D.J. and Langenhorst, F. 2007. Impurity diffusion and microstructure in diamonds deformed at high pressures and temperatures. **Diamond and Related Materials**, 16(3): 503-511

Thakur, V. K., Thakur, M. K., Gupta, R. K., Prasanth, R., Kessler, M. R. 2014. Green Composites: An Introduction. In: Green Composites from Natural Resources, (Thakur, V. K., Ed.), CRC Press, pp. 5-7, Boca Raton, FL.

Thomas, G. P. 2013. Composite Prepregs – Manufacturing, Benefits and Applications. http://www.azom.com/article.aspx?ArticleID=8353#3, Last accessed in July 2018.

Vilaseca, F., Mendez, J.A., Lopez, J.P., Vallejos, M., EBarbera, L., Pelach, M.A., Turon X. and Mutje P., 2007. Recovered and recycled Kraft fibres as reinforcement of PP composites. **Chemical Engineering Journal**, 38(1-3): 586-595.

Vlyssides, A.G., Loizidou, M., Gimouhopoulos, K., Zorpas, A. 1998. Olive oil processing wastes production and their characteristics in relation to olive oil extraction methods. **Fresenius Environmental Bulletin**, 7 (5-6): 308-313.

Williams, J. G. 2001. Introduction to Linear Elastic Fracture Mechanics In: Fracture Mechanics Testing Methods for Polymers, Adhesives and Composites. Volume 28. (Moore, D. R., Pavan, A., Williams, J.G., Eds.), Elsevier, pp. 3, Oxford, UK.

Zavareze, E. R., da Dias, A. R. G. 2012. Relation between Structural Anisotropy in Natural Fibres and Mechanical Properties in Composites In: Natural Polymers, Volume 1: Composites. (Maya John, J., Thomas S. Eds.) The Royal Society of Chemistry Publishing, pp. 66, Cambridge, UK.

Zweben, C. 2006. Composite Materials. In: Mechanical Engineers' Handbook: Materials and Mechanical Design, Volume 1, Third Edition, (Kutz, M., Ed.), John Wiley & Sons, Inc., pp. 381-382, New Jersey.

APPENDICES

This section includes the Tensile and Flexural test results:

Appendix A – Tensile Test Diagrams

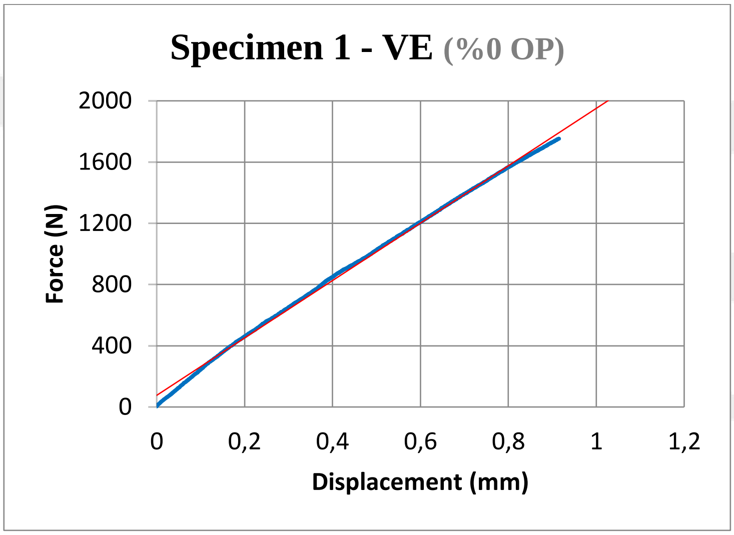

Figure A. 1. Specimen 1, Tensile Force – Displacement diagram

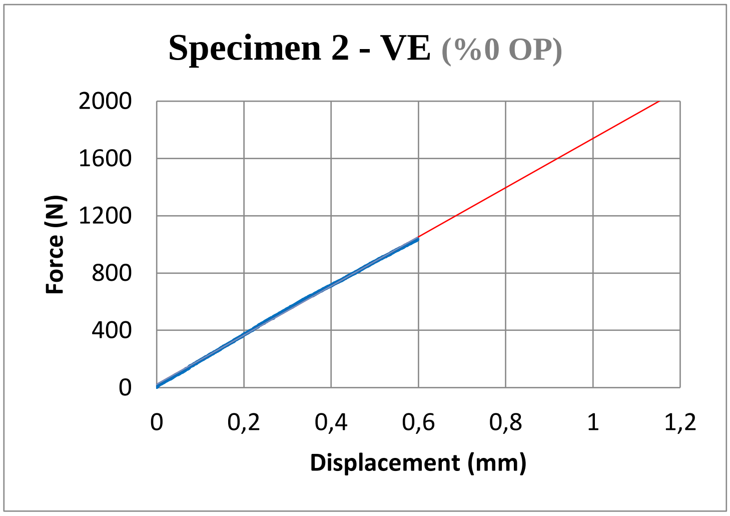

Figure A. 2. Specimen 2, Tensile Force – Displacement diagram

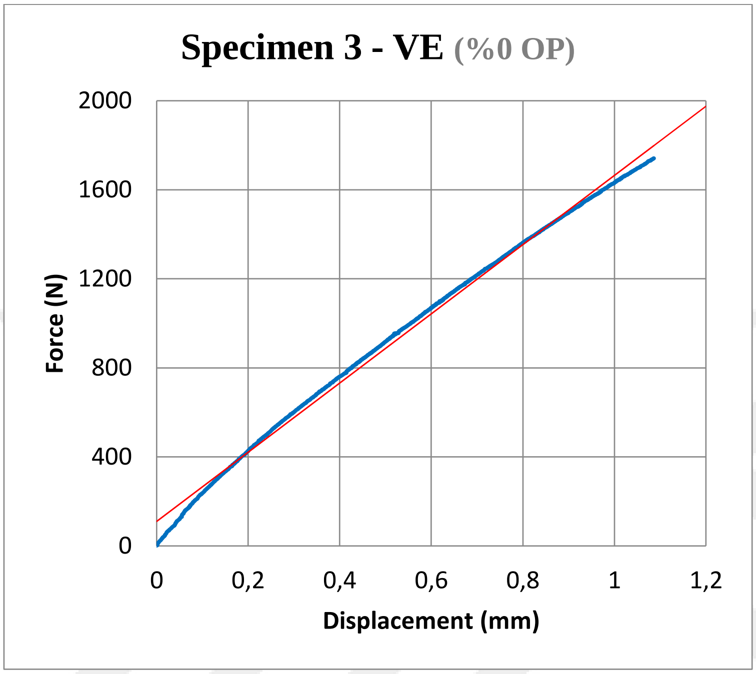

Figure A. 3. Specimen 3, Tensile Force – Displacement diagram

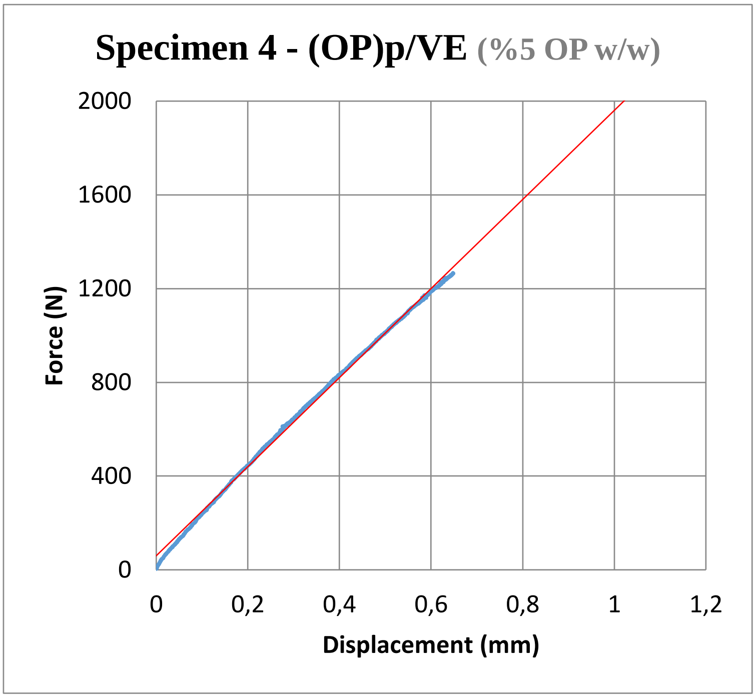

Figure A. 4. Specimen 4, Tensile Force – Displacement diagram

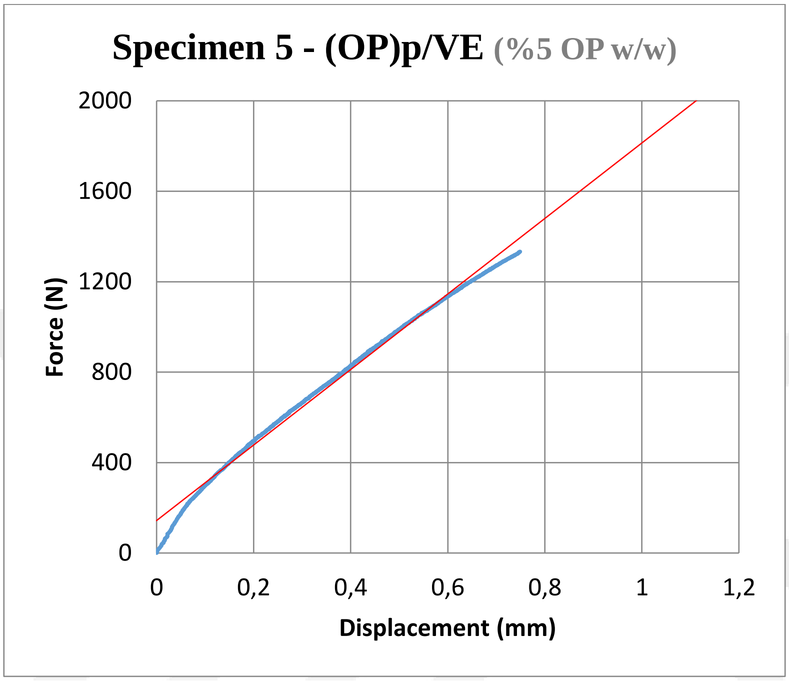

Figure A. 5. Specimen 5, Tensile Force – Displacement diagram

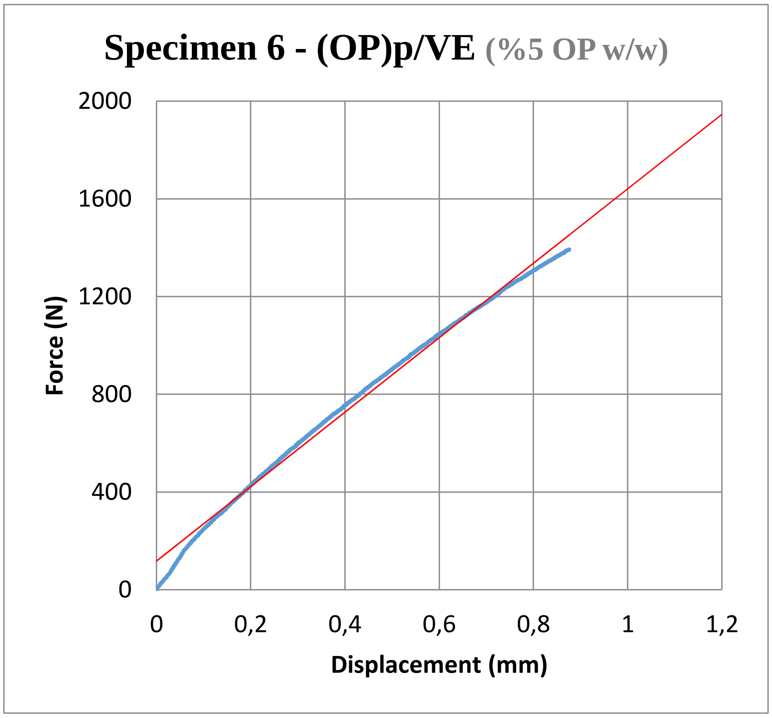

Figure A. 6. Specimen 6, Tensile Force – Displacement diagram

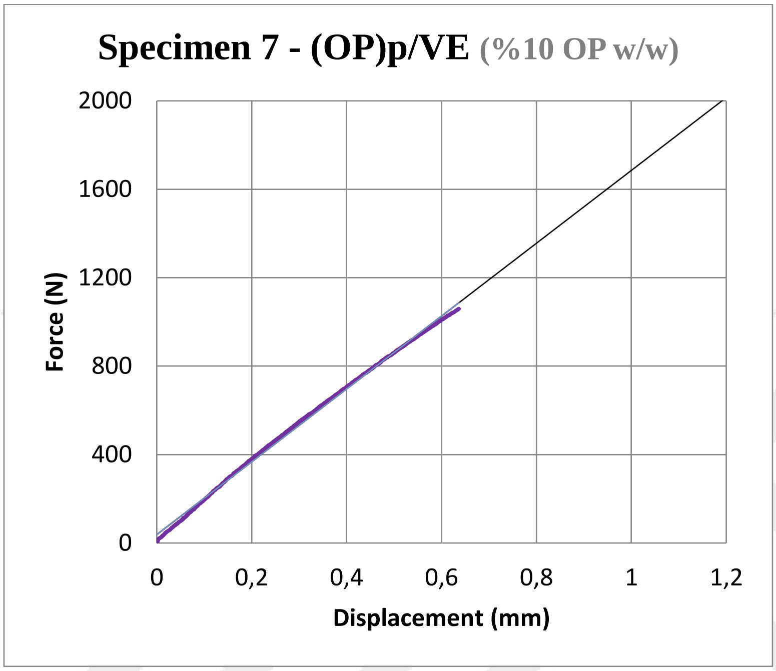

Figure A. 7. Specimen 7, Tensile Force – Displacement diagram

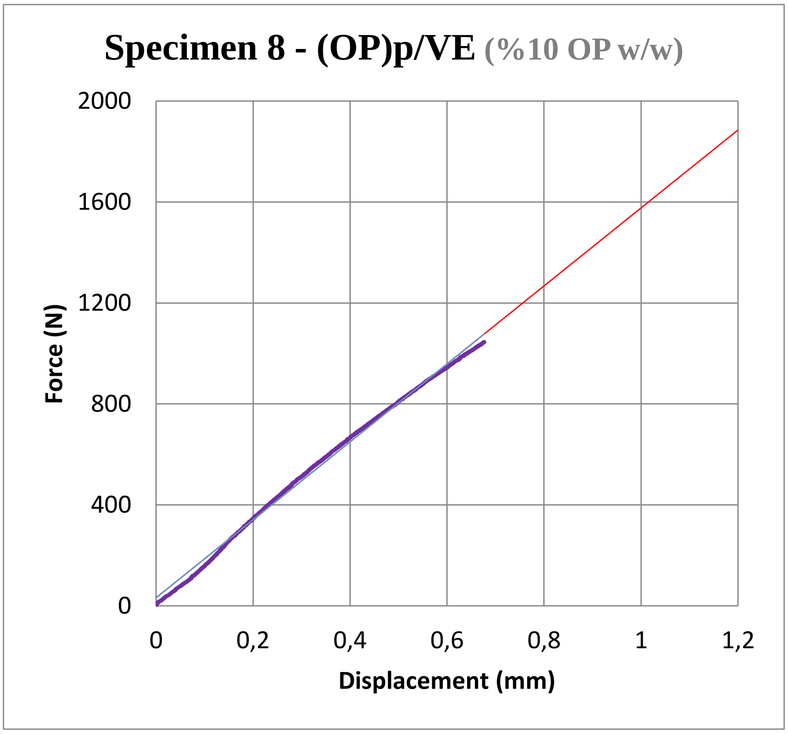

Figure A. 8. Specimen 8, Tensile Force – Displacement diagram

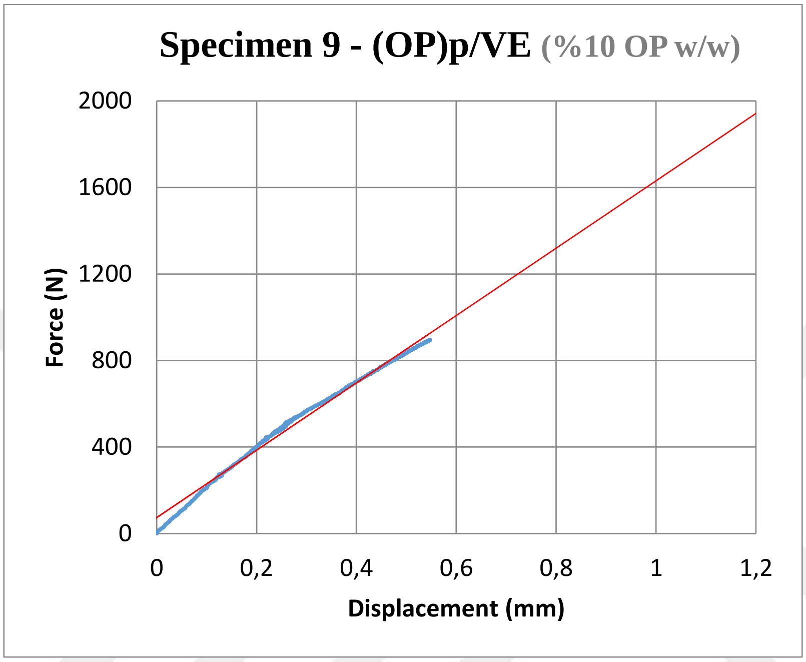

Figure A. 9. Specimen 9, Tensile Force – Displacement diagram

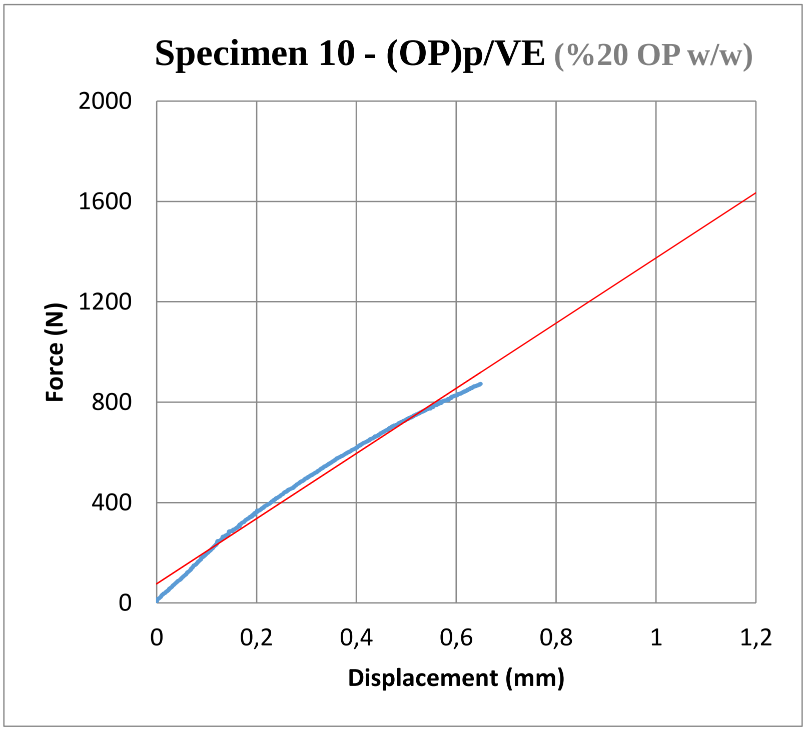

Figure A. 10. Specimen 10, Tensile Force – Displacement diagram

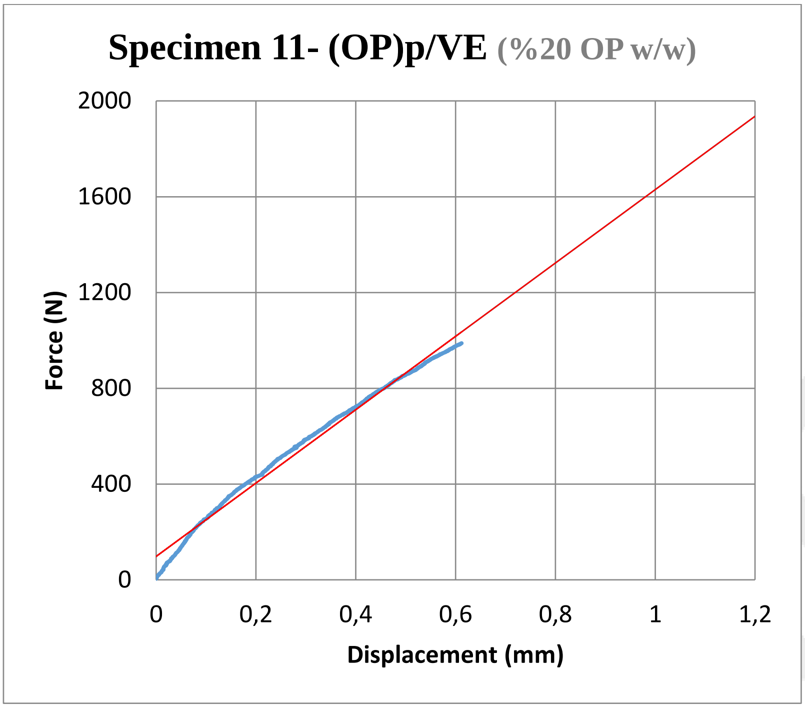

Figure A. 11. Specimen 11, Tensile Force – Displacement diagram

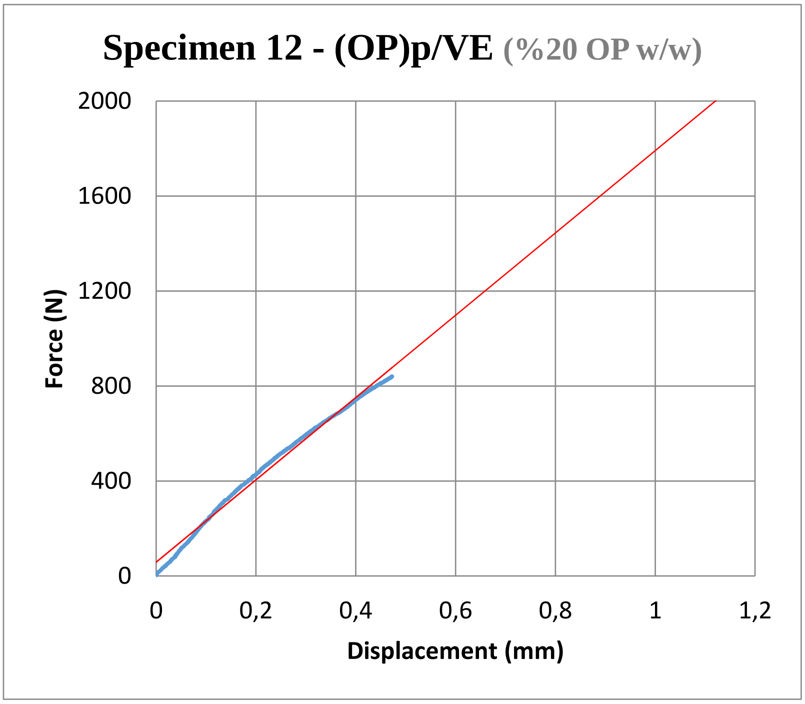

Figure A. 12. Specimen 12, Tensile Force – Displacement diagram

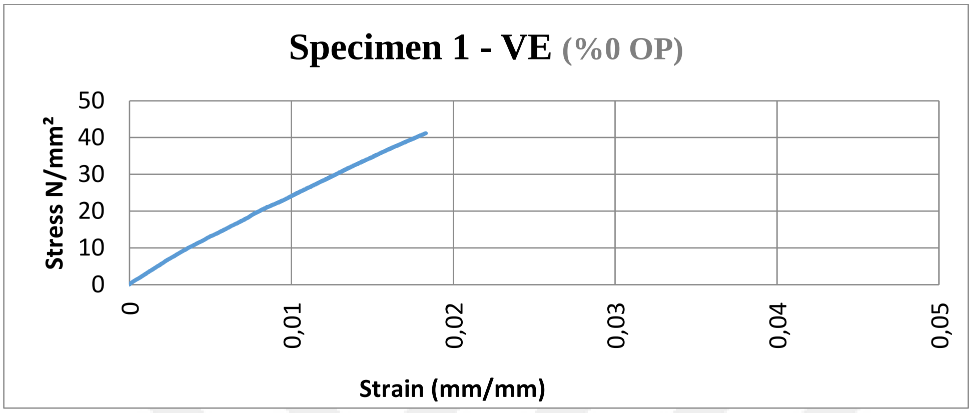

Figure A. 13. Specimen 1, Tensile Stress – Strain diagram

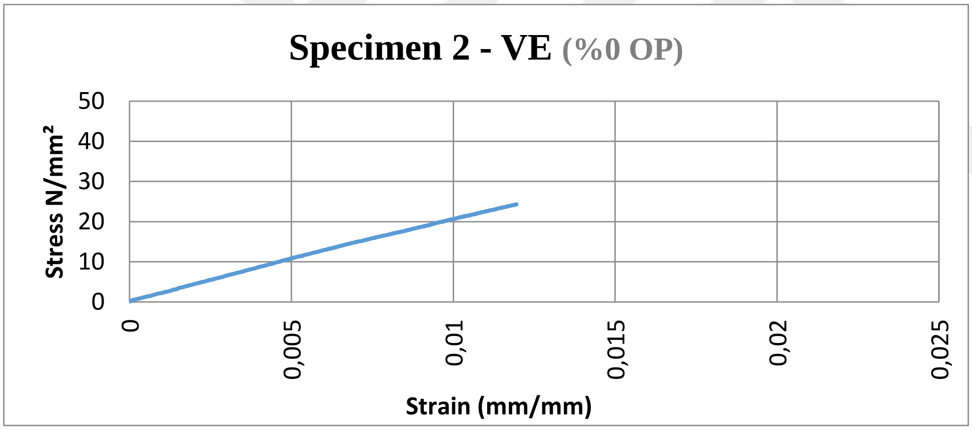

Figure A. 14. Specimen 2, Tensile Stress – Strain diagram

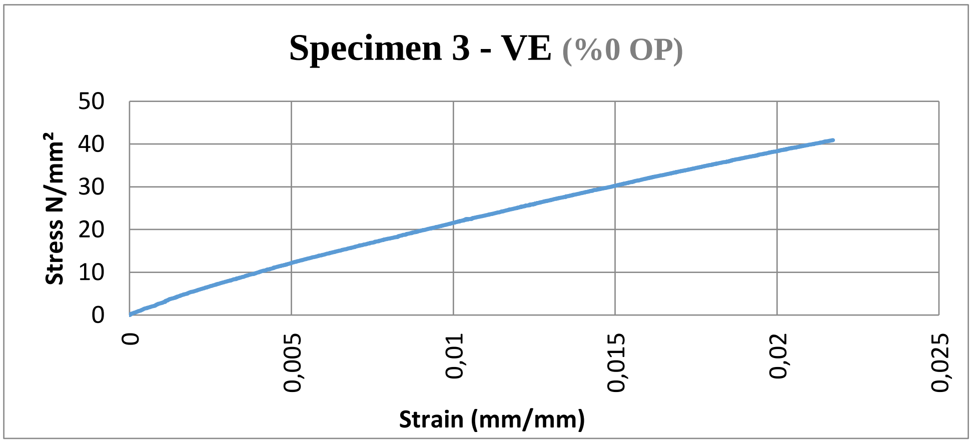

Figure A. 15. Specimen 3, Tensile Stress – Strain diagram

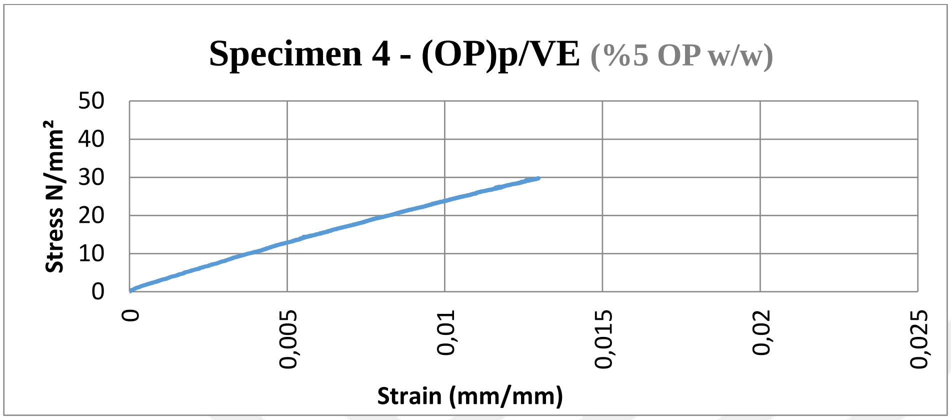

Figure A. 16. Specimen 4, Tensile Stress – Strain diagram

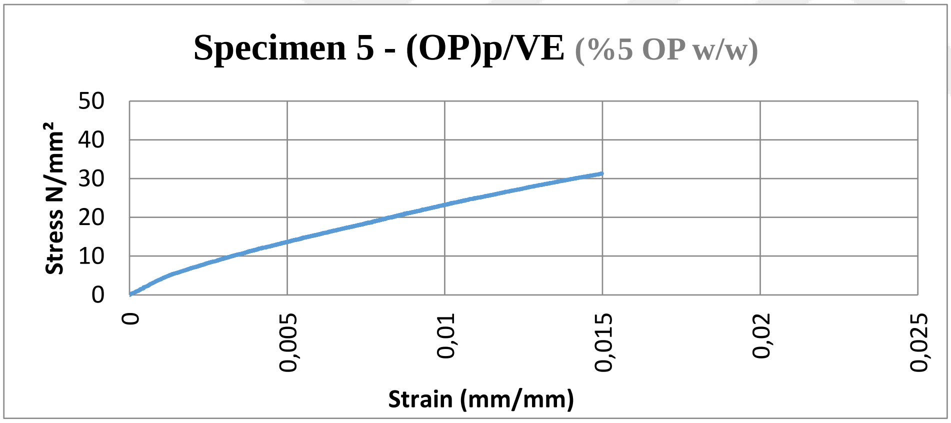

Figure A. 17. Specimen 5, Tensile Stress – Strain diagram

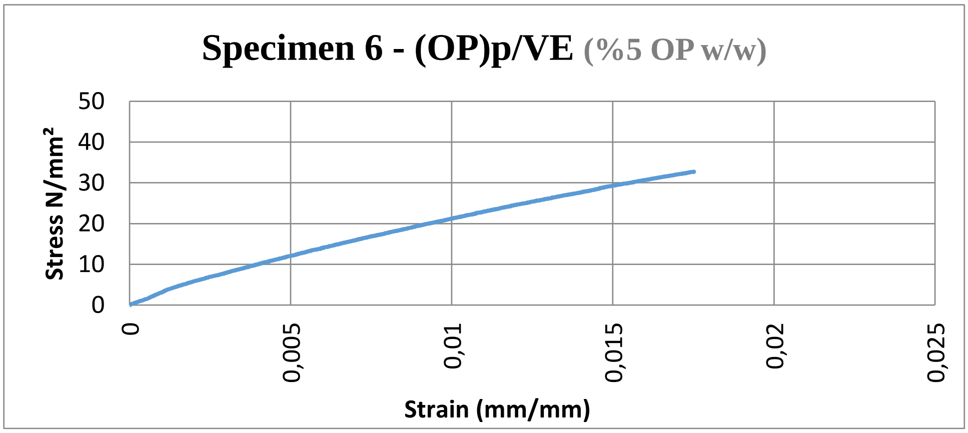

Figure A. 18. Specimen 6, Tensile Stress – Strain diagram

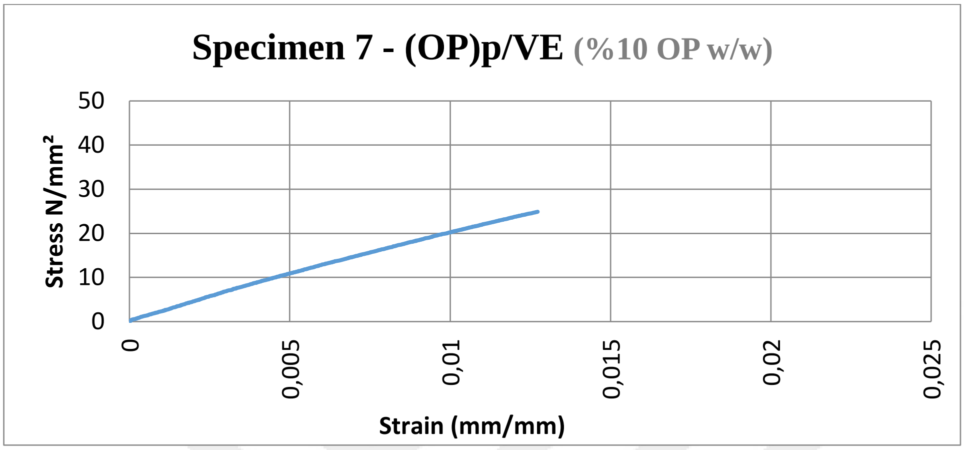

Figure A. 19. Specimen 7, Tensile Stress – Strain diagram

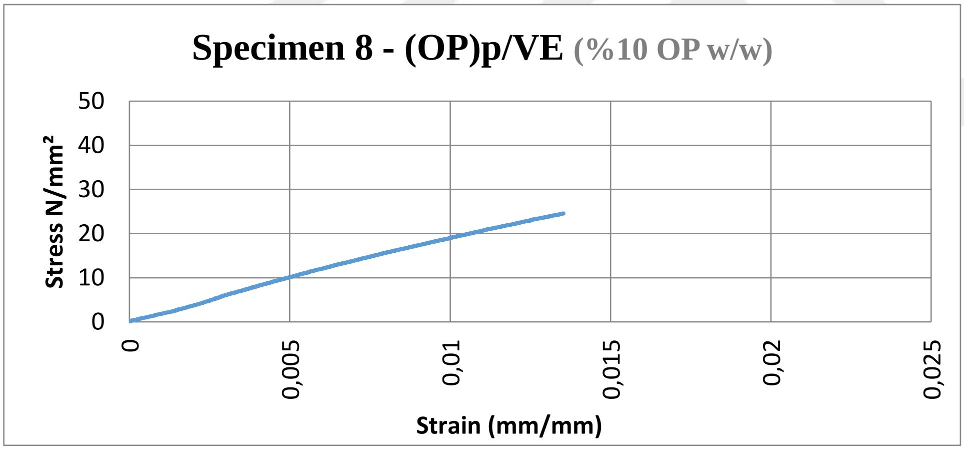

Figure A. 20. Specimen 8, Tensile Stress – Strain diagram

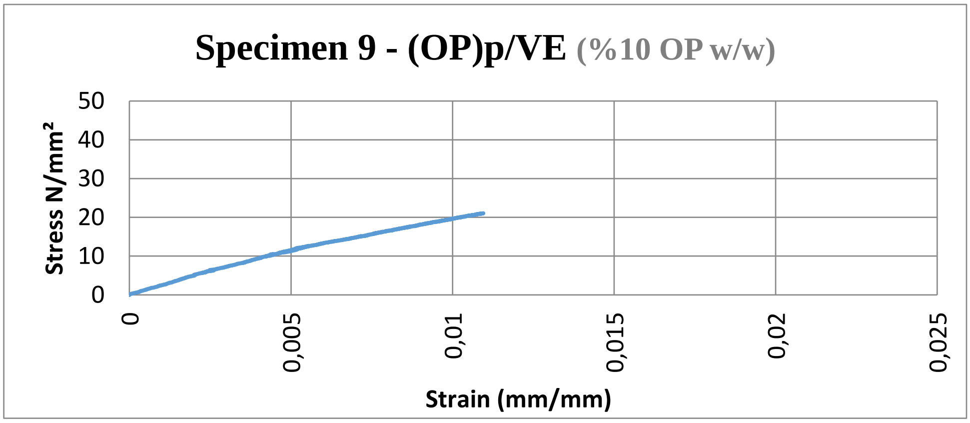

Figure A. 21. Specimen 9, Tensile Stress – Strain diagram

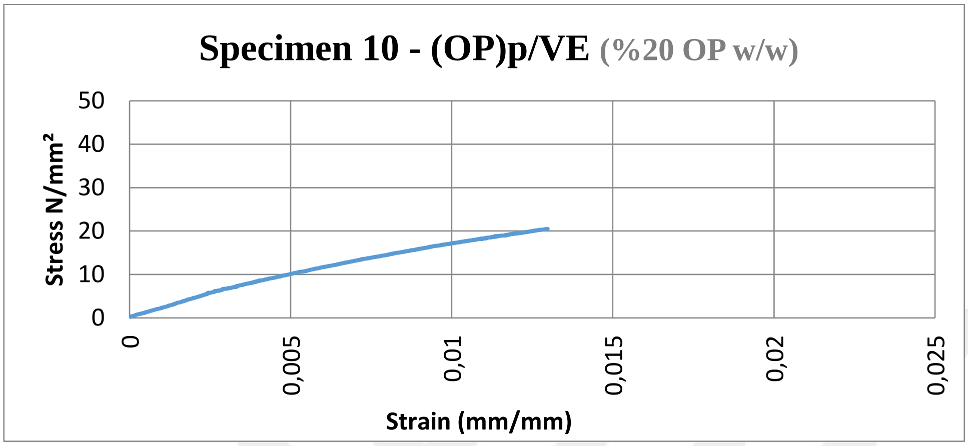

Figure A. 22. Specimen 10, Tensile Stress – Strain diagram

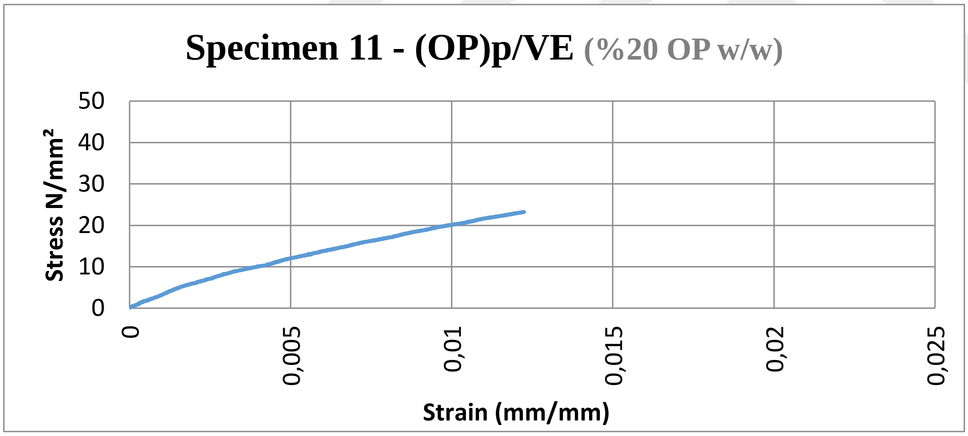

Figure A. 23. Specimen 11, Tensile Stress – Strain diagram

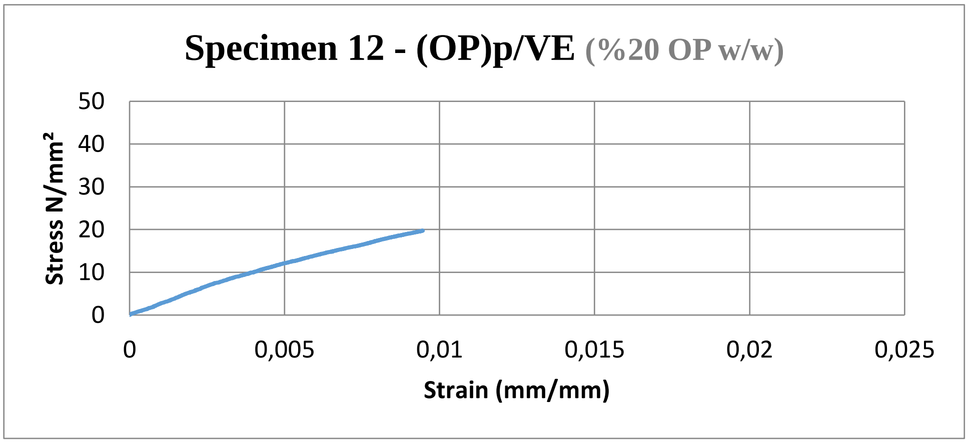

Figure A. 24. Specimen 12, Tensile Stress – Strain diagram

Appendix B – Flexural Test Diagrams

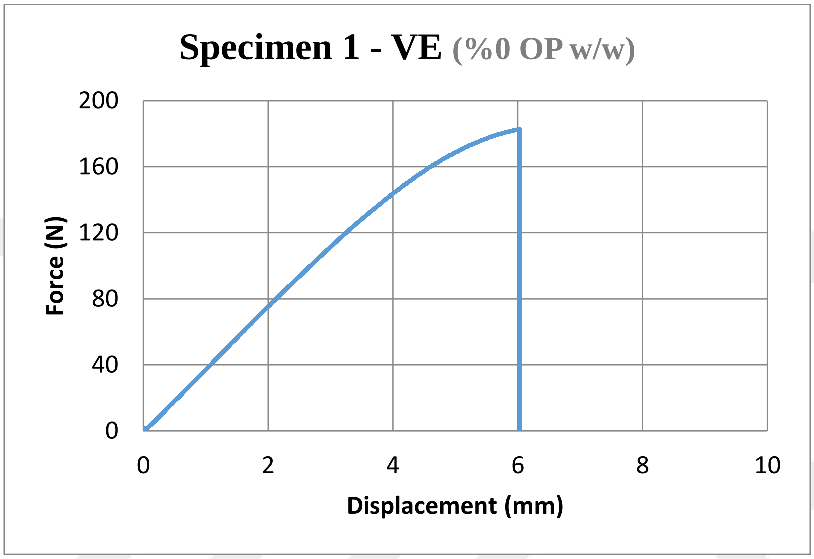

Figure B. 1. Specimen 1, Flexural Force – Displacement diagram

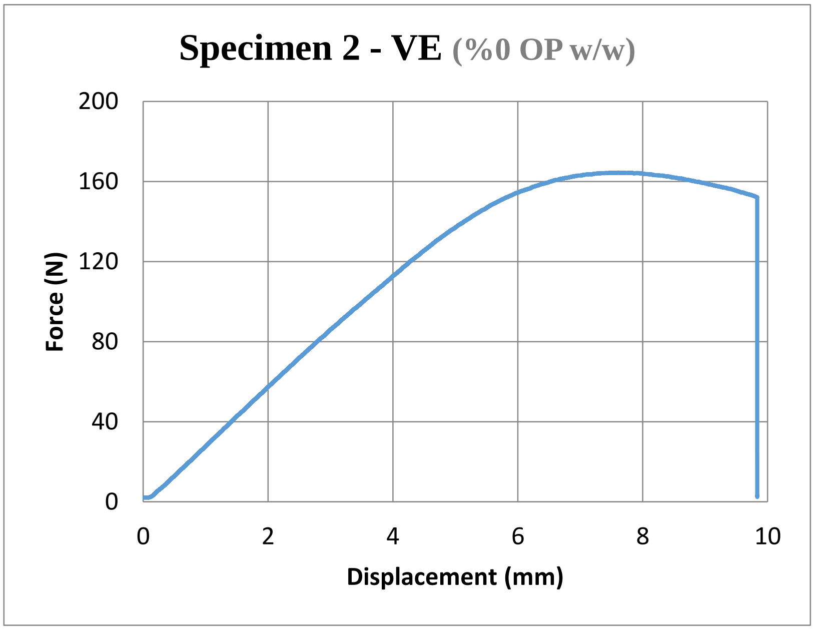

Figure B. 2. Specimen 2, Flexural Force – Displacement diagram

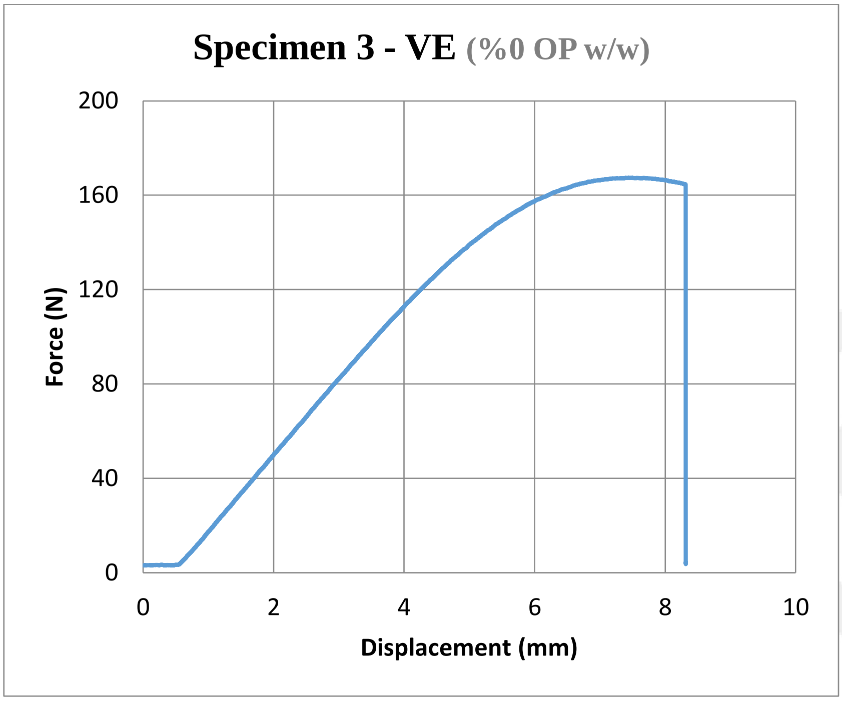

Figure B. 3. Specimen 3, Flexural Force – Displacement diagram

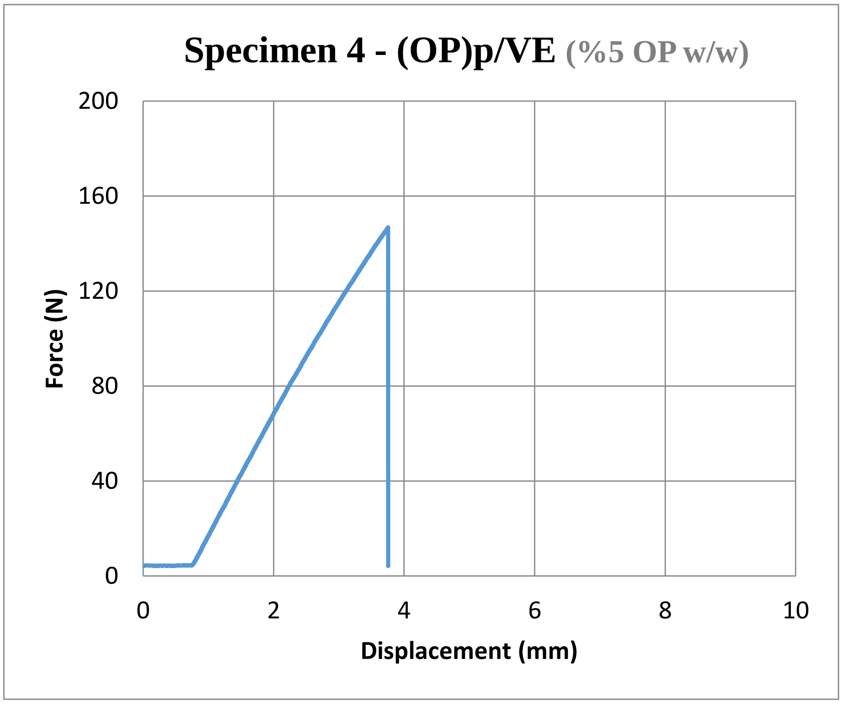

Figure B. 4. Specimen 4, Flexural Force – Displacement diagram

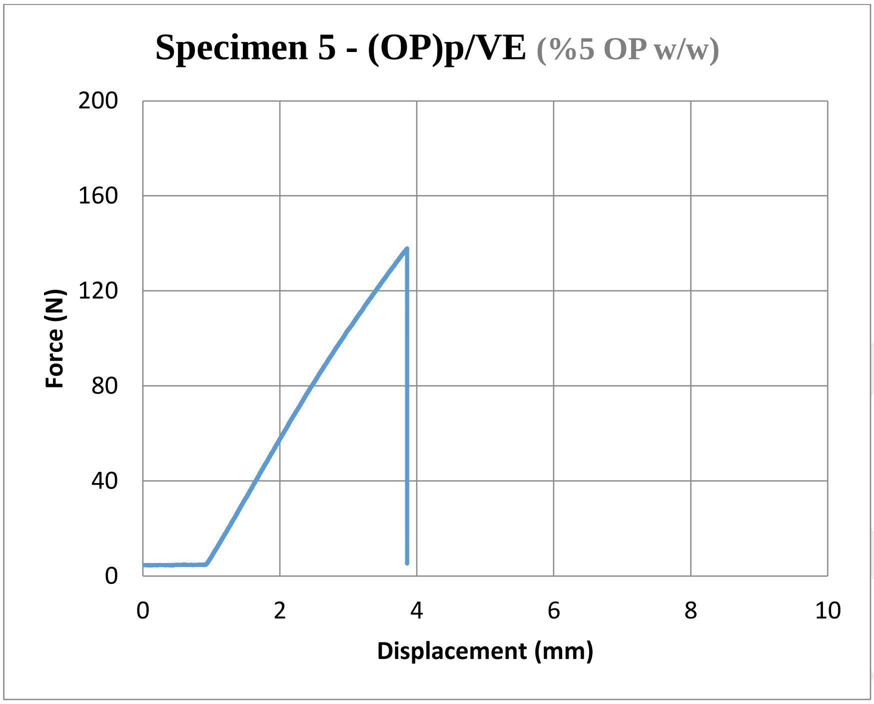

Figure B. 5. Specimen 5, Flexural Force – Displacement diagram

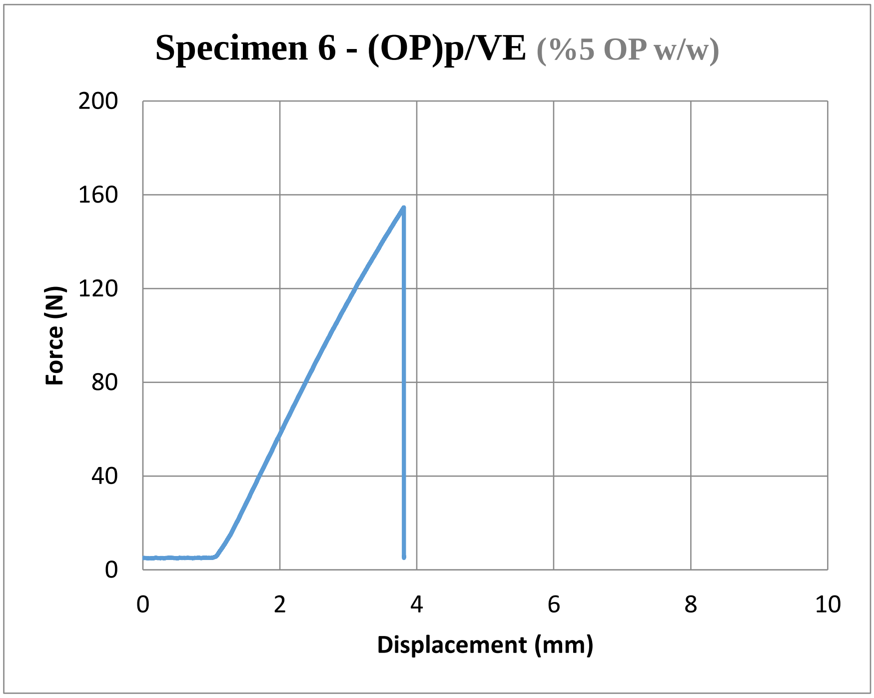

Figure B. 6. Specimen 6, Flexural Force – Displacement diagram

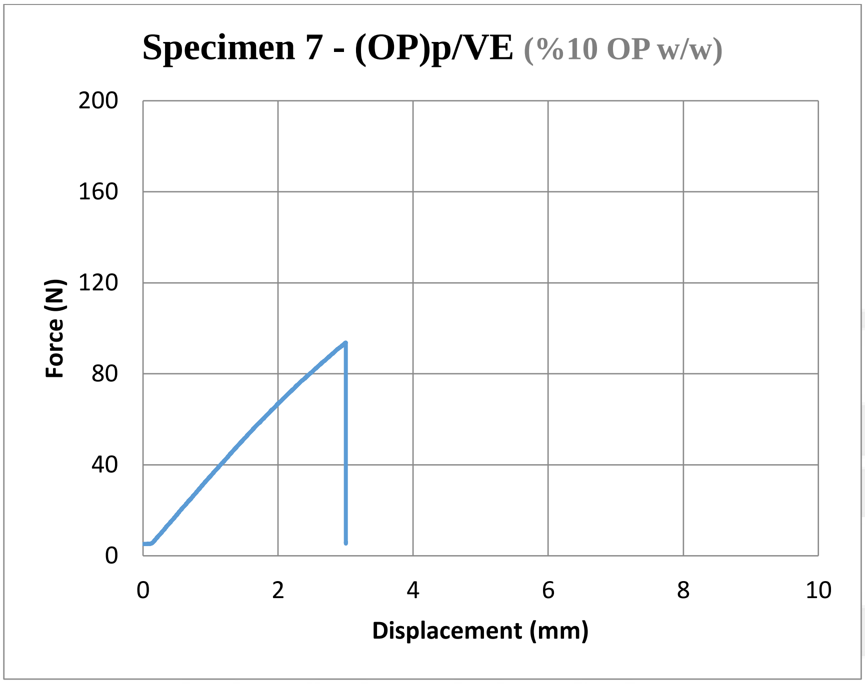

Figure B. 7. Specimen 7, Flexural Force – Displacement diagram

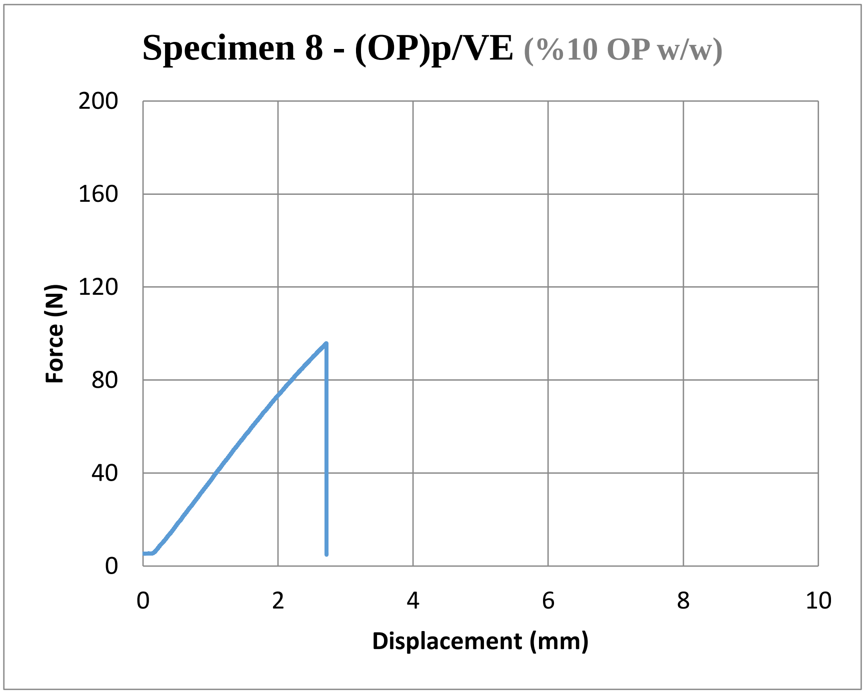

Figure B. 8. Specimen 8, Flexural Force – Displacement diagram

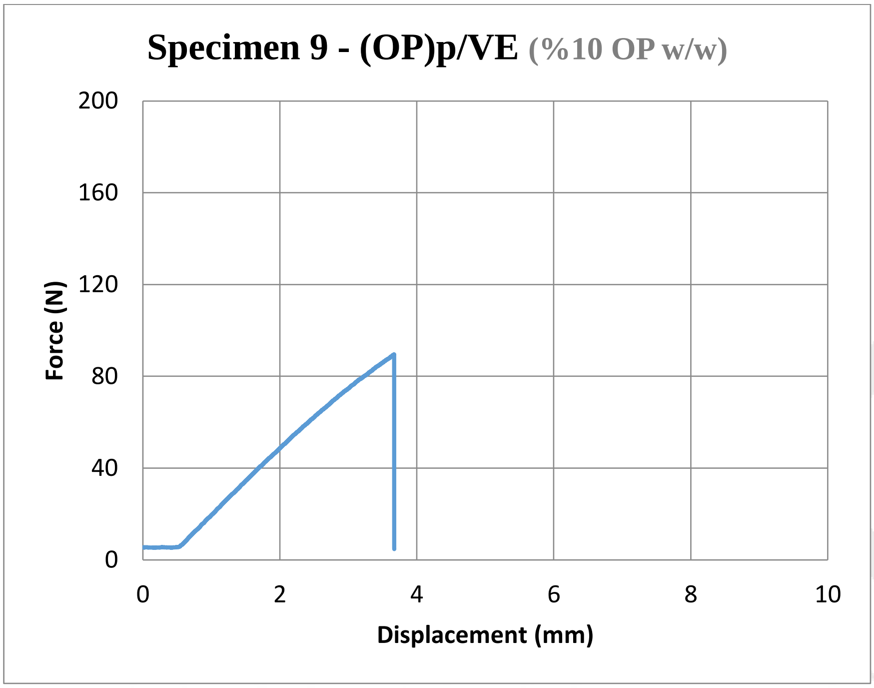

Figure B. 9. Specimen 9, Flexural Force – Displacement diagram

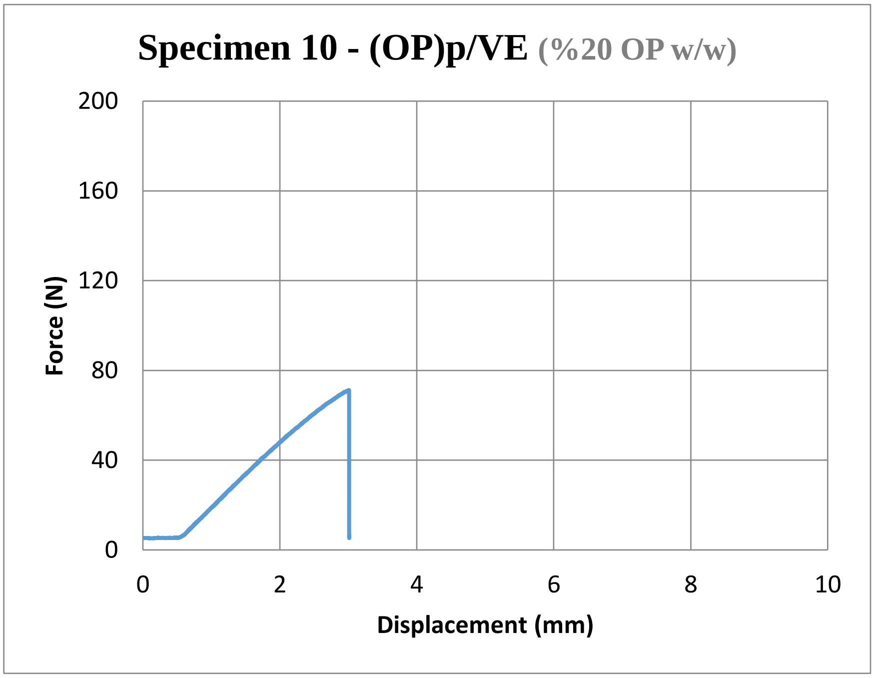

Figure B. 10. Specimen 10, Flexural Force – Displacement diagram

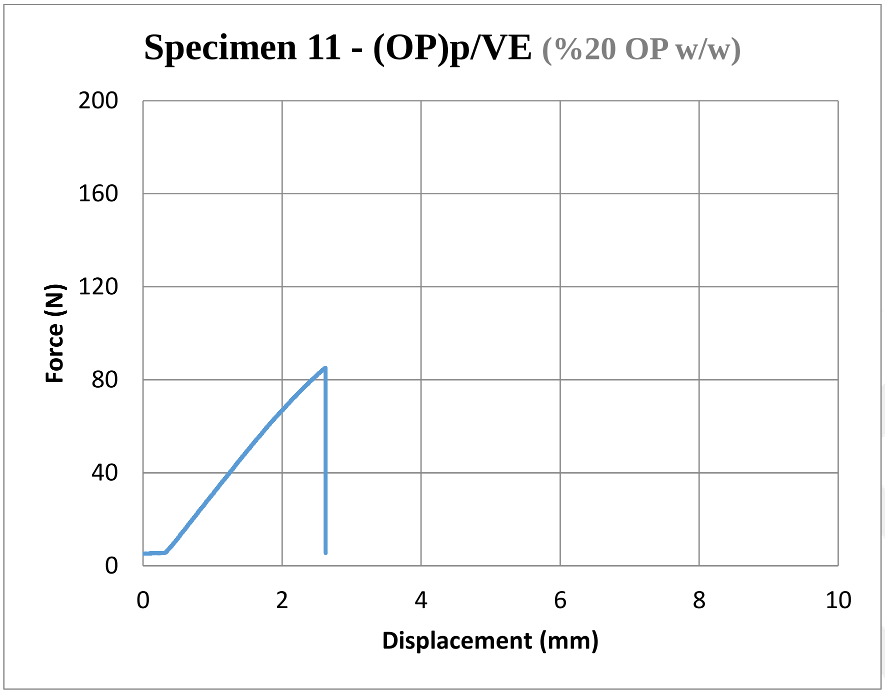

Figure B. 11. Specimen 11, Flexural Force – Displacement diagram

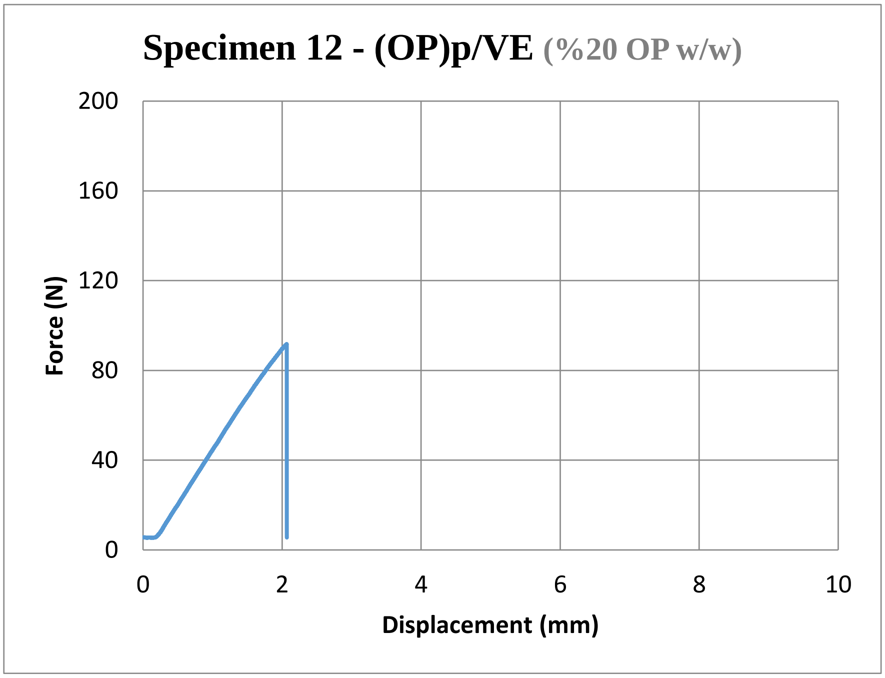

Figure B. 12. Specimen 12, Flexural Force – Displacement diagram

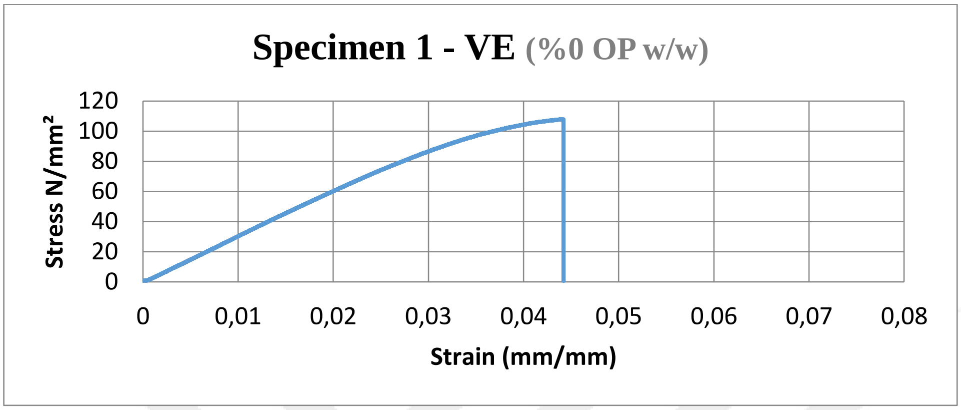

Figure B. 13. Specimen 1, Flexural Stress – Strain diagram

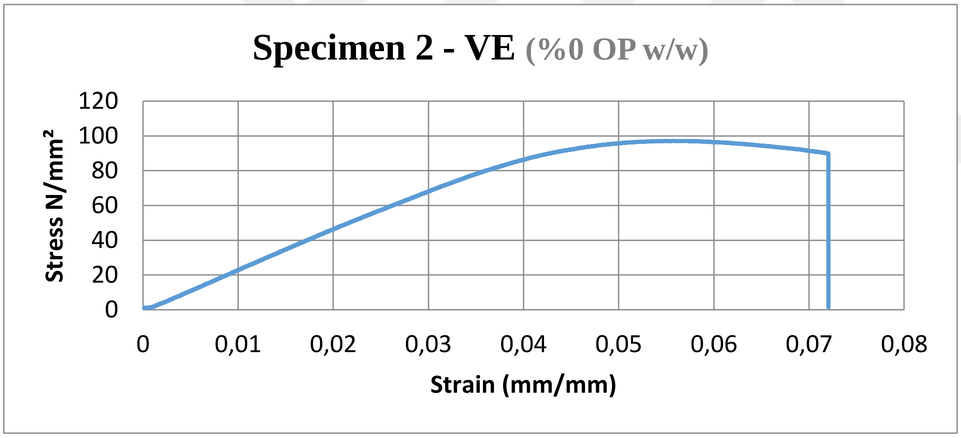

Figure B. 14. Specimen 2, Flexural Stress – Strain diagram

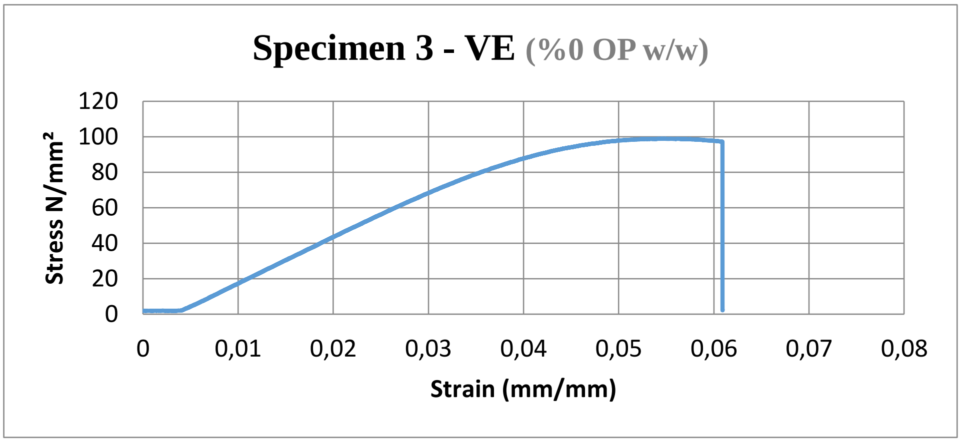

Figure B. 15. Specimen 3, Flexural Stress – Strain diagram

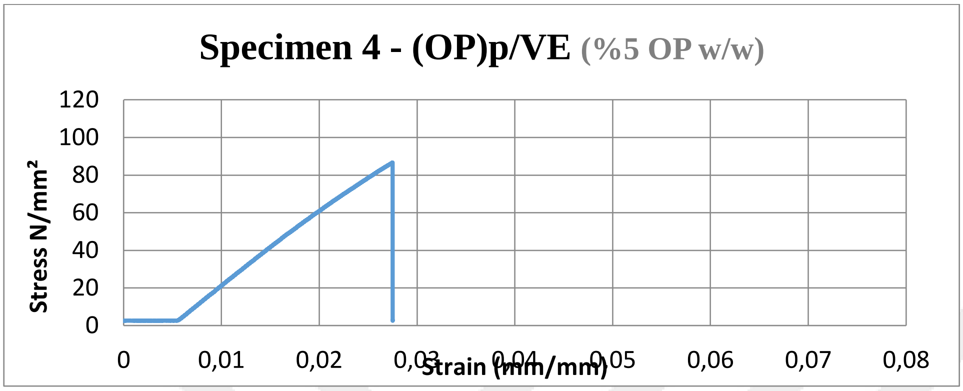

Figure B. 16. Specimen 4, Flexural Stress – Strain diagram

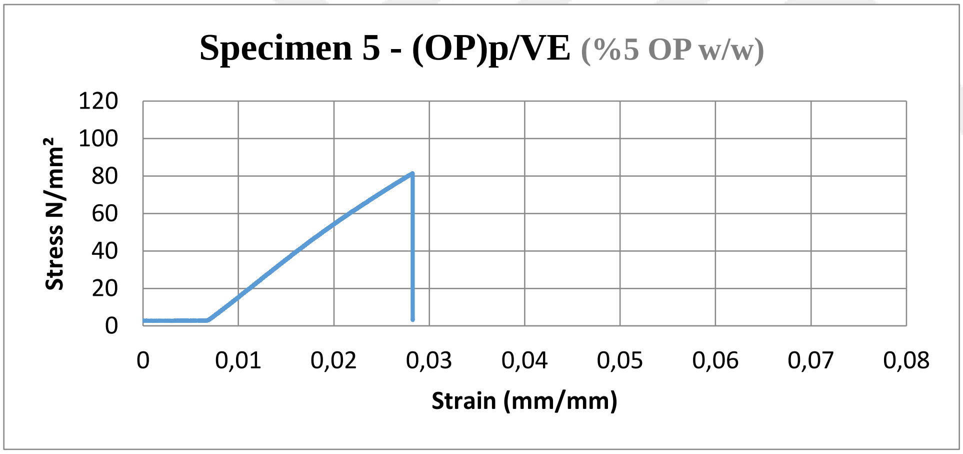

Figure B. 17. Specimen 5, Flexural Stress – Strain diagram

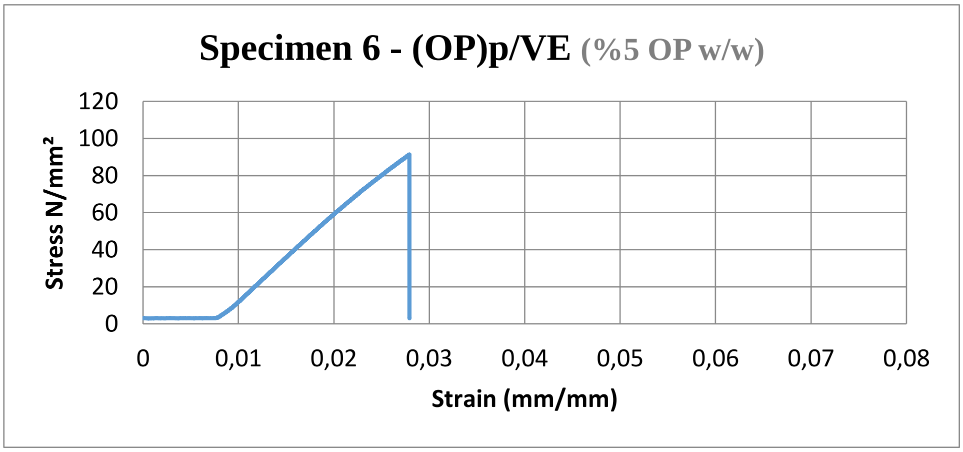

Figure B. 18. Specimen 6, Flexural Stress – Strain diagram

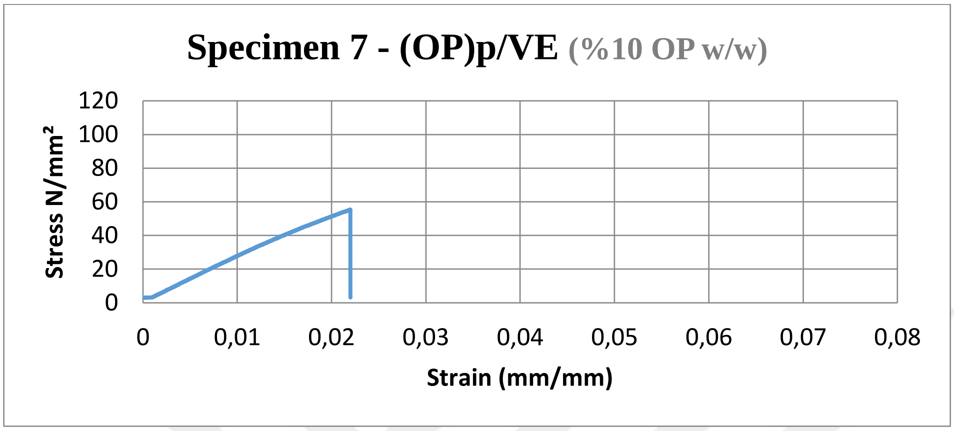

Figure B. 19. Specimen 7, Flexural Stress – Strain diagram

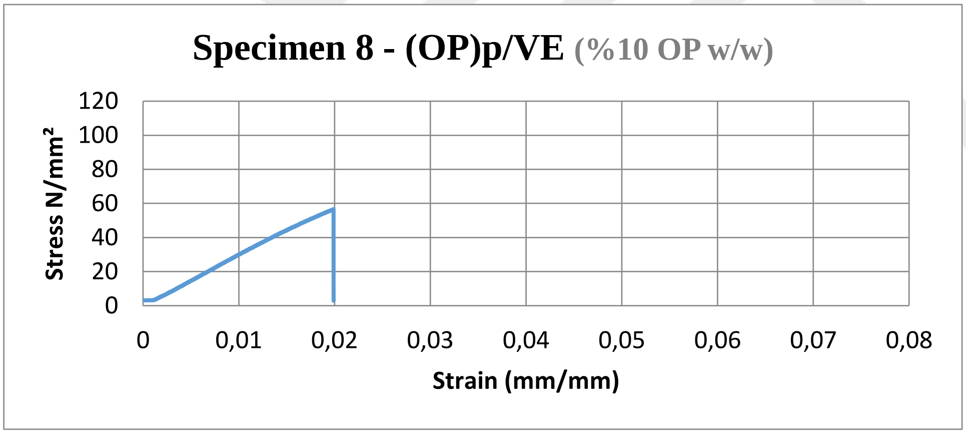

Figure B. 20. Specimen 8, Flexural Stress – Strain diagram

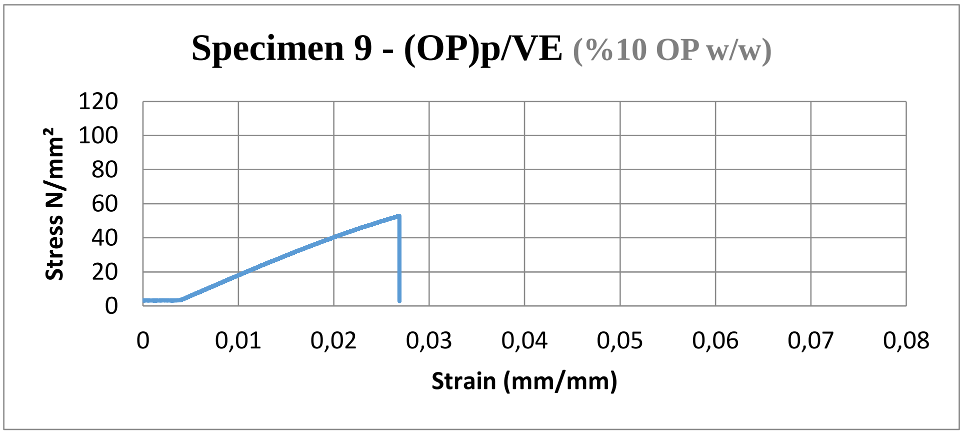

Figure B. 21. Specimen 9, Flexural Stress – Strain diagram

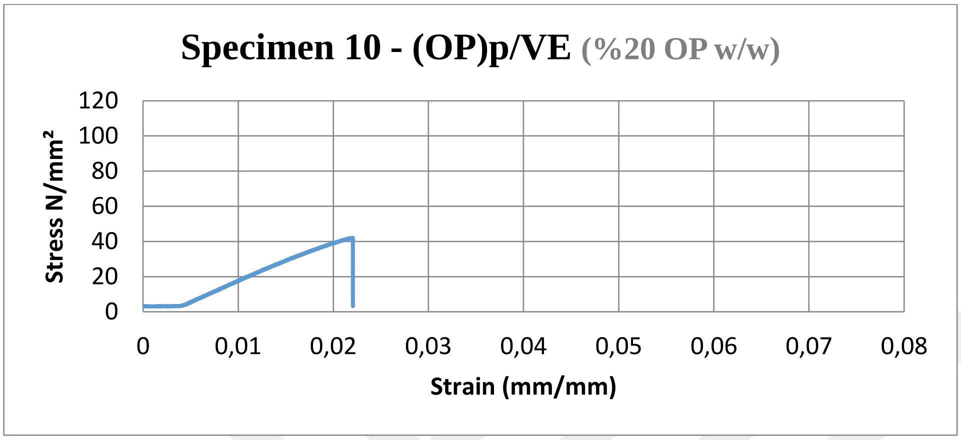

Figure B. 22. Specimen 10, Flexural Stress – Strain diagram

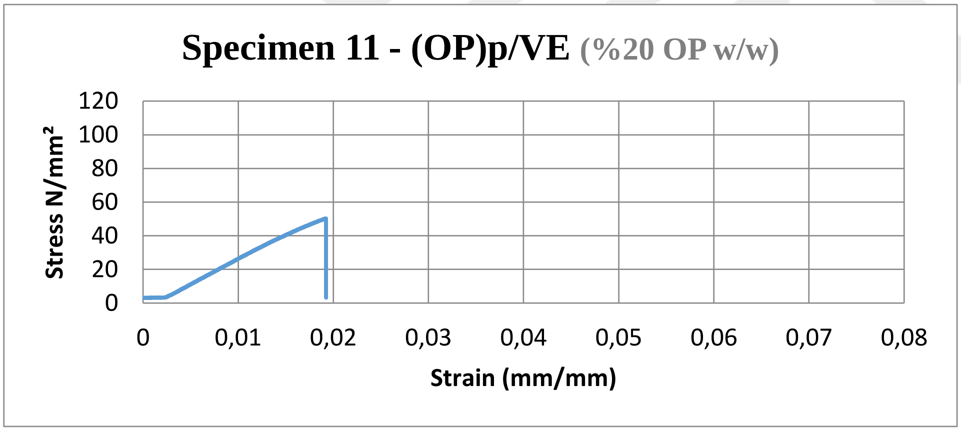

Figure B. 23. Specimen 11, Flexural Stress – Strain diagram

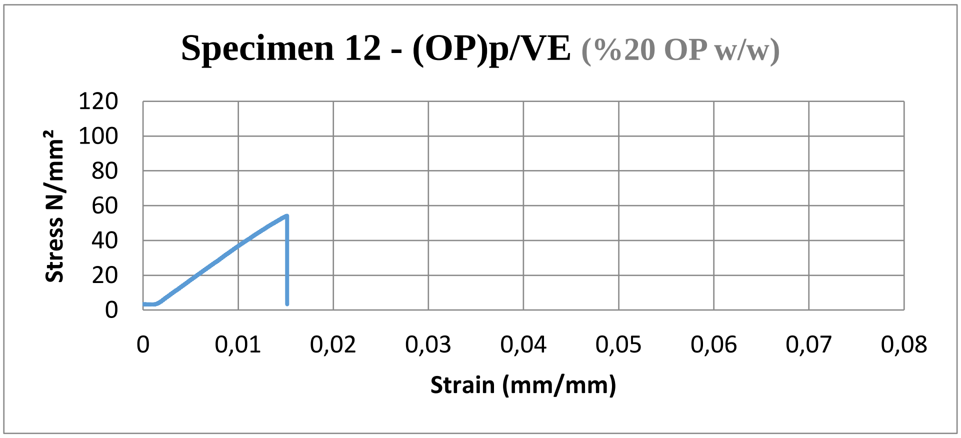

Figure B. 24. Specimen 12, Flexural Stress – Strain diagram

RESUME

Personal Information

Name Surname : Cihan ATİNTAŞ

Place and Date of Birth : Istanbul - 1986

Education

Undergraduate : Turkish Military Academy

Post Graduate : Aydın Adnan Menderes University

Foreign Languages : English (Advanced), Russian (Basic)

Experience

The Institution and Year:	Securitas - Turkey	2017 – Present
	Gendarmerie General Command	2016 – 2017
	Turkish Armed Forces	2009 – 2016

Contact

E-mail : cihanatintas@gmail.com

Date : 12/07/2018